Doctoral Dissertation

Doctoral Program in Civil and Environmental Engineering (34th Cycle)

Investigating green walls for greywater treatment and visualising enzymatic activity in constructed wetlands

Elisa Costamagna

******

Supervisor:
Prof. Fulvio Boano

Declaration

I hereby declare that, the contents and organization of this dissertation constitute my own original work and does not compromise in any way the rights of third parties, including those relating to the security of personal data.

This project received funding support provided by Compagnia di San Paolo through the project “SuperGreen - SUstainable Purification of waste- watER with GREEN walls”.

This project has received funding from the European Union’s Horizon 2020 research and innovation programme under grant agreement No 101003765

Elisa Costamagna

2022

This dissertation is presented in partial fulfillment of the requirements for **Ph.D. degree** in the Graduate School of Politecnico di Torino (ScuDo).

Si fractus illabatur orbis impavidum ferient ruinae

(Orazio, Odi III 3,8)

Ringraziamenti

Dedicata a tutti coloro che considerano il Dottorato di Ricerca un lavoro vero.

Dedicata a coloro che hanno contribuito, con incoraggiamenti, finanziamenti e ospitalità, a farmi girare il mondo per aprire i miei orizzonti.

Dedicata a coloro che mi fanno sorridere quando mi cercano e che vedo sorridere quando li cerco io, grazie a voi la fatica sparisce.

Dedicata a coloro che hanno speso del tempo per me quando ho chiesto loro consiglio, a coloro che si sono accorti che avevo bisogno di un aiuto anche quando non mi decidevo a chiederlo.

Dedicata a coloro che facendo il loro lavoro mi hanno aiutata a fare il mio, e anche a coloro a cui è capitato di rimandare le loro attività per darmi una mano.

Dedicata a coloro che mi incoraggiano ad avere una vita stimolante e favoriscono la mia curiosità mentre si lasciano contagiare dal mio entusiasmo e dalle mie riflessioni.

Dedicata a coloro che sono stati comprensivi quando li ho trascurati, quando sono arrivata tardi o quando ho messo la sveglia all'alba per riuscire a fare tutto.

Dedicata a coloro che hanno deciso di condividere pezzetti del loro cammino con me in questi anni e a coloro che per svariati motivi non fanno più parte della mia vita ma avrebbero gioito insieme a me per questo risultato.

Dedicata a coloro che sanno quanto sia importante il confronto, a volte anche acceso, ma che sono in grado di appianare le divergenze.

Dedicata a tutti coloro che contribuiscono con onestà intellettuale e gentilezza a rendere la nostra società accogliente ed equilibrata.

Sono sicura che vi siete riconosciuti.

Elisa

♦ Abstract

The European Research and Innovation Policy Agenda points Nature-Based Solutions (NBS) as key technologies to improve the sustainability of urban areas. NBS provide multiple benefits and ecosystem services, developing city resilience against climate change and improving water management, e.g., through increased stormwater retention and infiltration and through wastewater treatment. Green walls are an important type of NBS, recently studied for several applications such as thermal regulation and biodiversity preservation. The main limit of this technology is its water requirement for irrigation. However, wastewater could support the water and nutrient requirements of green walls, hence favouring the circular economy approach. The portion of wastewater that better fits the green wall irrigation and treatment purposes is greywater (GW), i.e. the portion of household wastewater that excludes toilet flushes and kitchen sinks, because it requires only mild treatment and it is available in high quantity. However, multiple challenges hinder the design of green walls for GW treatment, including the choice of the composition of the filter material, the contribution of the number of levels to treatment performance, and the influence of system operational time on GW treatment.

This thesis presents a green wall modular design tested along three years to evaluate the impact of design variation on GW treatment. The system is composed by modular panels with 12 planted pots each. The pots are organised in four columns that are fed separately with high HLR (around 740 $Lm^{-2}day^{-1}$) with water flowing vertically by gravity to the lower pots. Experiments have been performed in four phases, each one characterised by specific objectives, measuring the main physical-chemical and biological parameter from input and output water samples.

The first phase (December 2018 - March 2019) aimed to evaluate the effects of different filter media compositions on treatment performances. Preliminary tests were performed to select the plant species and the main filter medium composition. Four additives (compost, biochar, polyacrylate and granular activated carbon) were mixed with the base medium (BM), comparing 8 configurations. Possible compound release form BM was also evaluated testing a configuration fed with tap water. Removal performances were satisfactory for many parameters for most of the tested configurations. Compared to the base medium, biochar was the best performing additive over the highest number of parameters, compost also achieved high removal performances, but the frequent clogging events occurred during the monitoring period do not make its use recommendable. Granular activated carbon and the combination of biochar and polyacrylate performed

better than the base medium, but only for the removal of nitric nitrogen. The outcome of phase 1 led to the choice of configurations for the second phase.

The second phase (April - June 2019) tested the possible improvement of the best configuration arisen from the previous phase by adding graphene, which is a material with high potential for contaminant removal. Moreover, the possible influence of different system ages was verified comparing an older and a newer set of the best configuration of phase 1. Water samples were also collected along different levels of the green wall, to quantify the contribute of each level to the overall treatment performance and to obtain preliminary indications for the design geometry of the green wall. Results showed that the addition of graphene did not significantly improve treatment performance, that GW was mostly treated by the first two levels of the green wall, and that treatment performances slightly decreased after three months of operational time.

The third phase (January - March 2021) aimed to evaluate the impact of operational time on the system comparing two identical modules at two-year-distance as set up time difference. Water samples were collected along different levels of the green wall to better understand the contribution of each level of the module. Both panels exhibited very good removal efficiencies for TSS, BOD_5, COD, TN, MBAS. The newer panel reached satisfying pollutants removal after two levels, while the older one showed higher variability and clogging phenomena. This highlighted that the third level was necessary to guarantee good performances after over 2 years of operation for the chosen configuration.

The fourth phase (April - December 2021) consisted in stress tests aimed to test system resilience to feeding flow rate variations. The green wall design slightly changed in drainage system and filter medium composition, due to the lessons learnt during previous phases (e.g. due reduce the risk of clogging and waterlogging). The treatment performances increased along the columns in both panels, and the first two levels guaranteed a good removal during standard flow and underflow rates. On the other hand, the overflow rate caused a performance decrease for many parameters, followed by a visible plant stress. However, after one week of reverting to standard flow rate reduced the negative effects on plants of the three-weeks-overflow period.

Finally, the second part of this thesis focuses on a non-invasive methodology that allows a deeper comprehension of the microbial activities within a porous medium in CWs at mesocosm scale. This innovative photographical method was proposed by Dr. Gagnon and Dr. Chazarenc in 2014 and it is based on the use of fluorescein diacetate (FDA) and its response to UV-light after bacterial metabolic processes. During this thesis, the picture processing procedure has been optimised and automatized to visualise the enzymatic activity in 2D maps over time for three mesocosms planted with different vegetation species.

♦ Index

List of tables	**p. I**
List of figures	**p. III**
Introduction	**p. 1**
1.1 Greywater	p. 1
1.2 Nature-based Solutions (NBSs)	p. 7
1.3 Green walls	p. 7
1.3.1 Green walls for greywater treatment: state of the art	p. 8
1.3.2 Knowledge gaps and objectives	p. 11
1.4 Opening the black box	p. 12
Methods	**p. 15**
2.1 Greywater	p. 16
2.2 Filter media	p. 16
2.2.1 Base medium mix tests	p. 17
2.3 Plant selection	p. 18
2.4 Green wall modules	p. 19
2.4.1 Phase 1	p. 19
2.4.2 Phase 2	p. 21
2.4.3 Phase 3	p. 22
2.4.4 Phase 4	p. 22
2.4.5 Washing procedure	p. 23
2.4.6 Samples analysis	p. 23
2.4.7 Data analysis and statistical tests	p. 24
Results	**p. 25**
3.1 Greywater	p. 25

3.2 Preliminary tests on filter media p. 26
3.3 Preliminary tests on plants p. 28
3.4 Treatment performances p. 29
3.4.1 Washing procedure p. 29
3.4.2 Phase 1 p. 31
3.4.3 Phase 2 p. 41
3.4.4 Phase 3 p. 46
3.4.5 Phase 4 p. 54
Photographical method p. 57
4.1 Mesocosms set up p. 57
4.2 Collection of the pictures p. 58
4.3 Calibration p. 59
4.3.1 Calibration of FeS optical effects in white light p. 59
4.3.2 Fluorescein optical response p. 60
4.4 CW's picture processing p. 61
Results of photographical method p. 65
5.1 Calibration p. 65
5.1.1 Influence of FeS p. 65
5.1.2 Fluorescein p. 66
5.2 Picture selection and alignment p. 66
5.3 FeS maps p. 67
5.4 Enzymatic activity maps p. 68
Conclusions p. 75
6.1 Green wall design for GW treatment p. 75
6.2 Photographical method p. 77
References p. 79
Appendix A p. 91
Appendix B p. 95

♦ List of tables

Table 1.1.1. Conventional parameters to characterize domestic greywater (Boano et al. 2020)	p. 2
Table 1.1.2. Overview of regulation for GW reuse	p. 4
Table 1.1.3. Overview of guidelines for GW reuse	p. 5
Table 1.1.4. Proposed guidelines and reports for GW reuse. No standards or limits are available. (Boano et al. 2020)	p. 5
Table 2.1.0. Main objectives of the four sampling campaign	p. 16
Table 2.1.1. Synthetic light GW recipe modified by (Diaper et al. 2008)	p. 16
Table 2.2.1. Media for filter mix. The abbreviations are used hereafter to identify both the configuration with the specific medium (when "configuration" or "mix" is used) and the medium itself	p. 17
Table 2.4.1. Configuration tested during the first phase. Percentage in volume for the different additives	p. 20
Table 2.4.2. Configuration tested during the second phase. Percentage in volume for the different additives	p. 21
Table 2.4.3. Flow rate of variable panel. Feeding is set once per hour per 24 hours a day, all week. Values of underflow and overflow are inspired by (Osterreichisches Normungsinstitut 2005)	p. 22
Table 2.4.4. Water procedure sampling schedule for BM* in phase 1	p. 23
Table 3.2.1. Physical characteristics of media in the base mix. Values are average and standard deviation (in parentheses) from three replicates	p. 26
Table 3.4.1. List of *p* values of the statistical tests performed on contaminants' removal efficiencies. The Mann-Kendall test verified the presence of temporal trends (positive if not otherwise specified), and the Students' *t*-test verified if a filter medium mixture had better removal performance than the BM (*p*<0.05 in bold). Asterisks confirmed the statistically significance after false discovery rate procedure	p. 37

Table 3.4.2. p-values of Mann-Kendall test on all parameter removal efficiency. Bold numbers indicate an increasing trend ($p<0.05$) in temporal series; asterisks confirm the trend after false discovery rate adjustment. NaN occurs when all value in a data set are below the detection limit	p. 42
Table 3.4.3. p-values of the t-Student test comparing removal efficiency of each configuration. Bold numbers indicate that the tested configuration performed significantly better that the reference one. Asterisks confirm the test significance after false discovery rate adjustment. NaN occurs when all values were below the detection limit	p. 42
Table 3.4.4. Average and standard deviation (in parenthesis) over time of on-site parameters of input GW and outflow from each level	p. 54
Table 3.4.5. Average and standard deviation (in parenthesis) over time of laboratory parameters of input GW and outflow from each level	p. 54
Table 5.4.1. Average concentration of fluorescein (mg/L) for the last available image and at the outlet sample of each mesocosm.	p. 73
Table A.I. Synoptic view of the main design characteristics of green walls for greywater treatment in literature, limited to pilot and full scale studies.	p. 91
Table A.II. Synoptic view of the inflow GW characteristics of green walls for treatment in literature, limited to pilot and full scale studies. Parameters in mg/L (other units for turbidity in NTU, E. coli in MPN/100mL, EC in µS/cm, pH).	p. 92
Table A.III. Characteristics of the outflow treated GW of green walls for treatment in literature, limited to pilot and full scale studies. Parameters in mg/L (other units for turbidity in NTU, E. coli in MPN/100mL, EC in µS/cm, pH). Removal efficiency of each system (in percentage).	p. 93
Table B.I. Average and standard deviation (in parenthesis) over time of on-site and laboratory parameters of input GW and outflow from each configuration.	p. 95
Table B.II. Average and standard deviation over time of input GW and outflow GW.	p. 96
Table B.III. Phase 3. Average and standard deviation (in parenthesis) over time of on-site and laboratory parameters of input GW and outflow from each level.	p. 97
Table B.IV. Phase 4. Average and standard deviation (in parenthesis) over time of on-site and laboratory parameters of input GW and outflow from each level.	p. 98

♦ List of figures

Figure 1.3.1. Types of vertical greening system (Medl et al. 2017)	p. 8
Figure 2.2.1. Constant head permeameters with automatic data collection	p. 18
Figure 2.4.1. Green wall modular panel	p. 20
Figure 3.1.1. Boxplot of time series values for input GW in the four sampling campaigns. Median value (cross), 25th and 75th percentiles (box), range (whiskers) and outliers (dots) are shown	p. 25
Figure 3.2.1. Average values and standard deviations of hydraulic conductivity K_s (blue triangles) and bulk density ρ_b (red circles) for mixes with different percentages of coconut fibre and perlite	p. 27
Figure 3.2.2. Granulometric curve of the mix CF:PL 1:1 in wet and dry (120° for 2h) conditions	p. 27
Figure 3.2.3. Hydraulic conductivity of 1:1 CF:PL mix during columns washing. Values are average and standard deviation of five replicates	p. 28
Figure 3.3.1. Tested plant species after one month: (a) *L. nitida*, (b) *I. germanica*, (c) *C. morrowii*, (d) *R. asiaticus*, and (e) *H. helix*. Red (solid) and blue (dashed) lines indicate the greywater (GW) and tap water (TW) groups, respectively	p. 28
Figure 3.3.2. Chlorophyll variation rate normalised on the value of first measurement. Values shown are calculated from average of plants from the same configuration (five leaves per plant, three point per leaf)	p. 29
Figure 3.4.1. Qualitative evaluation on water colour in samples I to V during washing procedure	p. 30
Figure 3.4.2. Compounds that were significantly released from the columns during the preliminary washing procedure with tap water: a) pH, Electrical Conductivity; b) NO_3^--N, SO_4^{2-}, Cl^-	p. 30
Figure 3.4.3. Average and standard deviation of pH and Electric Conductivity (EC) measured in the outflows of panels P1 and input tap water values during the washing procedure	p. 31
Figure 3.4.4. a) Temperature, b) pH, c) Electric Conductivity (EC), and d) Dissolved Oxygen (DO) at the inlet and outlet of TW and GW columns	p. 32

Figure 3.4.5. Concentrations of a) COD and b) BOD5 at the inlet and outlet of TW and GW columns	p. 33
Figure 3.4.6. Concentrations of a) TKN, b) NO_3^--N, and c) TP at the inlet and outlet of TW and GW columns	p. 34
Figure 3.4.7. Concentrations of a) sulphate and b) chloride at inlet and outlet of TW and GW columns	p. 35
Figure 3.4.8. Concentrations of a) *E. coli* in the input and output of GW columns and b) MBAS at the inlet and outlet of TAP and GW columns	p. 35
Figure 3.4.9. Time series of a) temperature, b) pH, c) Electric Conductivity (EC) and d) Dissolved Oxygen (DO) of GW (dashed lines) and at the outlet of all filter medium mixtures. Filter medium mixtures are denoted as (see text for further details) BM: base medium; 10GAC: granular activated carbon; 20CO: compost; 20BC: biochar; 20PA: polyacrylate; 20PA20BC: polyacrylate and biochar; 20PA+: polyacrylate (old configuration)	p. 36
Figure 3.4.10. Average values of concentrations of a) BOD5, b) COD and c) TSS of input GW (dashed lines) and at the outlet of all filter media mixes (bars). Filter medium mixtures are denoted as (see text for further details) BM: base medium; 10GAC: granular activated carbon; 20CO: compost; 20BC: biochar; 20 PA: polyacrylate; 20PA20BC: polyacrylate and biochar; 20 PA+: polyacrylate (old configuration)	p. 38
Figure 3.4.11. Removal efficiency of a) TKN, b) NO_3^--N, c) TP, d) SO_4^{2-} over the monitoring period. Filter medium mixtures are denoted as (see text for further details) BM: base medium; 10GAC: granular activated carbon; 20CO: compost; 20BC: biochar; 20PA: polyacrylate; 20PA20BC: polyacrylate and biochar; 20PA+: polyacrylate (old configuration)	p. 39
Figure 3.4.12. Removal efficiency of a) *E. coli*, b) MBAS over the monitoring period. Filter medium mixtures are denoted as (see text for further details) BM: base medium; 10GAC: granular activated carbon; 20CO: compost; 20BC: biochar; 20PA: polyacrylate; 20PA20BC: polyacrylate and biochar; 20PA+: polyacrylate (old configuration)	p. 40
Figure 3.4.13. Boxplot of time series values for input water (TW and GW) and output water from all configurations for parameters measured on site with the multiparametric probe (Temperature: top left, pH: top right, EC: bottom left, DO: bottom right). Median value (red line), 25th and 75th percentiles (blue box), range (black whiskers) and outliers (red cross) are shown	p. 41

Figure 3.4.14. Boxplot of time series values for input water (TW and GW) and output water from all configurations for bio-chemical parameters (BOD_5 top left, TKN top right, NO_3^--N bottom left, NO_3^--N bottom right). Median value (red line), 25th and 75th percentiles (blue box), range (black whiskers) and outliers (red cross) are shown	p. 43
Figure 3.4.15. Boxplot of time series values for input water (TW and GW) and output water from all configurations for bio-chemical parameters (TP top left, SO_4^{2-} top right, Cl^- bottom left, MBAS bottom right). Median value (red line), 25th and 75th percentiles (blue box), range (black whiskers) and outliers (red cross) are shown	p. 43
Figure 3.4.16. Temperature values measured in the outflows of the different levels (L1, L2, and L3) of panels P1 (top) and P2 (bottom) and in input greywater (GW)	p. 46
Figure 3.4.17. pH values measured in the outflows of the different levels (L1, L2, and L3) of panels P1 (top) and P2 (bottom) and in input greywater (GW)	p. 47
Figure 3.4.18. Dissolved Oxygen (DO) concentration values measured in the outflows of the different levels (L1, L2, and L3) of panels P1 (top) and P2 (bottom) and in input greywater (GW)	p. 48
Figure 3.4.19. Electrical Conductivity (EC) values measured in the outflows of the different levels (L1, L2, and L3) of panels P1 (top) and P2 (bottom) and in input greywater (GW)	p. 48
Figure 3.4.20. Concentration of total suspended solids (TSS) in output water samples and input GW for all the levels in P1 (top) and P2 (bottom)	p. 49
Figure 3.4.21. Average cumulative removal efficiency (%) obtained at the different levels of panels P1 (newer) and P2 (older) for total suspended solids (TSS), chemical oxygen demand (COD), biochemical oxygen demand (BOD_5), total nitrogen (TN), ammonia nitrogen (NH_4^+-N), methylene blue active substances (MBAS), total phosphorous (TP), chloride (Cl^-)	p. 50
Figure 3.4.22. Concentration of COD in output water samples and input GW for all the levels in P1 (top) and P2 (bottom)	p. 51
Figure 3.4.23. Concentration of BOD_5 in output water samples and input GW for all the levels in P1 (top) and P2 (bottom)	p. 51
Figure 3.4.24. Concentration of total nitrogen (TN) in output water samples and input GW for all the levels in P1 (top) and P2 (bottom)	p. 52

Figure 3.4.25. Concentration of methylene blue active substances (MBAS) in output water samples and input GW for all the levels in P1 (top) and P2 (bottom)	p. 53
Figure 3.4.26. Comparison between outflow of variable load panel (left column) and constant load panel (right column) for TSS. Highlighted areas show help the visual comparison of the two panel during the different loading rate	p. 55
Figure 3.4.27. Comparison between outflow of variable load panel (left column) and constant load panel (right column) for BOD_5. Highlighted areas show help the visual comparison of the two panel during the different loading rate	p. 55
Figure 3.4.28. Comparison between outflow of variable load panel (left column) and constant load panel (right column) for COD. Highlighted areas show help the visual comparison of the two panel during the different loading rate.	p. 56
Figure 4.1.1. Scheme of the mesocosm, side and top view	p. 57
Figure 4.2.1. Schematic top view of the black box around the wetland, location of camera and UV-light	p. 58
Figure 4.3.1. Picture for the calibration in white light. Each box contains glass sand saturated with different concentrations of FeS. Image in greyscale at +70% brightness	p. 60
Figure 4.3.2. Picture for the calibration in UV-light. Each box contains glass sand saturated with different concentrations of fluorescein. Image in greyscale at +80% brightness	p. 61
Figure 4.4.1. a) subtraction of UV_0 from a non-aligned UV_N. b) subtraction of UV_0 from the same UV_N after alignment	p. 62
Figure 4.4.2. Selecting frame to cut the area of interest	p. 62
Figure 4.4.3. White light image after resolution decreasing. The image has been brightened to favour the visualisation of this step	p. 63
Figure 4.4.4. a) FeS concentration map from WL image in grey scale. b) Fluorescein concentration map from UV-A image at 25 minutes	p. 63
Figure 4.4.5. Flow chart that summarizes the picture processing to build concentration maps	p. 64
Figure 5.1.1. Correlation curve of FeS concentration in white light	p. 65
Figure 5.1.2. Correlation curve of fluorescein light emission at different concentration in UV light	p. 66
Figure 5.2.1. Timeline of the analysed picture per each series	p. 67

Figure 5.3.1 Examples of maps of FeS concentration for a) *Phragmites australis,* b) *Phalaris arundinacea* and c) *Typha angustifolia*	p. 67
Figure 5.4.1. Extract of time series of fluorescein concentration maps for *Phragmites Australis*, from the first to the last available UV-light pictures	p. 69
Figure 5.4.2. Extract of the time series of fluorescein concentration maps for *Phalaris Arundinacea*, from the first to the last available UV-light pictures	p. 70
Figure 5.4.3. Extract of the time series of fluorescein concentration maps for *Typha angustifolia*, from the first to the last available UV-light pictures	p. 71
Figure 5.4.4. Concentration maps (left) and white light picture (right) of a-b) *Phragmites australis,* c-d) *Phalaris arundinacea* and e-f) *Typha angustifolia*	p. 72
Figure 5.4.5. Complete time series of the average concentration of fluorescein calculated for all available pictures	p. 73

♦ Introduction

The material in this chapter is partially derived from (Boano et al., 2021a, 2021b, 2020; Costamagna et al., 2021)

It is estimated that one third of the world's population does not have access to clean drinking water (Ghaitidak and Yadav, 2013; ONU, 2018; Pruss-Ustun and World Health Organization, 2008; World Health Organization, 2017). Furthermore, over two-thirds of the world population, about 4 billion people, is already experiencing severe water scarcity during at least one month per year (Mekonnen and Hoekstra, 2016) and this scenario could be extended to approximately 4.8–5.7 billion people in 2050 (Burek et al., 2016). Global water shortage is due to a combination of population growth, economic development with extensive use of water in agriculture and industry, increasing standard of lifestyle, dietary changes, and climate change (Kummu et al., 2010). United Nations Sustainable Development Goals (UN SDGs) 6.3 and 6.4 promote novel strategies for overcoming the water stress scenario at the global level, giving safe water reuse an essential role in reducing freshwater withdrawals and improving water use efficiency, even at the household level. This is especially relevant in areas where water scarcity is already a reality, such as Cape Town, in South Africa, or Viseu, in Portugal, (Climate System Analysis Group, 2020) but these scenarios might become more frequent in the coming decades due to climate changes, with the Mediterranean being one of the most critical areas (Milano et al., 2012). Alternative water sources should be actively sought, so that the urban water cycle will become a true cycle, and reclaimed wastewater/greywater reuse will proficiently contribute to the circular economy and to the achievement of UN SDGs. Moreover, regulations for treating civil wastewater require progressively higher performances in removal of traditional and emerging contaminants (European Commission, 2012), increasing energy consumption and operating costs. A sustainable management of water resource is therefore essential (Grant et al., 2012). In this context, nature-based solutions (NBSs) are recommended to increase urban areas' resilience, contrast climate change effects, reduce clean water consumption and preserve natural ecosystems (European and Commission, 2015).

1.1 Greywater

Greywater (GW) is the share of household wastewater (WW) deriving from sinks, showers and laundry, representing up to 75% of total domestic WW. It means a volume

of 72−225 $LPE^{-1}day^{-1}$ in EU, North America and Asia (Boano et al., 2020; Boyjoo et al., 2013; Eriksson et al., 2002; Ghaitidak and Yadav, 2013). "Light" GW excludes kitchen sinks, and it is particularly suitable for local treatment due to its low pollution, also allowing non-potable water reuse and clean water saving. The source separation of GW can reduce the volume sent to WW treatment plants and to minimize the energy required for their treatment (Larsen et al., 2009; Remy and Jekel, 2008) because only the more polluted fraction of domestic WW is sent to the treatment plant (Otterpohl et al., 2002). Additionally, reclaimed GW can be locally recycled for other uses (e.g., toilet washing, irrigation) which would otherwise employ high-quality water; in this way, GW reuse has a fundamental role in creating a new model of urban water supply, integrating this new source with rainwater-harvesting practices. (Friedler and Hadari, 2006; Leong et al., 2017; Oteng-Peprah et al., 2018).

Household sources contribute differently to GW composition. The average contribution of three main different sources to the composition of GW are: 49% bath tubs, basins and showers; 27% kitchen sinks and dishwashers; 24% laundry sinks and washing machines. These values were calculated from twenty studies referring to sixteen countries (Australia, Brazil, Burkina Faso, Denmark, England and Wales, Greece, Holland, India, Israel, Jordan, North America, Oman, Yemen) (Al-jayyousi, 2003; Edwin et al., 2014; Ghaitidak and Yadav, 2013; Maiga et al., 2014; Noutsopoulos et al., 2018; Vakil et al., 2014).

GW quality is conventionally assessed through the parameters summarized in Table 1.1.1; typically, most studies focus only on a subset of them (e.g., Eriksson et al. 2002; Fowdar et al. 2017; Leonard et al. 2016). For pathogen assessment, different Faecal Indicator Bacteria (FIB) are employed – among which Escherichia coli is the most used – even though their correlation with enteric pathogens has been questioned (Benami et al., 2016). Xenobiotic Organic Compounds usually include surfactants, fragrance flavours, preservatives, and solvents.

Table 1.1.1. Conventional parameters to characterize domestic greywater (Boano et al., 2020).

Physical		**Chemical**	
Parameter	**Units**	**Parameter**	**Units**
Temperature	°C	pH	
Turbidity	NTU	Biochemical Oxygen Demand	mg/L
Total solids	mg/L	Chemical Oxygen Demand	mg/L
Total suspended solids	mg/L	Total Organic Carbon	mg/L
Total dissolved solids	mg/L	Dissolved Organic Carbon	mg/L
Biological		Nitrate	mg/L
Total coliforms	MPN/100mL	Ammonium	mg/L
Faecal coliforms	MPN/100mL	Oxidized nitrogen	mg/L
Escherichia coli	MPN/100mL	Total Nitrogen	mg/L
F-RNA bacteriophage	MPN/100mL	Total Phosphorus	mg/L
Clostridium perfringens	MPN/100mL	Phosphate	mg/L
Bacteroidales	MPN/100mL	Heavy metals	mg/L
		Xenobiotic Organic Compounds	mg/L

Almost all literature agrees that quantity and quality of domestic GW exhibit seasonal variations and depend on the characteristics of users (number, age, habits, activities), composition of commercial cleaning products, wastewater collection system, house

facilities (e.g., dishwasher, washing machine), area type (e.g., urban, countryside, seaside). Furthermore, source and mix play an important role in the compounds that are in greywater. Usually, bath and hand basin GW contains personal care products (e.g. soap, toothpaste, shampoo), human-derived components (e.g. shave residuals, hair, skin, sebum), and also traces of faeces and urine (Eriksson et al., 2002; Ghaitidak and Yadav, 2013); laundry GW contains high concentrations of chemical products (e.g. soaps and oils) and non-biodegradable fibres (Ghaitidak and Yadav, 2013; Morel and Diener, 2006); kitchen GW (from sinks or dishwashers) contains food, oils, fats, and detergents (Ghaitidak and Yadav, 2013; Noah, 2002). Both baths and laundry are the most frequent origins for faeces, skin, and food residuals, especially if there are babies in the house (Leonard et al., 2016). By definition, urine is not included into GW, but high concentration of phosphorus and nitrogen are usually considered indicators of urine contamination (Eriksson et al., 2002; Leonard et al., 2016). Storage time has also an impact on greywater characteristics: quality improves within the first day of storage but drastically decreases after 48 h (Eriksson et al., 2002; Liu et al., 2010). An extensive comparison of the properties of GW from different sources was proposed by Eriksson et al. (2002). According to this study, it is hard to find in literature comparable data about parameter ranges or average values: some authors split different sources, while others consider a mixed GW; sometimes average values are given (with or without standard deviation), while other times ranges are provided. Most of the published papers organize data on either country or source bases. Boano et al. (2020) summarised the country-based approach, comparing physical-chemical properties from published reviews and articles that analysed real domestic GW from 28 countries. None of the parameters exhibited a trend that allows grouping countries according to a geographic criterion. An income criterion has often been used to group countries (Ghaitidak and Yadav, 2013) but the review of the collected studies did not support this choice (Boano et al., 2020). Some parameters have similar ranges in almost all countries. For instance, pH fluctuates around the neutral value, and typical values of total suspended solids (TSS) are below 500 mg/L with peaks of the order of 1000 mg/L. Chemical Oxygen Demand (COD) and Biochemical Oxygen Demand (BOD_5) values are usually of the order of some hundreds mg/L, although a few values larger than 1000 mg/L have been reported (e.g., Israel, Malaysia, Jordan, United Arab Emirates). Total nitrogen (TN) and total phosphorus (TP) generally exhibit concentrations below a few tens mg/L and a few mg/L, respectively, with only a few exceptions (e.g. Palestine and Jordan). Faecal Indicator Bacteria (FIB) instead present a huge variability both among and within countries, with variations in concentration spanning many orders of magnitude. Some studies considered synthetic GW (Diaper et al., 2008; Hourlier et al., 2010) due to its reproducibility and consistency in composition. Synthetic GW is usually prepared combining specific amounts of laundry soap, shampoo, oil, hand soap, etc. Different recipes have been used in terms of kind and quantity of products. In order to ensure the consistency of synthetic GW recipe, it is necessary to confirm the availability of the specific products (brand or exact composition). For this reason, Hourlier et al. (2010) suggested a composition that uses only chemical products of technical quality. Abed and Scholz (2016) provided a comparison between different recipes: some of them use commercial products, others

chemical ones. There are also some studies that suggest different recipes (Charchalac Ochoa et al., 2015; Chrispim and Nolasco, 2017; Rodriguez-Chueca et al., 2014).

Quality requirements for GW reuse are available, as regulations and guidelines, in a number of countries. Quality requirements and reuse limits depend on type of reuse, on origin of GW, and on possibility of human contact with recycled water (Abu Ghunmi et al., 2011; Eriksson et al., 2002; Ghaitidak and Yadav, 2013; Hourlier et al., 2010; Leonard et al., 2016). Country reuse standard comparison has been provided in literature (De Gisi et al., 2016; Edwin et al., 2014), but a more widespread regulation has been highly recommended in recent studies (Al-ismaili et al., 2017). Table 1.1.2 shows mandatory standards for GW reuse are available for Great Britain (BSI, 2011), USA (NSF/ANSI, 2011), New South Wales – Australia (NSW-DEUS, 2007; Vuppaladadiyam et al., 2018), Italy (D.M. 185, 2003), and Japan (JSWA, 2016; Vuppaladadiyam et al., 2018).

Table 1.1.2. Overview of regulation for GW reuse.

	Great Britain		**USA**		**NSW-Australia**		**Japan**
Parameter	**Sprinkler**	**Non-sprinkler**	**Residential**	**Commercial**	**Irrigation**	**Household**	
pH	5–9.5	5–9.5	6–9	6–9	6	9	6–9
EC (µS/cm)	–	–	–	–	80	1	–
BOD_5 (mg/L)	–	–	<10	<10	<20	<20	<20
TSS (mg/L)	–	–	–	–	30	10	–
Turbidity (NTU)	<10	<10	<5	<2	–	–	Clear
MBAS (mg/L)	–	–	–	–	–	–	30
TN (mg/L)	–	–	–	–	–	–	20-30
TP (mg/L)	–	–	–	–	–	–	1-4
FIB (MPN/100 mL)	Not detected	25 (*E.coli*)	~0	~0	<1	<4	$<1 \cdot 10^5$

Table 1.1.3 lists the guidelines voluntarily adopted in Germany (Jokerst et al., 2011; USEPA, 2012), Slovenia (Šostar-Turk et al., 2005), Jordan (Abu Ghunmi et al., 2011), China (Zhu et al., 2018), India (Hosseinzadeh et al., 2015), and Canada (Chaillou et al., 2011). Even though the parameters are not fully consistent among different countries, standard limits have been proposed by the existing guidelines for pH, BOD_5, COD, total suspended solids (TSS), total phosphorus (TP), and faecal bacteria (FIB). Values of these standard limits in Table 1.1.3 exhibit considerable variations, with differences among countries that are larger than one order of magnitude.

Table 1.1.3. Overview of guidelines for GW reuse.

	Guidelines					
	Germany	**Slovenia**	**Jordan**	**China**	**India**	**Canada**
Parameter						
pH	6-9	7- 9	6-9	6-9	6-9	7-9
EC (µS/cm)	–	–	1000	–	–	–
BOD_5 (mg/L)	20	30	30-300	10-20	<30	200
COD (mg/L)	–	200	100-500	<15	<250	280
TSS (mg/L)	Near free	80	50-150	10-50	<200	<100
Turbidity (NTU)	Near clear	–	2-10	<10	–	<2
MBAS (mg/L)	–	1	30-100	0.5-1	<10	–
Sodium (mg/L)	–	–	230	–	–	–
TN (mg/L)	–	10	50-70	15-20	–	–
TP (mg/L)	–	1	30	1-5	–	–
Potassium (mg/L)	–	–	–	–	–	–
Boron (mg/L)	–	–	1	–	–	–
FIB (MPN/100 mL)	<10 (total) <100 faecal)	–	<1000 (faecal) 100 (*E.coli*)	–	–	<1000 (total) 2-200 (faecal)

Table 1.1.4 offers an overview of the guidelines for GW reuse in Europe and the world. These guidelines have been developed to encourage and enhance the reuse of GW and provide recommendations for a proper reuse, with a specific focus on managing health risks related to the use of non-treated GW.

Table 1.1.4. Proposed guidelines and reports for GW reuse. No standards or limits are available (Boano et al., 2020).

Country	**Guideline**	**Main finding**	**Reference**
Europe	Directive 91/271/EEC on urban waste water treatment (UWWTD)	- Wastewater shall be reused whenever appropriate - Member States shall minimise any adverse effects on the environment from wastewater reuse - The nutrient removal requirements concern Sensitive Areas (i.e. eutrophic/in danger fresh-water bodies, sources of drinking water, bathing waters, natural habitats, fish waters).	(Council of the European Communities, 1991)
United Nations	Guidelines for the safe use of wastewater, excreta and greywater	- Chapter 2: Technical perspectives - Chapter 8: Environmental aspects	(WHO, 2006)
Australia	National guidelines for water recycling: managing health and environmental risks (phase 1)	- Chapter 2: Framework for management of recycled water quality and use - Chapter 3.7: Managing health risks in recycled water, GW, microbial and chemical risks	(EPHC NRMMC AHMC, 2006)

Country	Guideline	Main finding	Reference
Australia	NSW guidelines for greywater reuse in sewered single household residential premises	GW reuse in urban area	(NSW-DEUS, 2007)
United Kingdom	Guidelines for greywater reuse: health issues	GW health risks	(Dixon et al., 1999)
Ireland	Rainwater harvesting and greywater treatment systems for domestic application in Ireland	- Coarse filtration + metal strainer to retain suspended particles - Membrane filtration to clarify water	(Li et al., 2010)
North America	Overview of greywater reuse: the potential of greywater systems to aid sustainable water management.	- Challenges and opportunities for GW reuse - GW as percentage of total water use - GW and energy - GW and agriculture	(Allen et al., 2010)
Israel	Greywater use in Israel and worldwide: standards and prospects	- Separated collection of GW from wastewater - Biological treat is based on membrane + UV disinfection - Reuse for 1 yard irrigation and/or toilet flushing	(Oron et al., 2014)
Europe	Technical guide for greywater recycling systems	- Treated GW shall only be used for the following applications: - Flushing of water closet (WC)/Urinal. - General washing (excluding high pressure jet washing and general washing at markets and food establishments) - Irrigation (excluding irrigation sprinklers) - Cooling tower makeup water.	(PUB, 2014)
Australia	Code of practice – onsite wastewater management	- Chapter 3: Onsite wastewater management in unsewered areas - Chapter 4.1: GW overview - Overview of GW policies, regulations, and laws around the world	(EPA Victoria, 2016)
Europe	Guidelines on integrating water reuse into water planning and management in the context of the WFD (Water Framework Directive)	- Water scarcity - Greywater reuse in agriculture - Greywater health risk	(EPA, 2016)
United Nations	United Nations: world water development report.	- Chapter 2: wastewater and the sustainable development agenda - Chapter 4: technical aspects of wastewater - Chapter 5: municipal and urban wastewater - Chapter 7: agriculture as a user of wastewater	(United Nations, 2017)
United Kingdom	BS8525 and the Water Supply (Water Fittings) Regulations	GW can be reused on site for: - ornamental, garden and lawn irrigation, - toilet flushing.	(BSI, 2011; UK government, 1999)

1.2 Nature-based Solutions (NBSs)

Nature-based solutions (NBSs) are defined as "actions to protect, sustainably manage, and restore natural or modified ecosystems, that address societal challenges effectively and adaptively, simultaneously providing human well-being and biodiversity benefits" (Cohen-Shacham et al., 2016) and also as ''living solutions inspired by, continuously supported by and using nature, which are designed to address various societal challenges in a resource-efficient and adaptable manner and to provide simultaneously economic, social, and environmental benefits" (European and Commission, 2015). Thus, NBSs are techniques that mimic natural processes in urban landscapes, including in WW management, with low inputs of energy and chemicals. Different NBSs have been implemented, including constructed wetlands (CWs), green roofs, green walls/living walls, and urban green spaces (e.g., parks, street trees). NBSs contribute to save energy through reduced cooling loads (Alexandri and Jones, 2008; Castleton et al., 2010), reduce flooding risk (Rizzo et al., 2018), and promote a sustainable economic growth (Maes and Jacobs, 2017). Several studies have demonstrated the positive effects induced by greening vacant urban land on the well-being of the people (Ling and Chiang, 2018; South et al., 2018; Tzoulas et al., 2007). Finally, NBSs support biodiversity by providing habitats for different species (Francis and Lorimer, 2011). Planning and design aspects should be taken into account when implementing NBSs. The aesthetic appearance is essential for their integration with the surrounding landscape and acceptance from local communities. One of the most critical limits to the application of NBS in densely built urban areas is the lack of available space. However, the outer surfaces of buildings can provide unused spaces in densely inhabited areas. From this perspective, green roofs and green walls represent two examples of NBSs that are well suited to urban areas, saving horizontal space (Castellar da Cunha et al., 2018). The main critiques addressed to urban greening are maintenance costs and the large amount of water to maintain it. However, around two decades ago NBSs for GW treatment emerged and provided interesting preliminary results in water treatment. Constructed wetlands were the first low-cost NBSs for wastewater treatment and have also been used to successfully treat GW (Alfiya et al., 2013; Arden and Ma, 2018; Avery et al., 2007; Ramprasad et al., 2017).

1.3 Green walls

Vertical greening systems are an important technique for urban reconciliation ecology (Francis and Lorimer, 2011), and are becoming integrated parts of modern building in many countries. There are several types of vertical greening systems (Figure 1.3.1), with different water needs and support media for the plants, with systems simulating an assembly of pots, while others use fabric mats or similar materials to support the plants (Manso and Castro-gomes, 2015).

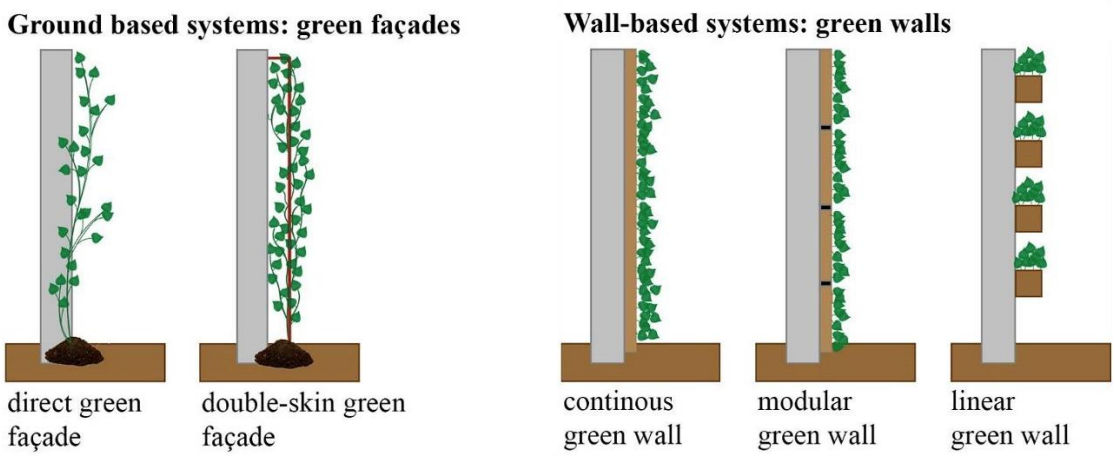

Figure 1.3.1. Types of vertical greening system (Medl et al., 2017).

All of these configurations provide multiple benefits, such as high thermal/energy performance, air quality improvement, urban heat-island mitigation, and better quality of life (Bauduceau et al., 2015; Bustami et al., 2018; Castellar da Cunha et al., 2018), in addition to biodiversity protection and real estate valorisation (Castellar da Cunha et al., 2018; Francis and Lorimer, 2011; Seyam, 2019). These green infrastructures were originally developed for aesthetic and insulation purposes (Teotónio et al., 2018), and they have only been recently proposed for wastewater treatment systems. In particular, green walls are vertical systems usually attached to internal or external walls, and are made up of planted containers attached to the wall itself. The vegetation is hence rooted across the entire vertical structure of the wall and not only at its base as for green facades (Manso and Castro-gomes, 2015). Green walls for GW treatment operate similarly to reed beds, in which GW percolates through planted pots filled with a combination of granular media such as vermiculite, sand, growstone, expanded clay, phytofoam, coco coir, and perlite (Prodanovic et al., 2017). However, their low space requirements represent a relevant advantage compared to the conventional reed beds (Masi et al., 2016). The choice of plants must fulfil multiple criteria: fitness to local climatic conditions and high survival capacity, aesthetic appearance (e.g., perennial species), low space required for root growth, low weight, and good removal capacity of nutrients (Castellar da Cunha et al., 2018). Additional features such as potential use for agricultural or medical purposes are certainly added values (Eregno et al., 2017). The use of green walls to produce reclaimed water has several advantages compared to wastewater treatment plants; the decentralized approach represents a sustainable strategy, reducing the load on existing wastewater treatment plants, while also maintaining all of the mentioned benefits of traditional green walls. Furthermore, the drained water can be locally reused for non-potable uses, such as toilet flushing, garden irrigation, street washing (Masi et al., 2016; Svete, 2012; Wolcott et al., 2016).

1.3.1 Green walls for greywater treatment: state of the art

Unfortunately, there is currently a lack of well-established criteria to guide the design of green walls and green roofs as NBS for greywater treatment. The possibility of exploiting green walls for GW treatment and reuse is still in the preliminary stage, with few studies

available in the literature. Most studies focused on the treatment performance of different filter media and plant species, analysing the removal of organic matter and nutrients.

A review on specific issues such as the mechanisms of contaminant removal by plants and growing media, system longevity, and socio-cultural implications (Pradhan et al., 2019a) has been recently published. In particular, Pradhan et al. (2019a) addressed: significant issues related to the design of green walls for GW treatment; pollutants removal mechanisms (both considering the plants and the growing media); problems that may compromise the durability of the systems; reduction in produced treated GW due to intense evapotranspiration in arid climates; potential damages to buildings due to the roots growth; reluctance to the reuse of treated GW, which is seen as contaminated in some cultural contexts; potential health issues related to the reuse of treated GW; costs for maintenance and operation.

The first application of vegetated walls for GW treatment was developed in Norway and consisted in a wall-adapted biological filter intermittently dosed with domestic GW (Svete, 2012). In spite of the limited spatial footprint (filter surface area around 0.54 m^2), the system was able to operate with good removal performance as enhanced aerobic conditions and residence times supported fast biogeochemical reaction rates. The system included three different sections, among which the planted one showed higher removal rates, satisfying all the expected treatment performances for biological filters in Norway, with the exception of *E. coli*. However, an Anova analysis demonstrated that the contribution of vegetation to treatment was not relevant, suggesting that the higher performance was most probably due to higher residence time and confirming the importance of this parameter. A pilot installation of a green wall was conducted by Masi et al. (2016) for the treatment of GW produced by an office building in Pune (India). The system involved a series of pots filled with porous media (LECA mixed with either sand or coconut fibres) and with different plant species. The pots were arranged in 12 vertical columns (6 pots per column), and perforated pipes fed the upper row while the lower rows of pots received water through vertical percolation. The effluent collected at the bottom of the wall was then reused for garden irrigation. The main conclusion of the study was related to the importance of the substrate used in the green wall. Even though TN removal was limited, the system was successful in minimizing the treatment footprint while ensuring an effluent quality that respected the Indian regulations on reuse for irrigation purposes and, in some samples, for toilet flushing.

Considering the importance of filter media, preliminary and pilot studies were performed, suggesting that mixes with coconut fibre guarantee a favourable hydraulic retention time for removing pollutants and avoiding clogging (Masi et al., 2016; Prodanovic et al., 2018, 2017). It was also observed that expanded clay mixes provide good removal results, (Gattringer et al., 2016; Masi et al., 2016) while Fowdar et al. (2017) realized good performances with inert material (sand, gravel) and planted with ornamental species (climbers and flowers) to reproduce a living wall system. The study investigated different operational and design aspects in terms of loading rates, saturated zone design, vegetation species, filling materials, inflow concentrations, and dosing

frequency. It was observed that denitrification was limited by the availability of organic matter in the saturated layer. The only carbon source provided by the GW was quickly removed in the upper layers, limiting the presence of biodegradable matter where denitrification could occur. The performance of the system in terms of BOD_5 removal proved to be very high, while some improvements were still required for nitrogen and phosphorous removal. Another laboratory study (Prodanovic et al., 2017) examined different growing media for green walls. The study aim was to identify the underlying pollutant removal processes and to maximize the treatment capacity of the system. Experimental tests were performed in vertical columns filled with different porous media and without vegetation. The tested materials were selected on the basis of physical and chemical characteristics such as specific weight, water and nutrient retention capacity, porosity, capacity to distribute water and support plant growth, sustainability, and local availability. Among the hydraulically fast and slow media identified as suitable media, the analysis identified perlite and coconut coir as the two best performing media, suggesting their combined use as best option. Mixing two materials with different hydraulic behaviour allows, on one hand, to limit clogging issues, and, on the other hand, to increase the treatment efficiency, providing enough time for biological processes. A following study (Prodanovic et al., 2018) examined the removal performance of different mixes of coir and perlite in terms of TSS, TN, TP, COD and *E. coli*, providing a complete picture about the physical-chemical removal processes. It was observed that biological removal processes dominate nitrogen and COD removals, while physical-chemical processes dominate removal in fast media. Another example of full-scale application (VertECO-Vertical Ecosystem) was installed in a hotel in Lloret de Mar (Spain) by Gattringer et al. (2016). It consisted of an indoor living wall aimed to treat 1 m^3 of GW per day. An interesting outcome of the study deriving from the application of a Life Cycle Assessment was that the environmental impact of such systems could be improved by using alternative materials, such as plastics or wood, for the realization of the wall, and by employing sustainable energy sources, such as photovoltaic energy. The effluent water quality was also analysed in terms of micropollutants (endocrine disrupting compounds and pharmaceutical active compounds), obtaining generally high removal efficiencies apart from a few exceptions. Recently, the use of a mixture of recycled materials (date seeds and spent coffee grounds) was shown to perform similarly to the mixture of coco coir and perlite (Pradhan et al., 2020). Plant selection is also an important design aspect, even if their influence on treatment performance is still being debated. Some studies (Fowdar et al., 2017, 2018; Prodanovic et al., 2019a) found a strong dependency of nitrogen and phosphorus removal on plant species, probably due to the development of roots and the rate of growth of plants, indicating the importance of the correct choice of plants. An extensive study (Prodanovic et al., 2019a) with 13 plants based on a perlite/coconut coir mix (1:2 ratio) reported a slight variation among species in removal of TN, but a strong dependency on plant species in removal of TP. However, a recent study (Kotsia et al., 2020) tested ornamental plants usually used in green walls and found no significant difference in TP, BOD_5, or COD removal efficiency, although plants showed different levels of well-being under high-moisture conditions. An even more limited number of studies addressed the removal of biological pollutants of green walls in GW treatment (Boano et al., 2021a, 2021b; Prodanovic et al., 2020; Svete, 2012). A

different application was proposed by Eregno et al. (2017). The GW biofilter system was composed of a sequence of a primary settler, an unsaturated fixed-film biofilter, and a secondary clarifier, followed by an infiltration system (unvegetated filtration columns). The effluent from the filtration columns was then used for the hydroponic cultivation of lettuce in a green wall, with the addition of urine as a nutrient source for plant growth. The focus of the study concerned the reliability of using treated greywater to cultivate food crop and the consecutive possibility of consuming lettuce irrigated with treated GW without health risks through a quantitative microbial risk assessment. The quality of the effluent from the infiltration columns was satisfactory in terms of nutrient and bacteria removal.

Appendix A presents a synoptic table describing the main real scale and pilot green walls for GW treatment available in literature.

1.3.2 Knowledge gaps and objectives

The optimization of the removal processes in NBS involves the selection of appropriate plant species and substrates as growing materials, the assessment of optimal hydraulic parameters, and the definition of suitable operating conditions. While these issues have been widely addressed for constructed wetlands, much less information are available for green walls and green roofs. As examined in 1.3.1, some works started to discuss and analyse the selection criteria for defining the best combination of design parameters involved in the realization of vegetated GW treatment systems (Castellar da Cunha et al., 2018; Pradhan et al., 2019b). However, a fundamental issue that has not been fully clarified yet is the influence of operational factors on removal efficiencies. The most relevant issue that limits the application of these systems for GW treatment is the lack of sizing principles to predict the amount of GW that can be fed and efficiently treated by a specific system. The identification of optimal design parameters for green walls is essential to ensure high pollutant removal and an efficient use of space. Another important issue that will require further research efforts is how to ensure the durability of these systems. Problems that can mine durability of these NBS span from clogging of porous medium to structural ageing, and long-term studies will be necessary to understand these issues and avoid loss of treatment efficiency over time. Finally, as stressed by Pradhan et al. (2019a), difficulties related to social acceptance of treated GW reuse should not be dismissed.

This work aims to investigate GW treatment performances of a pot-based green wall under conditions that are more challenging compared to more controlled laboratory (Fowdar et al., 2017; Prodanovic et al., 2018; Svete, 2012) and pilot studies (Castellar da Cunha et al., 2018; Fowdar et al., 2018; Prodanovic et al., 2020, 2019a, 2019b), i.e., considering open-air conditions and a high hydraulic loading rate (HLR). After preliminary tests on plants and filter media, experiments were performed at pilot scale on an outdoor green wall designed with a modular outline, thus providing easy scaling-up possibilities. The system was fed with high flow rates of synthetic GW to minimize the required space, reaching a considerable HLR compared to those of common practices. Treatment performances were quantified for a wide array of physical-chemical and

biological parameters (e.g., suspended solids, organic substances, nutrients and *E. coli*). The effects of different additives mixed with a base filter medium (made of coconut fibre and perlite) was compared, easily modifying the base filter media properties with minimum impact on construction time and costs. Four carbon-based additives (compost, biochar, granular activated carbon, and polyacrylate) were tested in different combinations. Then, the dimensional design was evaluated, in terms of optimal number of treatment levels needed to achieve good treatment performances (i.e., to obtain water that can be reused for non-potable uses), to better understand how the treatment efficiency varies within the system instead of observing only its overall performances. The choice of a correct number of treatment levels (i.e., rows of pots in the green wall system) would impact on the investment costs and allow to better evaluate the necessary surface of the green wall depending on the flow rate and pollutants load of the inflow. The effect of system operational time was also assessed by comparing two vertical flow systems of different age, estimating for how long a green wall could be able to guarantee satisfactory treatment performances. The resilience of the system was also tested with HLR variations, simulating possible system failure or anomalous GW production.

1.4 Opening the black box

In NBS, the processes involved in pollutant removal are of physical, chemical and biological nature. The porous medium performs filtration and sorption, depending on its specific physical-chemical characteristics. Plant contribution is still under debate for small systems while for large scale systems it is recognised that plant roots provide indirect benefits (e.g. contrasting clogging and supporting biofilm growth) and, to a lesser extent, directly contribute to nutrient uptake. Degradation of organic compounds depends on biofilm development and conditions, as the bacterial community employ these compounds as source of organic matter and releases enzymes that decompose them.

The evaluation of treatment performances usually consists in a comparison between concentrations of inlet and outlet water samples. This method does not perturb the system and it is the most appropriate in real operating conditions. However, the improvement of treating NBS technology requires to better understand the specific contribution of the three main removing categories (i.e. filter media, plants and bacteria). To reach this goal, conventional samplings are performed, perturbing the system or even destroying it in case of mesocosm systems. In the first case, small samples (e.g. filter media or plants root portions) are collected; in the second case all the system is reduced in smaller portions. Both cases perform destructive analyses that give back precise information about the systems, in specific points (1D information with point samples) or mapping the volume of the system (3D data if sectioning the mesocosms). Unfortunately, these methods do not allow to see the evolution over time nor to analyse the system in normal operating conditions. In this context, the necessity to better understand removal mechanisms in CWs over time led to propose a new imaging method that is non-destructive, performable along time analysing the same mesocosm, and that provides 2D spatial information. This method, based on the imaging of fluorescent reactive tracers, has been proposed in the École Polytechnique de l'Université de Nantes by Dr. Vincent Gagnon and Dr. Florent

Chazarenc in 2014, conducting experiments and proving the proof of concept. The resulting dataset and the support of Dr. Gagnon allowed to further develop this method as a part of this thesis work. This new method measures the spatial and temporal distribution of enzymatic activity within a horizontal subsurface flow CW by using a transparent organic molecule, fluorescein diacetate (FDA), which releases a highly fluorescent molecule (fluorescein) when degraded by microbial enzymes. To measure this fluorescence in situ, transparent CWs containing glass sand were constructed and planted with a monoculture of macrophyte species. The photographic method relied on a box placed against one of the transparent sides of the CW, where the rhizosphere was illuminated with UV-A lights, exciting the fluorescein molecules which emitted a green fluorescent light that was captured by a digital camera. A sequential series of photos were taken and the resulting dataset was used in this thesis to improve the imaging method. Specifically, the method was automatized to enhance its application. An algorithm was developed to analyse the images to measure the change in the green fluorescent intensity with time. The intensity was then correlated with the spatial and temporal distribution of enzymatic activity in the CWs.

♦ Methods

The material in this chapter is partially derived from (Boano et al., 2021a, 2021b; Costamagna et al., 2022, submitted).

The design of a green wall system requires some main elements to choose: structure (e.g. ground based or wall based, continuous or modular), materials for filter media, plant species. Each part was evaluated and preliminary tests were performed on media and plants during 2018. After that, twelve modular panels were built and four campaigns were performed from December 2018 to December 2021, each with specific objectives (Table 2.1.0).

The first campaign started in December 2018 and lasted until March 2019. During this phase, the objective was to evaluate the effects of different filter media compositions on treatment performances. The mix of coconut fibre and perlite selected during the preliminary tests was used as main growing medium (BM). Four additives (compost, biochar, polyacrylate and granulate active carbon) were mixed with BM, in order to compare 8 configurations. The outcome of phase 1 led to the choice of configurations for phase 2.

The second campaign (phase 2) was performed between April and June 2019. This phase aimed to test high performing material (i.e. graphene) as further additive to evenly increase the best configuration arisen from the previous phase. Moreover, the possible influence of the start-up period was verified comparing an older and a newer set of the best configuration. Water samples were also collected along different levels of the green wall, to preliminarily evaluate the design geometry of the green wall itself.

The third campaign (phase 3) aimed to evaluate the durability of the system comparing two identical modules at two-year-distance as set up time difference. Water samples were regularly collected along different levels of the green wall to evaluate the contribution of each pot of the module, during three months from January 2021.

The fourth campaign (phase 4) was performed between April and December 2021, aiming to test system resilience to feeding volume variations, considered as stress tests. The green wall design slightly changed in drainage system and BM composition, due to critical issues arose during previous phases (e.g. clogging).

Table 2.1.0. Main objectives of the four sampling campaign.

Phase	Aim	Sampling period	No of sampling dates
1	- Evaluate treatment performance of different filter mix - Evaluate possible release from base medium configuration	Jan 2019 Mar 2019	9
2	- Evaluate the effect of graphene addition (removal and release) - Evaluate the impact of set up aging	May 2019 July 2019	8
3	- Evaluate the effect of system aging on performances - Better understand the distribution of treatment contribute along the system	Jan 2021 Mar 2021	10
4	- Evaluate system resilience to feeding volume variations	Apr 2021 Dec 2021	16

2.1 Greywater

The use of synthetic GW favours experimental reproducibility. To ensure the recipe consistency, it is necessary to confirm the availability of the specific products for the whole experimental campaign. Many recipes have been compared in literature (Abed and Scholz, 2016) but they can be divided in two groups: recipes that use only chemical products of technical quality (Hourlier et al., 2010) and recipes that mainly use commercial products in different mixes (Charchalac Ochoa et al., 2015; Chrispim and Nolasco, 2017; Rodriguez-Chueca et al., 2014). The studies on green walls that use synthetic greywater (Bakheet et al., 2020; Fowdar et al., 2017; Kotsia et al., 2020; Prodanovic et al., 2017) usually adapt the recipe by Diaper et al. (2008) to local availability of commercial products, as done in this study (Table 2.1.1).

Table 2.1.1. Synthetic light GW recipe modified by (Diaper et al., 2008).

Product	Brand	Quantity in 100 L
Bodycream (g)	Leocrema	1.50
Toothpaste (g)	Pasta del Capitano	3.25
Deodorant (g)	Sauber and Prep	1.00
Handsoap (g)	Dermomed	72.00
Laundry (g)	Soft	15.00
Na_2SO_4 (g)	analytical grade	3.50
$NaHCO_3$ (g)	analytical grade	2.50
Na_2PO_4 (g)	analytical grade	3.90
Clay (g)	bentonitic	5.00
Boric acid (g)	analytical grade	0.14
Lactic acid (g)	analytical grade	2.80
E. coli tablets	Ielab BAControl	instead of the prescribed secondary effluent

2.2 Filter media

Filter media used in green wall for greywater treatment must combine properties typical of green hanged structures (such as light weight and suitability for plants growth) with hydraulic characteristics that allow a good drainage but at the same time a hydraulic retention time (HRT) suitable for water treatment. Avoiding clogging but guaranteeing a

contact time between water and particle is fundamental for the main growing medium of a green wall. Furthermore, additives were used in the green wall to increase treatment performances, in proportions that did not drastically modify the physical characteristics of the main growing media.

A mix of coconut fibre and perlite was chosen as base filter medium (BM) accordingly to previous studies (Prodanovic et al., 2018, 2017). Coconut fibre (BioFiore®) is commonly used in green walls due to its physical properties (e.g. the organic composition favour plant growth) and the capacity of avoiding excessively fast drainage (Masi et al., 2016). Perlite is another material often used in green walls due to its very low density (less than water) that depends on the high number of close pores. The use of perlite in the base medium mix would help water drainage, contrasting clogging.

The additives that were chosen during this study (Table 2.2.1) have different specific properties and advantages. Compost is obtained from a six-month dynamic composting of waste and provides high nutrient component. Biochar is a material obtained by pyrolysis of wooden chips. These two low cost materials are usually used as soil amendants from recycled materials, providing multiple environmental benefits (Kotsiris et al., 2013; Moges et al., 2015). Granular active carbon has high adsorption capacity (Thompson et al., 2020); polyacrylate (i.e. hydrogel) is a polymer with high water retention capacity and very low dry weight and volume, thus its transportation costs and installation could be competitive in hard accessible areas (Deska et al., 2020). Both granular active carbon and polyacrylate would increase the contact time between biofilm and greywater. Paragraph 2.4.1 provides more details on the use of all the media in the tested configurations.

Table 2.2.1. Media for filter mix. The abbreviations are used hereafter to identify both the configuration with the specific medium (when "configuration" or "mix" is used) and the medium itself.

Medium	**Abbreviation used also for filter media configuration mix**	**Provider**
Coconut fibre	CF	Centro Evergreen
Perlite	PL	Centro Evergreen
Polyacrylate	PA	New PolyPlants, Italy
Biochar	BC	Agrinewtech, Italy
Compost	CO	Agrinewtech, Italy
Granular active carbon	GAC	SHG, Italy
Graphene	GR	Directa Plus S.p.A.

2.2.1 Base medium mix tests

The suitable ratio of CF and PL were identified with preliminary tests at microcosm scale, analysing physical and hydraulic properties for different mixes, as proposed in (Prodanovic et al., 2017). Triplicate tests were performed on plexiglass columns (Ø = 6 cm; height = 50 cm; mix height = 30 cm) to evaluate the hydraulic behaviour of the different mixtures without plants. For all five mixes (volume percentages of CF: 60%, 70%, 80%, 90% and 100%) porosity, particle density and bulk density were measured, weighting each column before and after saturation with water. The saturated hydraulic conductivity (K_s) was evaluated using Darcy's falling head method.

Before phase 4, a mix with CF 50% was tested in five replicates in a constant head permeameter (Figure 2.2.1). Each column was 30 cm high filled with around 25 cm of testing media mix, with a 5 cm diameter. Hydraulic head was around 1 m and imposed pressure was 0.1 bar. 10 tests were performed in each column at 2-hour distance. In that interval of time tap water flew through the columns in order to simulate the washing procedure to be performed on the green wall panels.

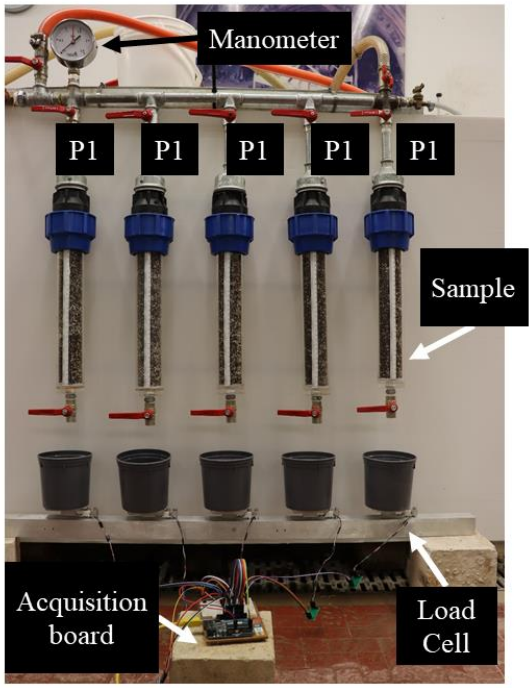

Figure 2.2.1. Constant head permeameters with automatic data collection.

2.3 Plant selection

The multi-functionality of the green walls structure requires the use of living plants, excluding the opportunity of using plastic plants or unplanted configurations. The plants commonly used in NBS treatment plants hardly fit in vertical systems, due to space requirements. Thus, a literature review (Cameron et al., 2014; Castellar da Cunha et al., 2018; Fowdar et al., 2017; Pérez et al., 2011; Rysulova et al., 2017; Serra et al., 2017) was necessary to identify some species suitable for green walls. The specific characteristics that drove the choice were related to adaptation to continental climate conditions and to all seasons of the year, high tolerance to soil moisture, limited space for roots growth, small plant size, aesthetical appearance, possibly evergreen and locally available.

Five plant species (*Hedera helix*, *Carex morrowii*, *Iris germanica*, *Lonicera nitida*, and *Ranunculus asiaticus*) were tested for GW and soil moisture tolerance in two campaigns, from March 20th to June, 28th 2018 (test 1) and from July, 16th 2018 to March, 4th 2019 (test 2).

During test 1, one group with three plants per species were fed with synthetic GW (cfr. 2.1) 3−12 mm d^{-1} per pot, fed 5 days per week, while a control group received the same amount of tap water. Plants growth was visually evaluated for all species, in order to see the impact of the different types of feeding water. The length of *Hedera* leaves and *Lonicera* branches were measured (three per plant) to numerically evaluate if there was any difference in the growing rate.

After a first selection, the three more resistant species (*Carex*, *Hedera*, *Lonicera*) were chosen for the green wall modules and a parallel test was also performed on two new groups. Test 2 aimed to evaluate the effects of more aggressive chemical compounds added to the GW recipe: cleaning product (*Smac*^{TM} 200 mL in 20 L) and different type of hair dye (20 mL in 20 L) were added twice per week. The second group was fed with tap water as control. The length of *Hedera* leaves and *Lonicera* branches were measured (five per plant) to numerically evaluate if there was any difference in the growing rate.

Plant well-being was also evaluated on the green wall modules by visual inspection. Furthermore, in January 2019, a Chlorophyll concentration meter MC-100 (Apogee Instruments) was weekly used for 11 weeks to collect data from each *Hedera* plant (five leaves, three point per leaf) to evaluate the impact of different growing media mix on plants growth. This parameter allows a non-destructive measurement and it is easy to use but not quantitatively precise, as multiple measurements in the same date showed considerable variability. Thus, this measure was not prolonged in all experimental phases, due to the uncertainty of results interpretation.

2.4 Green wall modules

Some design parameters remained constant in all experimental phases, while others were changed. In this section the complete set up will be presented starting from the first phase and highlighting the changes in each following phase.

2.4.1 Phase 1

The experimental real scale set up was located in the Hydraulics Laboratory courtyard at Politecnico di Torino, on the north-east facing wall. It is an open air modular green wall, built with six modular units (1 m^2) with 12 pots (0.18 × 0.18 × 0.22 m, 6.5 L bulk volume) each. Triplicate tests were made for each mixture using three identical columns, each one composed of three pots filled with a 0.2 m layer of the same mixture, and different ornamental plant species (from top to bottom in Figure 2.4.1: *Carex morrowii*, *Hedera helix*, *Lonicera nitida*). The use of different plant species reduces the risk of phytodiseases, increase biodiversity and favours aesthetical appearance (Castellar da Cunha et al., 2018).



Figure 2.4.1. Green wall modular panel.

Eight configurations were set up, combining the base medium mix (BM, 80% coconut fibre and 20% perlite in volume) with four additives that are not conventionally used in green walls (compost, biochar, granular active carbon, polyacrylate), in order to increase removal capacity. One BM configuration was fed with tap water (named hereafter with BM*) in order to identify background values for the different compounds, comparing the results with a BM configuration fed with GW. Three configurations were prepared mixing 80% BM and 20% CO, BC, or PA (also named 20CO, 20BC, and 20PA), one configuration was made of 90% BM and 10% GAC (10GAC; a lower additive volume was chosen due to its strong sorption potential). One configuration combined the effects of multiple additives using 60% BM with 20% BC and 20% PA (20BC20PA) and an older mixture of 80% BM and 20% PA (20 PA+) was also tested (it was set up four months before the other and employed for preliminary design). Table 2.4.1 summarizes the tested configuration tested during this phase.

Table 2.4.1. Configuration tested during the first phase. Percentage in volume for the different additives.

Configuration ID	Coconut fibre	Perlite	Additive	Set up
BM* (fed with tap water)	80%	20%		Dec 2018
BM	80%	20%		Dec 2018
CO	64%	16%	Compost 20%	Dec 2018
BC	64%	16%	Biochar 20%	Dec 2018
PA	64%	16%	Polyacrylate 20%	Dec 2018
GAC	72%	18%	Granular active carbon 10%	Dec 2018
BCPA	48%	12%	Biochar 20% Polyacrylate 20%	Dec 2018
PA+ (previously set up)	64%	16%	Polyacrylate 20%	Sept 2018

The green wall was fed with a volume of 96 Ld^{-1} per panel, aiming to reproduce the mean daily GW production per capita in high income countries (Boano et al., 2020; Ghaitidak and Yadav, 2013), thus the design rationale is one square meter per person. This amount lead to a hydraulic loading rate (HLR) of 740.8 $Lm^{-2}d^{-1}$, that falls at the highest range of usual HLR in vertical CWs and green walls for water treatment (Boano et al., 2020; Castellar da Cunha et al., 2018; Dotro et al., 2017). This feeding volume allows to neglect the contribution of daily precipitations (0-30.8 $Lm^{-2}d^{-1}$ during the sampling period). Each column works independently as a vertical flow system in which water flows to the bottom pot by gravity through 4-mm plastic tubes located in the middle of vases base. GW was provided in a pressurised distributing system of plastic pipes, flowing through drippers at 4 Lh^{-1} flow rate. A separate piping system with the same structure was used to provide tap water to BM* directly from the water supply network. Each column was independently fed by batches every hour, providing 1 L flush in 15 minutes, followed by a 45-minute rest, in order to favour aerobic degradation (Dotro et al., 2017). The final outflow was collected in 10 L tanks (one per panel) and then discharged in the sewer system. GW was prepared every 2 days and stored in a 1.5 m^3 HDPE tank, hourly mixed by a recirculating system following the feeding schedule.

Water samples were collected between January 8th and April 2nd, 2019, scheduling a weekly sampling in the first two months, as reported in literature (Kotsia et al., 2020; Masi et al., 2016; Ramprasad et al., 2017) aiming to detect the possible start-up period, and twice per months in the last period. Nine sampling date led to analyse a total of 234 water samples (216 output and 18 input water). Input GW and TW were analysed as discussed in section 2.5 to correctly evaluate water treatment.

2.4.2 Phase 2

Four configurations (nine pots each) were compared during this experimental phase, mixing coconut fibre, perlite, biochar and graphene in different proportions (Table 2.4.2). The configuration BCGR* received tap water to verify release from the filter medium, while the other configurations continued to receive 24 $Ld^{-1}col^{-1}$ of synthetic GW, as in phase 1. Drainage connections between different levels were changed: the small central tube at the bottom of each pot was replaced with a spiral of metal wire that supported water spreading on the lower pot. Water output at the bottom level was still collected into the 10-litre-tank through the 4-mm-tubes.

Table 2.4.2. Configuration tested during the second phase. Percentage in volume for the different additives.

Configuration ID	Coconut fibre	Perlite	Biochar	Graphene	Set up
BC_old	64.0 %	16.0 %	20.0 %	-	Jan 2019
BC	64.0 %	16.0 %	20.0 %	-	Apr 2019
BCGR	60.8 %	15.2 %	19.0 %	5.0 %	Apr 2019
BCGR*	60.8 %	15.2 %	19.0 %	5.0 %	Apr 2019

Eight samplings were planned once per week from May 2019 to July 2019, collecting output water from each column and from the input GW. The output water from the first

and second level of treatment was also collected in three sampling dates. Thus, 140 water samples were analysed in the whole period.

2.4.3 Phase 3

Two modules are the focus of this phase, aiming to evaluate the durability of the system: P2 was the BM configuration set up for phase 1 and a newer configuration (P1) with the same BM composition (80% coconut fibre and 20% perlite) was set up in December 2020. The water freely flowed from one pot to the lower one through unique central hole without any tube or metal wire, to enhance drainage and facilitate sampling operations. During the sampling period, air temperatures in the courtyard ranged between 0.4 and 20.3 °C; the cumulative precipitation was 106 Lm^{-2}, again considered negligible compared with the hydraulic loading rate (HLR) of the system (740.8 $Lm^{-2}d^{-1}$).

Water outflow was weekly sampled from mid-January 2021 to the end of March 2021, with 10 sampling dates in total. The outflow from each pot (18 samples plus input GW for each date, 190 samples in total) was collected and analysed to evaluate the contribution of the different level of treatment.

2.4.4 Phase 4

This phase compares two modules fed with different flow rate schedules, aiming to simulate the variability of GW quantity production. This scenario could arise from possible seasonal or weekly variations in building use or due to malfunctioning of the distribution system. The pots design was slightly different from the previous one: the new ones were 3 cm higher, they were filled with a different mix of coconut fibre and perlite (1:1 in volume) to guarantee a better drainage and the water flew vertically from 16 holes (1 cm diameter protected with a metallic net) at the bottom of each pot and 8 rectangular holes promote oxygenation of the system. The control panel was regularly fed with a standard flow rate of synthetic GW (24 $Ld^{-1}col^{-1}$), the other was fed with different flow rates (schedule in Table 2.4.3), and output water samples were weekly collected from each pot from June to December 2021 (304 analysed samples in total). The contribution of evapotranspiration and precipitation (127 mm cumulate during the most raining month) was neglected due to the very high HLR provided to the system.

Table 2.4.3. Flow rate of variable panel. Feeding is set once per hour per 24 hours a day, all week. Values of underflow and overflow are inspired by Osterreichisches Normungsinstitut (2005).

Phase	Flow rate ($Lcol^{-1}d^{-1}$)	HLR ($Lm^{-2}d^{-1}$)	Weeks	Nr. of samples
Standard	24.0	741	5	2
Underload (-50%)	12.8	395	3	3
Standard	24.0	741	3	3
Summer maintenance	0.5	15	9	-
Standard	24.0	741	2	2
Overload (+50%)	36.8	1136	3	3
Standard	24.0	741	3	3

2.4.5 Washing procedure

Washing procedure was tested on BM* columns before phase 1. It consisted in a preliminary irrigation with tap water, to remove the finest particles that could clog the system and to verify the possible release of compounds from the main filter media. The three columns were irrigated continuously with 4 Lh^{-1} for two plus one days, reaching 122 L in total per column. Water samples were collected at the outlet (schedule in Table 2.4.4) and different physical-chemical parameters were measured (temperature, pH, EC, TDS, TSS, sulphate, TKN, ammonium, nitrate, chloride, TP, COD, BOD_5) in order to understand the water volume to be used in start-up washing procedure. A two-week stop was done, to evaluate the stabilisation of the measured parameters. The column washing was then performed on all system configurations (without sampling) to remove the finest particles and favour plant and biofilm establishment.

Table 2.4.4. Water procedure sampling schedule for BM* in phase 1.

Sampling	Date	Mix	Cumulate water volume (L)	Cumulate irrigation time (h)
I	15/10/2018	BM	4	1.0
II	15/10/2018	BM	14	3.5
III	15/10/2018	BM	26	6.5
IV	15/10/2018	BM	80	20.0
V	16/10/2018	BM	82	20.5
VI	05/11/2018	BM	82	20.5
VII	05/11/2018	BM	100	25.5
VIII	05/11/2018	BM	120	30.5

All columns set up in April 2019 (phase 2) were washed with tap water (85 $Lcol^{-1}$) in about 15-minute-batch mode during 82 consecutive hours, in order to remove the finest particles and prevent clogging events.

Before phase 3 starting, the newest panel (P1) was washed with a total of 160 $Lcol^{-1}$ of tap water for 4 non-consecutive days (10th, 14th, 16th and 18th December, 2020), divided in 40 L $d^{-1}col^{-1}$ with a continuous irrigation to remove the finest particles and the possible dissolved compounds released from the base medium. The outflow was hourly collected and temperature (T), pH and electrical conductivity (EC) were analysed. After the washing, a setup phase followed to stabilize the system, providing 12 $Ld^{-1}col^{-1}$ of GW to both panels in the period 12/22/2020 – 01/07/2021, when the system became fully operational with the design HLR.

Before phase 4 all columns were washed with 127 L $d^{-1}col^{-1}$ but no samplings were collected.

2.4.6 Samples analysis

Physical-chemical and biological parameters were measured on site and in the Circular Economy Lab facilities at Politecnico di Torino. During the third and fourth phases I personally performed these analyses after collecting the samples.

Dissolved oxygen (DO), pH, temperature (T), and electrical conductivity (EC) were measured using a WTW Multi 3320 portable two-channel probe, with specific sensors and electrodes. Total suspended solids (TSS) were analysed by filtering the water samples

through 0.45 μm cellulose membranes. Sulfate (SO_4^{2-}), chloride (Cl^-), total Kjeldhal nitrogen (TKN), total nitrogen (TN), nitric nitrogen (NO_3^--N), ammonia nitrogen (NH_4^+-N), total phosphorus (TP), chemical oxygen demand (COD), and methylene blue active substances (MBAS, i.e., anionic surfactants) were analysed with Nanocolor™ reagent kits, a VELP COD ECO 16 thermoreactor (for TN, TP, and COD), and a model AL450 Multidirect photometer. BOD_5 was measured through a VELP FOC 215E cooled incubator equipped with 24 BOD sensor systems. *E. coli* was analysed through Colitag™ water test reagents after 24 h according to EPA Standard Method 9221 in phase 1 and 2, while Colilert-18 IDEXX was used with Quanti-Tray/2000 during phase 4, in compliance with ISO 11133:20004.

Some parameters were not measured in all phases, as will be evident in the result section. For example, TKN was measured in phases 1 and 2, TN in phases 3 and 4, due to different kits used; *E. coli* was not analysed in phases 3 and 4 due to logistic issues; SO_4^{2-} was not measured after phase 2 due to low impact of this parameter in system efficiency evaluation. Values of concentration below the detection limit were set equal to the limit itself to allow calculation of the removal efficiency (see paragraph 2.4.7).

2.4.7 Data analysis and statistical tests

The output concentration from each configuration was evaluated as average value and standard deviation from the three replicates of the configuration itself. Then, removal efficiency was calculated for each configuration with the average output concentration (C_{out}) of the configuration itself, using the following equation: $Rem_{eff} = \frac{C_{GW} - \overline{C_{out}}}{C_{GW}}$.

Two statistical tests were used to identify possible temporal trends and evaluate if differences in treatment performances were significant. A two-tailed non-parametric Mann−Kendall test was performed on time series (each configuration was treated separately) to verify the presence of significant monotonic trends over time. The test was performed on the observed time series for the on-site parameters measured (T, pH, EC, DO), while removal efficiency was used for the other parameters.

Then, aiming to compare the performance of each configuration with the reference one (that depend on the experimental phase) differences between values of removal efficiency of each mixture and those of the reference mix were calculated for each sampling date; a one-tailed Student's *t*-test was performed to verify if the mean value of the differences was significantly higher than zero. For the considered parameters, positive test results on the removal efficiencies indicated that the tested filter mixture was significantly more effective ($p < 0.05$) than the reference mix. The test was also applied to identify differences in temperature, pH, EC, and DO between GW and outflow samples. Finally, since multiple comparisons were performed, a false discovery rate procedure (Benjamini and Hochberg, 1995) was applied on all test results to correct *p*-values and avoid the inflation of Type-I error.

♦ Results

The results presented in this section are extracted from (Boano et al., 2021a, 2021b; Costamagna et al., 2022, 2021) or under peer review (Costamagna et al., n.d.).

3.1 Greywater

GW composition was the same in all experimental phases, but some differences were observed during input GW sample (Figure 3.1.1), probably due to the time interval between tank filling and sampling date, that was constant only within the same phase.

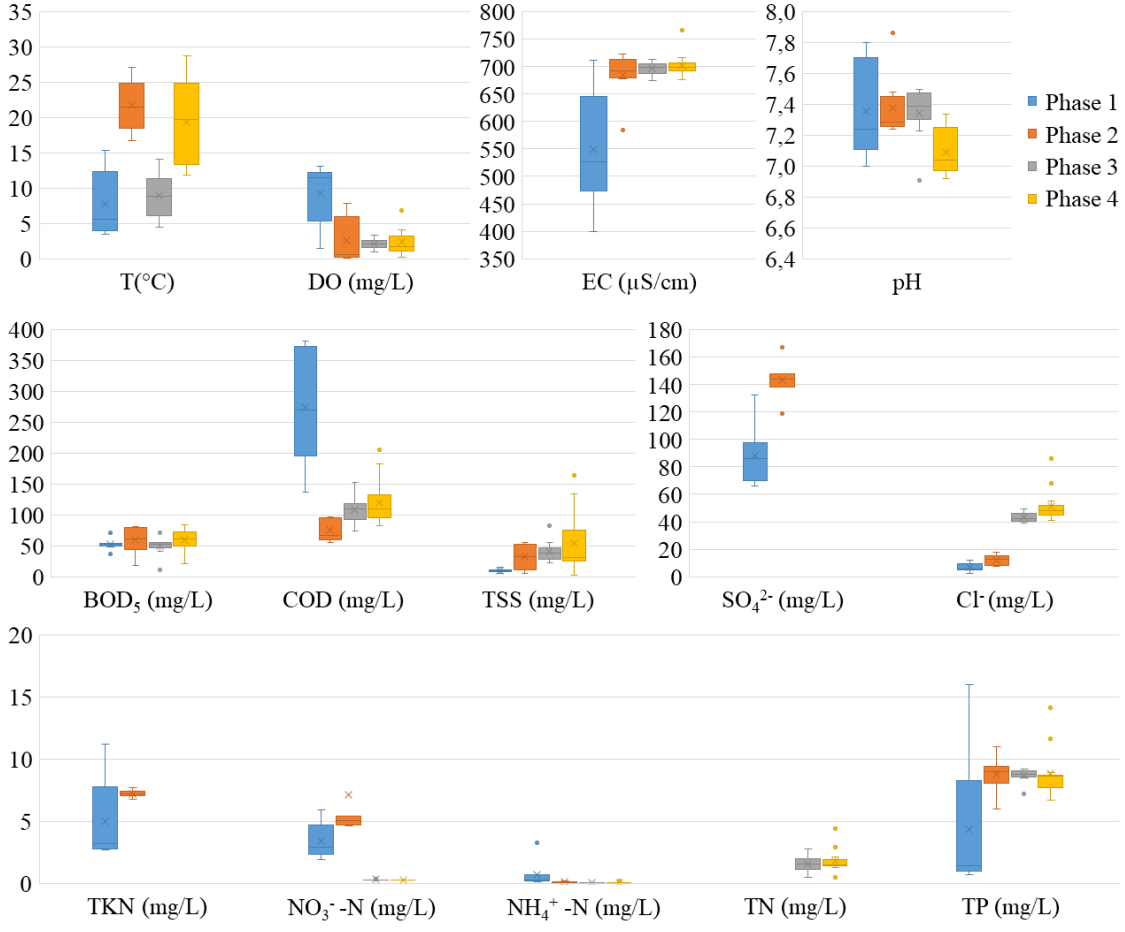

Figure 3.1.1. Boxplot of time series values for input GW in the four sampling campaigns. Median value (cross), 25th and 75th percentiles (box), range (whiskers) and outliers (dots) are shown.

The parameters that showed more variability between phases were DO, COD and TP, while the parameters that showed high variability within phase 1 were EC, pH, COD, TKN and TP. On the other hand, phases 2, 3 and 4 showed low variability in all parameters. MBAS revealed a different order of magnitude in phases 1 and 2 (average and standard deviation over time, phase 1: 3645±521 mg/L, phase 2: 790±650 mg/L) compared to phases 3 and 4 (phase 3: 11±6 mg/L, phase 4: 24±8 mg/L), but with a small standard deviation within the phases themselves.

3.2 Preliminary tests on filter media

Table 3.2.1 shows the physical Characteristics of Coconut Fibre (CF) and Perlite (PL) in terms of porosity and density. The particle density of CF is almost 3 times higher than that of PL, and the bulk density is more than double. Perlite is less dense than water; thus, it floats. CF adsorbs water and reaches a particle density around that of water (0.997 g/cm3).

Table 3.2.1. Physical characteristics of media in the base mix. Values are average and standard deviation (in parentheses) from three replicates.

Medium	Porosity	Particle density (g/cm^3)	Bulk density (g/cm^3)
Coconut fibre	0.652 (0.009)	1.023 (0.046)	0.355 (0.006)
Perlite	0.583 (0.013)	0.362 (0.103)	0.150 (0.013)

Figure 3.2.1 shows the comparison among different CF:PL mixes in terms of hydraulic conductivity (K_s) and bulk density (ρ_b). As expected, K_s strongly increased with PL content, because CF are hydraulically slower than PL. (Prodanovic et al., 2017) The average value of K_s varied between 0.066 ± 0.016 cm/s for pure CF and 0.217 ± 0.060 cm/s for the 60% CF/40% PL mix, showing a strong linear correlation between K_s and PL content (R2 = 0.998). The average ρ_b decreased with PL content (R2 = 0.577), varying between 0.415 ± 0.01 (pure CF) and 0.320 ± 0.01 (60% CF/ 40 % PL mix). The slopes of the trend lines in Figure 3.2.1 indicates that the hydraulic conductivity was more sensitive to PL content than ρ_b. While an increase in PL content is positive in terms of reducing the weight of the filter medium, the increase in K_s may not provide adequate contact time for the removal of contaminants. On the basis of the results presented here, the 80% CF:20% PL mix was chosen for the experiments as it allowed us to reduce ρ_b while matching the typical values of K_s of porous media employed in constructed wetlands with good removal performances (Dotro et al., 2017). This choice was regarded as a good compromise between weight (0.337 ± 0.02 g/cm^3) and hydraulic conductivity (0.146 ± 0.013 cm/s).

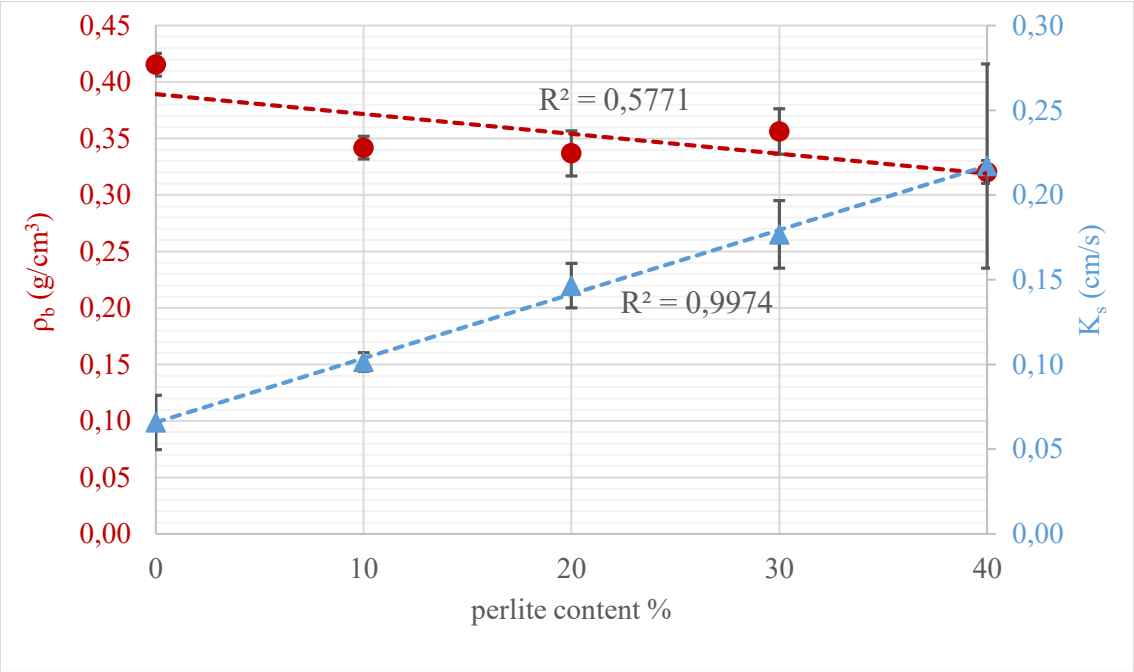

Figure 3.2.1. Average values and standard deviations of hydraulic conductivity K_s (blue triangles) and bulk density ρ_b (red circles) for mixes with different percentages of coconut fibre and perlite.

Before phase 4, the base medium mix was reconsidered, based on the experience developed during the previous campaigns on the green walls modules. Figure 3.2.2 reports the granulometry in dry and wet conditions of the mix 50% CF and 50% PL, in which the most of the grains fall between 0.5 mm and 2 mm in both cases.

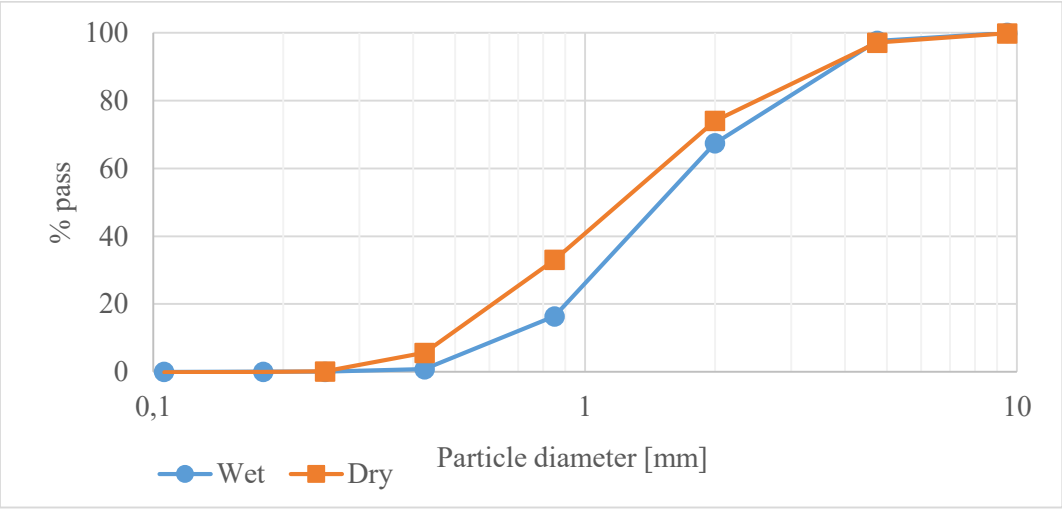

Figure 3.2.2. Granulometric curve of the mix CF:PL 1:1 in wet and dry (120° for 2h) conditions.

The permeameter tests for this new mix highlighted a strong decreasing in K_s during the washing with tap water up to 30 L, while the following decreasing was more moderate (between $7.55e^{-2}$ and $4.70e^{-2}$ m/s) as shown in Figure 3.2.3.

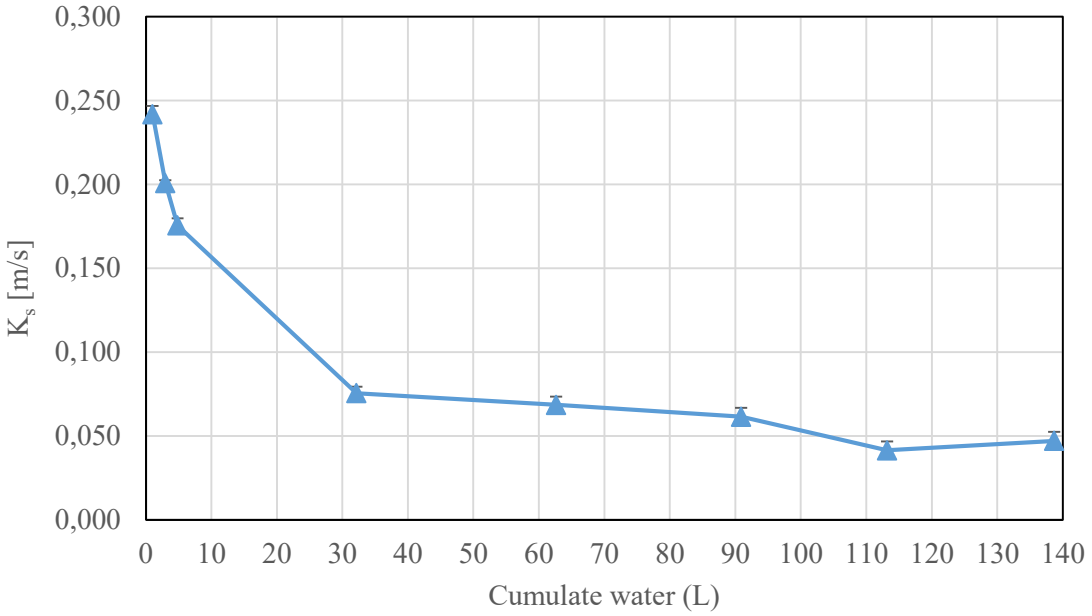

Figure 3.2.3. Hydraulic conductivity of 1:1 CF:PL mix during columns washing. Values are average and standard deviation of five replicates.

3.3 Preliminary tests on plants

Among the tested plant species, *Ranunculus* and *Iris* were discarded due to their intolerance to moisture since the first test on plants. *Lonicera*, *Carex* and *Hedera* did not show any problem with GW compounds nor high soil moisture, thus they were selected for the green wall design and for test 2 on plants resistance to more the aggressive GW formulation. Qualitative observations on these three species showed no particular differences in plant conditions and growth in both test phases (Figure 3.3.1).



Figure 3.3.1. Tested plant species after one month: (a) *L. nitida*, (b) *I. germanica*, (c) *C. morrowii*, (d) *R. asiaticus*, and (e) *H. helix*. Red (solid) and blue (dashed) lines indicate the greywater (GW) and tap water (TW) groups, respectively.

The numerical evaluation of plant wellness (i.e. observing the grow rate by measuring leaves and branches growth) cannot be considered totally trustable due to practical uncertainty noticed after data collection, thus numerical data will not be shown.

During phase 1, plants well-being was visually evaluated and chlorophyll content was measured for *Hederas*. Unfortunately, this parameter cannot be used to directly compare plants conditions numerically, but no regular pattern was observed in any configuration comparing the average chlorophyll variation rate (Figure 3.3.2). However, is important to qualitatively observe that the plants in compost mix suffered many situations of excessive moisture due to frequent clogging events, thus is possible that this has impact on the aesthetical appearance of plant and on their growth.

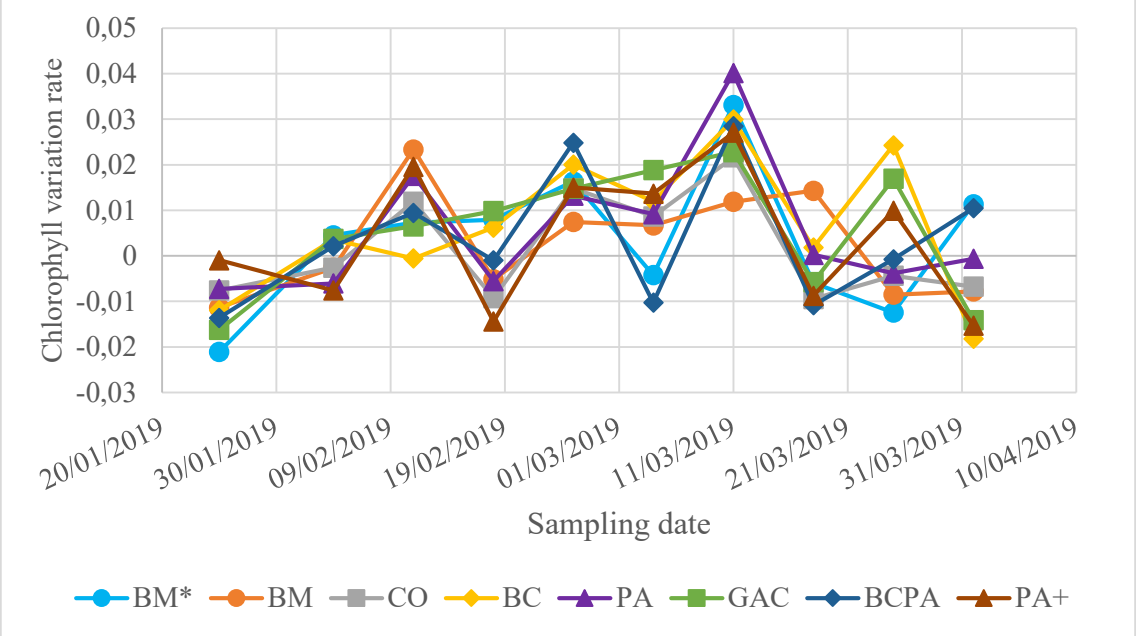

Figure 3.3.2. Chlorophyll variation rate normalised on the value of first measurement. Values shown are calculated from average of plants from the same configuration (five leaves per plant, three point per leaf).

3.4 Treatment performances

3.4.1 Washing procedure

The first washing procedure was performed in two steps (80 $Lcol^{-1}$+38 $Lcol^{-1}$ of tap water) before phase 1, to evaluate possible release of substances from the filter medium (80% CF and 20% PL). Qualitative observation showed improvements in water aspect (Figure 3.4.1) and physical-chemical parameter confirmed this properties changes. In fact, pH remained around neutrality (6.97±0.37) with a slight alkalinisation trend (Figure 3.4.2-a). EC strongly decreased along time and rapidly became uniform within the three replicates Figure 3.4.2-a. The release of NO_3^--N, SO_4^{2-} and Cl^- decreased along time (Figure 3.4.2-b). Cl^- passed from 92.93±44.35 mg/L to 6.57±0.95 mg/L, while NO_3^--N showed the same trend with smaller concentrations (from 30.63±1.52 mg/L to 2.76±0.71 mg/L). The filter medium released a higher concentration of SO_4^{2-} (103.92±22.96 mg/L) with a smoother

decrease and an initial rebound on the second washing day. Standard deviation among samples usually decreased over time for all the three solutes.

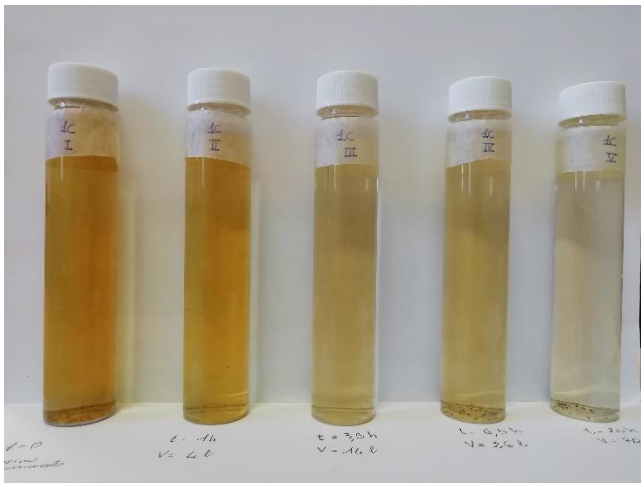

Figure 3.4.1. Qualitative evaluation on water colour in samples I to V during washing procedure.

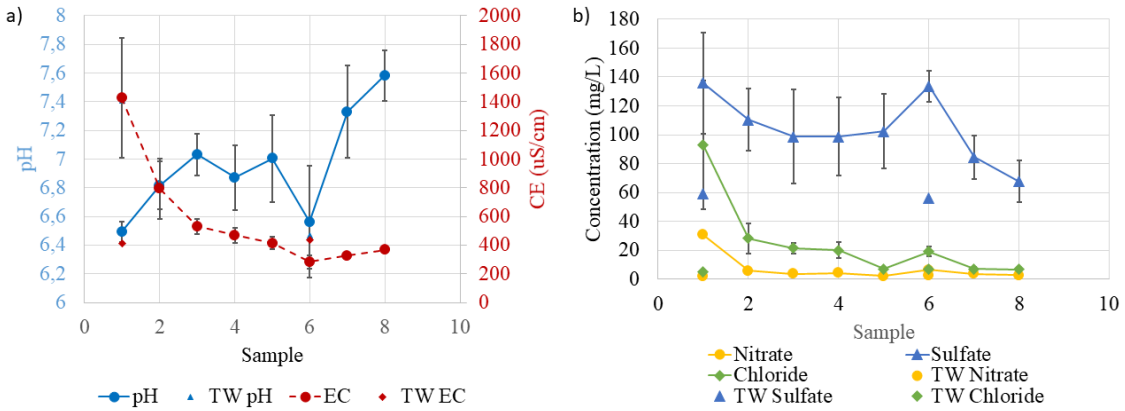

Figure 3.4.2. Compounds that were significantly released from the columns during the preliminary washing procedure with tap water: a) pH, Electrical Conductivity; b) NO_3^--N, SO_4^{2-}, Cl^-.

The other tested parameters did not show significant concentration values and in many cases were below the detection limits. The effectiveness of the preliminary washing procedure is demonstrated by the fact that all parameters eventually attained a concentration that was similar to the concentration in clean TW (with the exception of pH, which is expected to reach an equilibrium with the growing medium). Before phases 1 and 2, all columns were washed with 120 L but no samples were collected.

Before phase 3 a similar washing procedure was performed on the new configuration columns (Panel 1-P1, see paragraph 2.4.5). The outflows from each column of P1 were collected and on-site parameters such as temperature, pH and EC were measured. Temperature was strongly influenced by winter conditions. Since the washing procedure was performed in December 2020, temperature decreased as water flowed through the panel, reaching values between 5 and 14°C (compared to 12-16 °C measured in input tap water). The range of pH in input tap water was between 6.7-7.2 and it increased up to 7.6 after 80 L of washing (Figure 3.4.3), after which it remained stable and slightly higher

than previous results. EC quickly stabilized around 490-500 µS/cm after only 40 L of washing (Figure 3.4.3) and remained stable, even if during the first 20 L a high increase was observed (from 500 µS/cm in input to 2100 µS/cm in output), possibly due to the release of dissolved substances from the base medium.

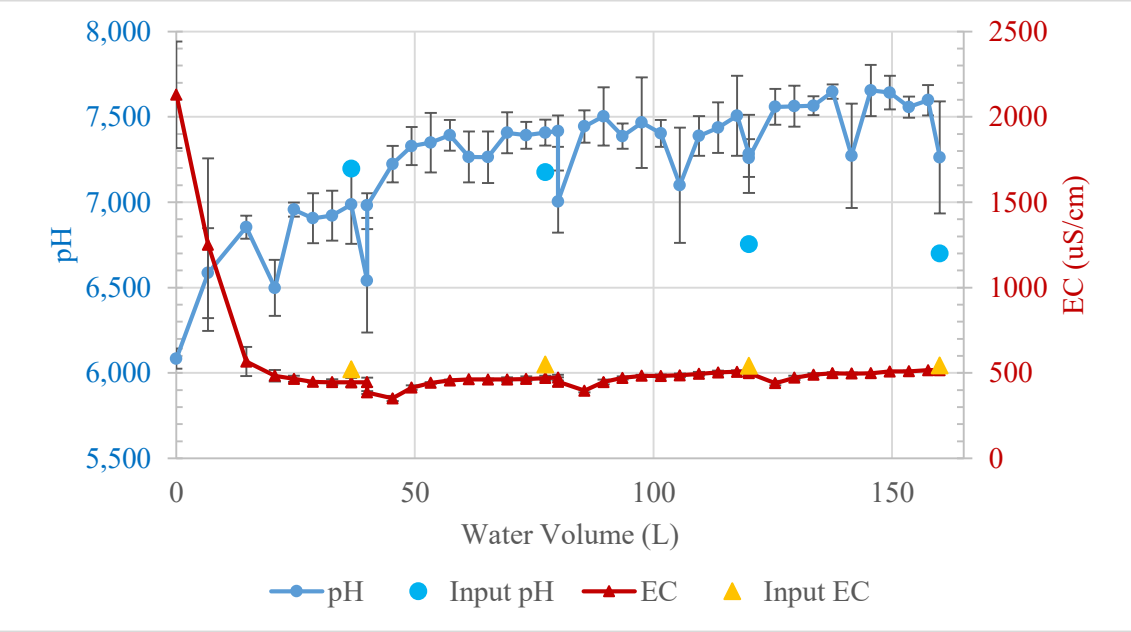

Figure 3.4.3. Average and standard deviation of pH and Electric Conductivity (EC) measured in the outflows of panels P1 and input tap water values during the washing procedure.

3.4.2 Phase 1

Release of compounds from base medium

This results compared the two configurations with base medium (80:20 coconut fibre-perlite), one (BM*) fed with tap water (TW) and the other (BM) fed with synthetic greywater (GW). The aim of this comparison is to test the possible release of compounds from the base medium itself.

Figure 3.4.4-a shows average temperature values of TW and GW at the inlet and outlet of the green wall. The recorded temperature range (3.5–15.3 °C, 7.7 ± 4.6◦C on average for GW) is comparable with winter experiments in greenhouses (minimum value of 4°C) and obviously lower than summer temperatures (maximum values of 44 °C and 45 °C) (Dal Ferro et al., 2021; Fowdar et al., 2017; Prodanovic et al., 2019b). Inlet average pH values (Figure 3.4.4-b) were neutral for TW (7.01+0.30) and slightly alkaline for GW (7.35± 0.31); the outlet pH was 7.24 ± 0.09 for BM* and 7.40 ± 0.04 for BM, both values within the recommended range of 6−7.5 for plant growth (Prodanovic et al., 2020) and within the optimal range of 6.5−8.5 for nitrogen removal (Yin et al., 2016). EC showed the same increase trend from inlet to outlet (Figure 3.4.4-c), even if inlet and outlet values were similar in the last samples for both TW and GW. DO values (Figure 3.4.4-d) were similar for BM* and BM due to the aerobic conditions of vertical flow systems that resulted in oxygen concentrations close to saturation (10−13 mg/L for the observed temperatures) and promoted aerobic reactions in the columns. Inlet GW showed a strong

DO decrease over time from 11.7 to 1.5 mg/L, due to an increase in the outdoor temperature, possibly because of aerobic reactions occurring in the storage tank.

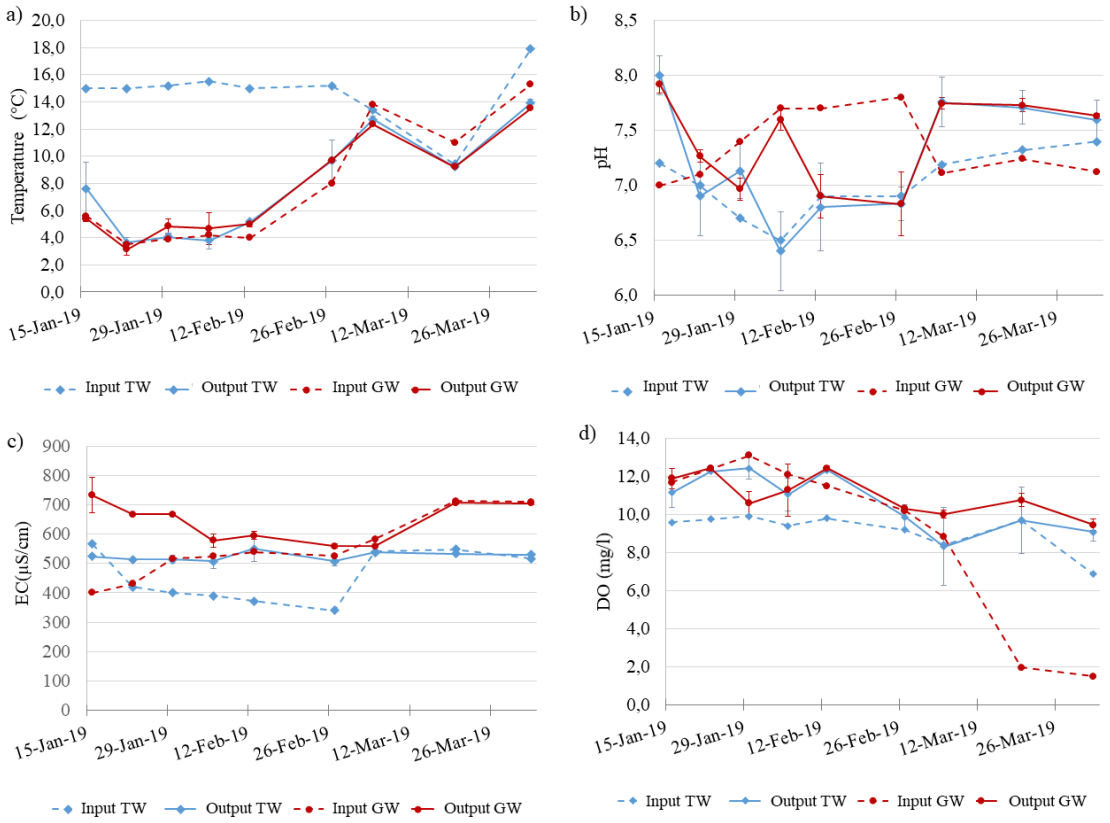

Figure 3.4.4. a) Temperature, b) pH, c) Electric Conductivity (EC), and d) Dissolved Oxygen (DO) at the inlet and outlet of TW and GW columns.

Average TSS concentration in inlet GW (9.63 ± 2.94 mg/L) was lower than usual values for synthetic GW (50–100 mg/L) (Fowdar et al., 2017; Hourlier et al., 2010; Pradhan et al., 2020), probably due to settling in the GW storage tank before the feeding system (Abed et al., 2020), but still in the range observed for real GW (e.g., 5–252 mg/L; in Prodanovic et al., 2020). The average outlet TSS concentration from GW columns (9.37±0.96 mg/ L) was in line with common outflow values from vertical constructed wetlands with similar TSS loads (6−60 mg/L) (Kadlec and Wallace, 2009), suggesting that lower outflow concentrations cannot be attained for this TSS load.

Figure 3.4.5-a shows average COD concentrations at the inlets and outlets of the green wall columns along the sampling period. Despite the prewashing, the filter medium released an average of 47.63 mg of COD/h, as shown by the comparison between inlet (67.67±29.9 mg/L) and outlet (122.00±4.93 mg/L) concentrations of BM* samples. In contrast, COD was always removed in GW-fed columns with removal rates in the range of 12.33−184.00 mg/h. The removal efficiency significantly increased over time from 4.7% to 82.3%, possibly due to a decreasing rate of release from the filter medium, an increase in temperature, and/or progressive biofilm growth (Masi et al., 2016; Prodanovic et al., 2017). This trend agrees with the literature findings where after an establishing phase COD removal performances increased up to 86% (Masi et al., 2016). On average,

this study found 40.4±25.0% COD removal efficiency in GW columns (102.67 mg/h average removal rate), similar to the range of 46.0−49.3% in (Jin et al., 2018) but lower than the values of 92.4% in (Prodanovic et al., 2020), in which sampling started after 16 weeks, and 95% in (Gattringer et al., 2016). These results indicate a good efficiency for the removal of COD from BM, within the range observed in laboratory studies of green walls. As opposed to COD, the BOD_5 average removal efficiency (97.7±1.3%) did not change over time, suggesting a fast removal by physicochemical processes (e.g., sorption on the filter medium) followed by biological degradation under favourable aerobic conditions (Dotro et al., 2017). The BOD_5 removal efficiency in columns fed with GW ranged between 96.1% and 99.3%, exhibiting a performance at the higher range of previous studies showing 86−98% (Fowdar et al., 2017; Gattringer et al., 2016; Masi et al., 2016). Figure 3.4.5-b reveals a low rate of release of BOD_5 from the filter medium in BM* columns (inlet, 0.43±0.45 mg/L; outlet, 1.18±0.33 mg/L). However, the release of BOD_5 was offset by removal processes in BM columns. In GW, BOD_5 ranged between 36.2 and 71.3 mg/L, with an average value of 52.4±9.0 mg/L (Figure 3.4.5-b), close to literature values for synthetic GW (65±6 mg/L) (Hourlier et al., 2010) and within the range of Western European countries (20–756 mg/L) (Boano et al., 2020).

The COD:BOD_5 ratio in inlet GW was 5.25±1.61, higher than those of typical real GW that are between 1.05 and 3.86 (Boano et al., 2020) but within the upper boundary of 6.98 for synthetic GW (Hourlier et al., 2010). The average value for outlet GW was much higher (182.82±177.18) and two orders of magnitude higher than values (2.3−3.6) reported in other studies (Gattringer et al., 2016; Masi et al., 2016). This difference probably derives from the limited removal of COD during the establishment period.

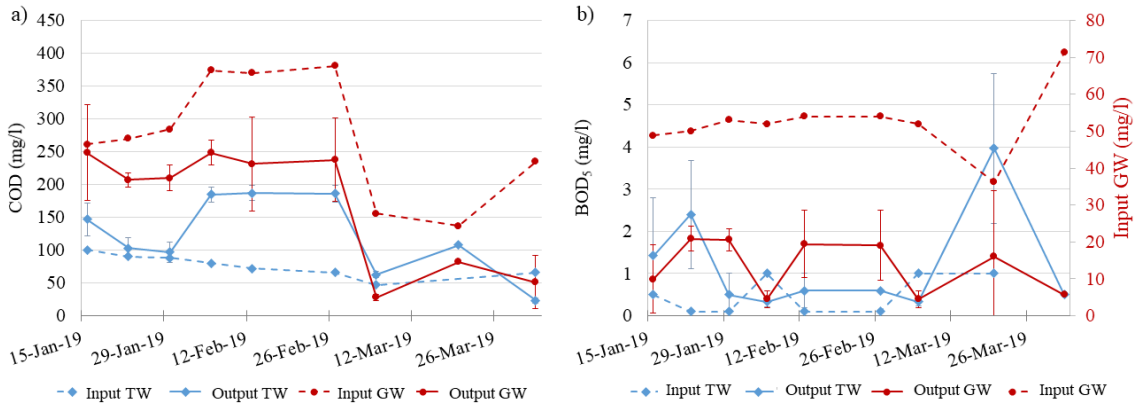

Figure 3.4.5. Concentrations of a) COD and b) BOD5 at the inlet and outlet of TW and GW columns.

Figure 3.4.6 shows the concentration of nitrogen species (TKN and NO_3^--N) and TP. A release of TKN from BM* columns (inlet, 2.42±2.54 mg/L; outlet, 4.34 ± 0.19 mg/L) occurred (Figure 3.4.6-a), possibly due to the organic components of coconut fibre, but a removal in BM columns (inlet, 5.01±3.11 mg/L; outlet, 2.66±0.14 mg/L) was observed. TKN was mainly composed of organic nitrogen due to the very low NH_4^+-N concentrations (mostly <1 mg/L) in BM* and BM inlets. The TKN removal efficiency in BM samples strongly increased over time, up to 92.7±2.4% (in agreement with the value of 94% in (Gattringer et al., 2016)), possibly due to the progressive development of

biological processes (e.g., microbial and plant uptake (Fowdar et al., 2018)) favoured by an increase in temperature and system growth, with an average removal equal to 34.6±29.7%. NO_3^--N was released from the filter medium in BM* columns (inlet, 1.94±1.79 mg/L; outlet, 2.19±0.15 mg/L) (Figure 3.4.6-b); however, BM columns removed NO_3^--N up to 55.6±13.7% (average rate of 25.7±28.8%). Literature results vary significantly, with removal efficiencies as high as 98.6% (Prodanovic et al., 2020); however, a strong (440.3%) release was also reported in a study (Gattringer et al., 2016) with a NO_3^--N outlet concentration (3.61 mg/L) close to the one in the present phase of this study. The observed NO_3^--N removal could be caused by denitrification in anaerobic micro-zones inside the pots and by plants and microbial uptake. As inlet concentrations were limited and vertical flow systems are not specifically designed for NO_3^--N removal, the observed removal performances for NO_3^--N obtained in this work were considered satisfactory. TP (Figure 3.4.6-c) was characterized by low inlet concentrations (often <1.70 mg/L), compared to values in the literature for real and synthetic GW (0.01−51.58 mg/L) (Boano et al., 2020; Prodanovic et al., 2020; Rodriguez-Chueca et al., 2014). TP concentrations varied negligibly in BM* columns, while BM columns showed a positive removal efficiency, as also observed by Prodanovic et al., possibly due to plant uptake, microbial activity, and sorption (Prodanovic et al., 2019a; Vymazal, 2002) and favoured by the increasing temperature (Ramprasad et al., 2017). The average output concentration (2.76±0.25 mg/L) and removal efficiencies (−22% to 56.7%) are consistent with previous studies (1−2.6 mg/L and 35−72.6%, respectively, on average) (Fowdar et al., 2017; Jin et al., 2018; Prodanovic et al., 2020, 2019a).

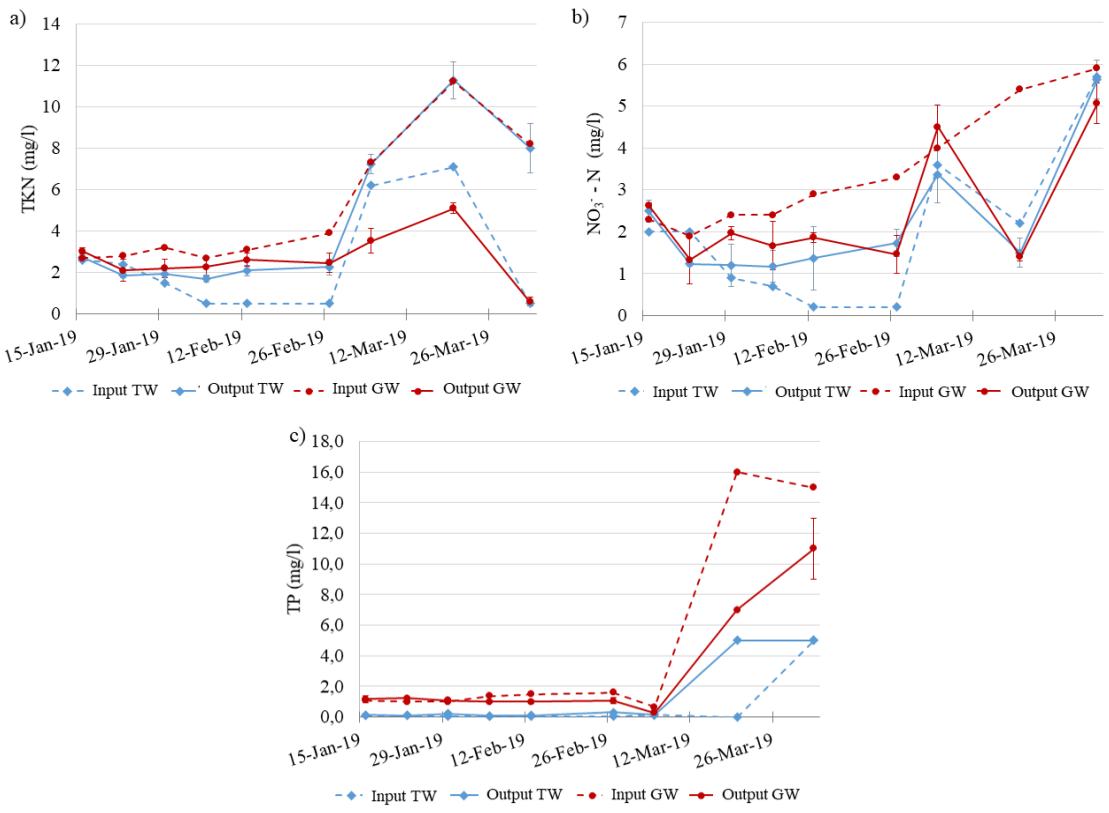

Figure 3.4.6 Concentrations of a) TKN, b) NO_3^--N, and c) TP at the inlet and outlet of TW and GW columns.

Chloride and sulphate (Figure 3.4.7) exhibited a slight release in BM* columns but exhibited rather conservative behaviour in BM columns.

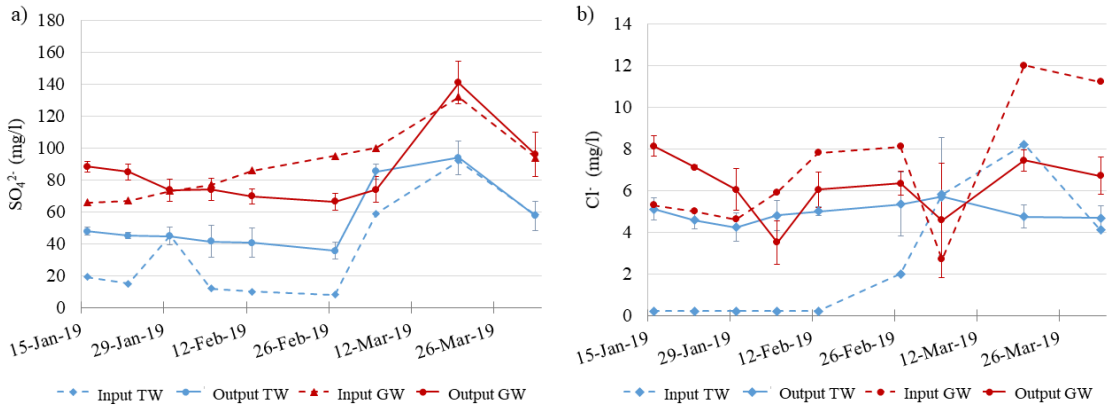

Figure 3.4.7. Concentrations of a) sulphate and b) chloride at inlet and outlet of TW and GW columns.

The *E. coli* average removal efficiency (Figure 3.4.8-a) was excellent (98.9±1.8% and 2.74±1.55 log units) and significantly improved over time ($|S| = 20$), ensuring a very low average concentration in the output (25 MPN/100 mL) compared to that of another vegetated pot system with values of 2.72×10^3 MPN/100 mL (Prodanovic et al., 2020) or 0.3−0.6 log unit (Kotsia et al., 2020). Hence, a single modular panel reduced the *E. coli* concentration by 4 orders of magnitude. Figure 3.4.8-b indicates that MBAS were released from BM* columns for all samples (inlet, 0.15±0.09 mg/L; outlet, 1852±172 mg/L), probably because of the leaching of natural organic substances from the filter medium that react during MBAS analysis. However, along BM columns, MBAS concentrations decreased remarkably, and output BM concentrations reached the values of output BM*. Thus, the system achieved very good performances (63.0±13.6% average removal efficiency) in removing anionic surfactants from GW.

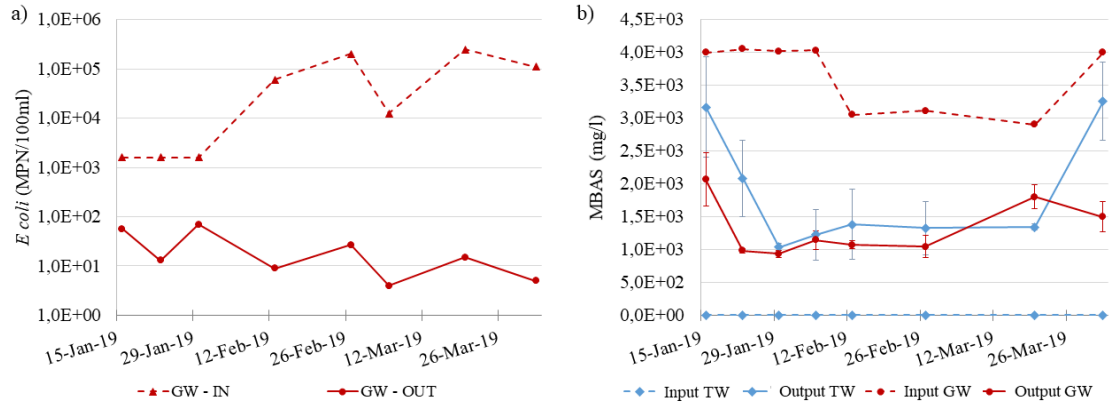

Figure 3.4.8. Concentrations of a) *E. coli* in the input and output of GW columns and b) MBAS at the inlet and outlet of TAP and GW columns.

Effects of additives on BM removal performances

The impact of additives on filter medium treatment efficacy was evaluated comparing the output concentrations and removal efficiency of the different configurations with BM.

Results for the tested physicochemical parameters are shown in Figure 3.4.9. For pH (Figure 3.4.9-a), no temporal trend was found for either GW or output water (Table 3.4.1). Output samples were on average slightly alkaline (Figure 3.4.9-b) and remained similar to GW for all mixtures (Table 3.4.1). Even though EC showed an increasing trend for GW from 400 to 712 µS/cm, no significant trend was present for the output samples (Table 3.4.1), suggesting that the water solution reached equilibrium with the porous medium. All mixtures showed higher EC values than GW, especially in the first two months of the monitoring period. In the whole monitoring period, no filter medium mixture exhibited significant differences in EC compared to BM (641±7 µS/cm) (Figure 3.4.9-c, Table 3.4.1). Average DO concentration in output samples was close to saturation for all filter medium mixtures (Figure 3.4.9-d). This indicates that oxygen exchange between soil and atmosphere produced aerobic conditions in the pots and increased DO concentrations. The compost mixture (CO) was characterized by the lowest average DO value (10.23±0.35 mg/L), possibly due to its low effective porosity (0.05±0.02 Table 3.4.1) and frequently observed clogging events that may have compromised soil aeration and oxygen exchange with open air.

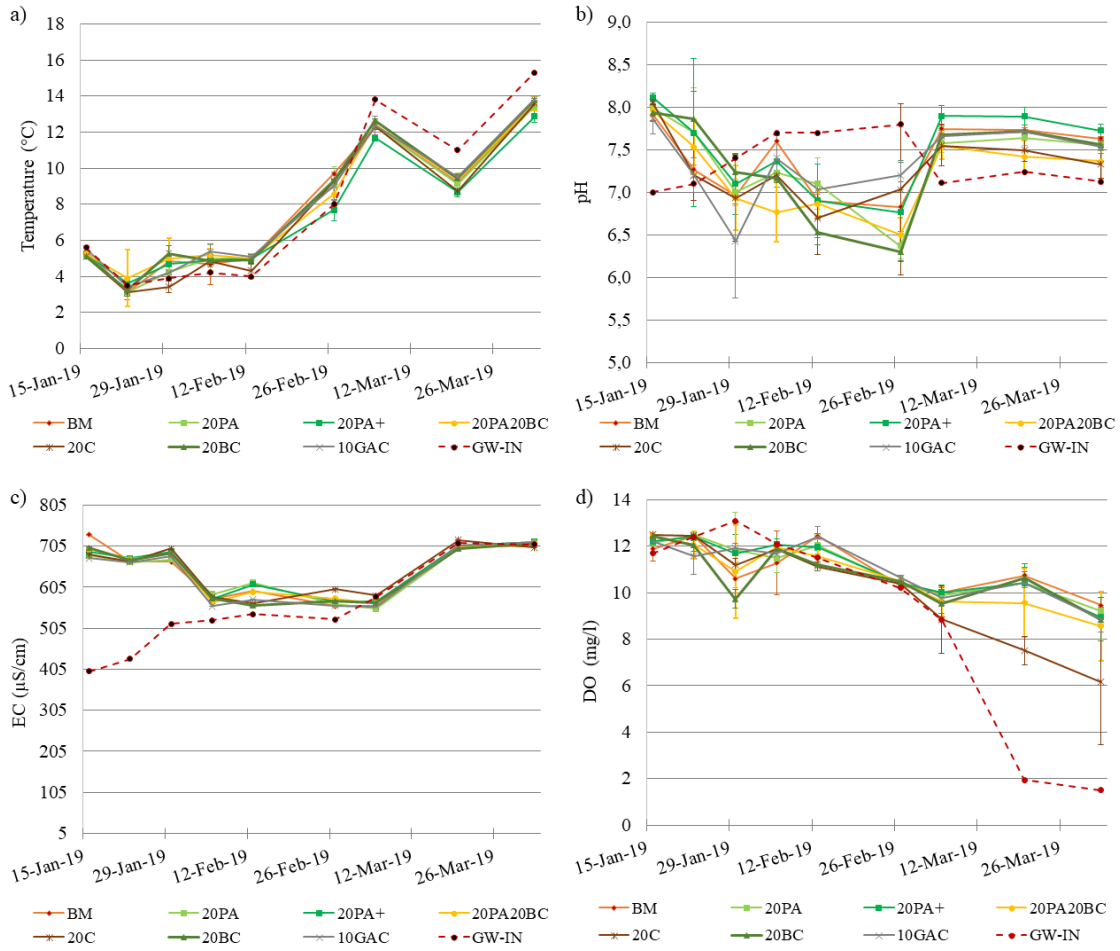

Figure 3.4.9. Time series of a) temperature, b) pH, c) Electric Conductivity (EC) and d) Dissolved Oxygen (DO) of GW (dashed lines) and at the outlet of all filter medium mixtures. Filter medium mixtures are denoted as (see text for further details) BM: base medium; 10GAC: granular activated carbon; 20CO: compost; 20BC: biochar; 20PA: polyacrylate; 20PA20BC: polyacrylate and biochar; 20PA+: polyacrylate (old configuration).

Table 3.4.1. List of *p* values of the statistical tests performed on contaminants' removal efficiencies. The Mann-Kendall test verified the presence of temporal trends (positive if not otherwise specified), and the Students' *t*-test verified if a filter medium mixture had better removal performance than the BM ($p<0.05$ in bold). Asterisks confirmed the statistically significance after false discovery rate procedure.

Mixture	BOD_5	COD	TSS	TKN	NO_3^--N	TP	SO_4^{2-}	*E. coli*	MBAS
					Temporal trend				
BM	0.317	**0.001***	0.266	**0.005***	0.252	0.076	0.175	**0.019***	0.266
10GAC	0.114	**0.029***	0.902	**0.005***	0.302	**0.009**	**0.048**	**0.019***	0.174
20CO	0.602	**0.005***	0.387	**0.017***	1.000	0.118	**0.048**	**0.019***	0.536
20BC	0.094	**0.004***	1.000	**0.029***	0.602	0.076	0.348	0.108	0.902
20PA	0.916	0.108	0.387	**0.005***	0.175	0.174	0.252	**0.035***	0.536
20PA20BC	0.602	**0.029***	0.266	0.076	0.917	0.252	0.175	**0.013***	0.902
20PA+	0.917	**0.029***	0.266	**0.005***	0.348	**0.017**	**0.029**	**0.019***	0.266
					Comparison with BM				
10GAC	0.894	0.349	0.903	0.077	**0.020***	0.081	0.039	0.242	0.515
20CO	0.961	0.857	0.862	**0.014***	**0.017***	0.938	0.217	0.104	0.601
20BC	0.808	**0.011**	0.971	**0.005***	**0.004***	0.173	**0.001***	0.403	0.093
20PA	0.980	0.087	0.498	0.831	0.753	0.777	0.909	0.092	0.636
20PA20BC	0.889	0.592	0.500	0.100	**0.023***	0.870	**0.004***	0.232	0.378
20PA+	0. 677	0.208	0.289	0.979	0.916	0.504	**0.010***	0.723	0.627

No significant temporal trend was detected for TSS along the monitoring period (Table 3.4.1). Due to the low concentrations in input GW and despite a small reduction in the average output concentration for BM and PA+ mixtures (9.37±0.96 and 9.08±0.70 mg/L, respectively), the average removal efficiency resulted in a slight TSS release for all mixes (Table 3.4.1, Figure 3.4.10c). According to the results of the Student's t-test, no filter medium mixture performed significantly better than BM (Table 3.4.1). The low input TSS load hence prevented further removal by the additives.

All the mixtures exhibited an average removal efficiency >93% for BOD_5 (Figure 3.4.10a), in line with the best literature performances for common filter media (96–99%) (Fowdar et al., 2017; Gattringer et al., 2016; Kotsia et al., 2020) and for GAC (97±3%) (Dalahmeh et al., 2012). None of the tested filter medium mixtures showed any temporal trend in BOD_5 removal efficiency (Table 3.4.1). According to the test results, no mix performed significantly better than the BM (Table 3.4.1). Apparently, the very high removal efficiency of the BM was not altered by the additives for this parameter. These results confirm the high potential of green wall application for removing BOD_5 from GW (Boano et al., 2021a; Gattringer et al., 2016). COD removal efficiency significantly increased over time for all mixtures except for 20PA (Table 3.4.1). This improvement of removal efficiency may have been caused by a combination of plants growth and biofilm development and of temperature increase during the monitoring period (Boano et al., 2021a). Removal efficiency varied among the mixtures between 29.6±45.5% for 20CO and 50.7±28.5% for 20BC (Figure 3.4.10b). The best removal performance was found for 20BC (50.7±28.5%), which was higher than for BM (40.4±25.1%) although the difference was not classified as statistically significant (corrected p=0.07). (Table 3.4.1). Output COD concentration for 20BC varied between 20 mg/L and 267 mg/L (147±8.9 mg/L on average), and its removal efficiency ranged between a slight (2.43%) release at the first sampling date to >86% removal (Figure 3.4.10). This increasing trend over the observation period led removal efficiency to gradually reach values reported in literature studies on green walls (64–98%) (Gattringer et al., 2016; Jin et al., 2018; Kotsia et al.,

2020; Masi et al., 2016; Pradhan et al., 2020; Prodanovic et al., 2020). Dalahmeh et al. (2012) reported COD removal efficiency up to 94% with an unplanted GAC filter; however, this performance was obtained with a HLR value (32 $Lm^{-2}d^{-1}$) that was about 20 times lower than in the present value. This comparison confirms previous results that increases in HLR up to 600–800 $Lm^{-2}d^{-1}$ lead to relatively mild reductions in COD removal efficiency (Boano et al., 2020).

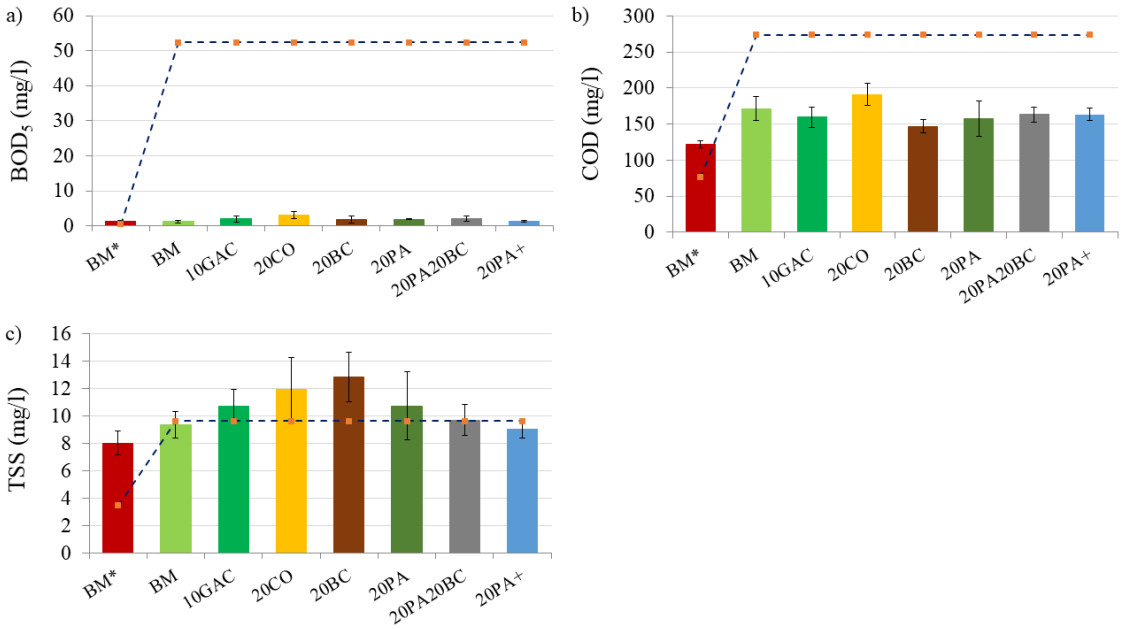

Figure 3.4.10. Average values of concentrations of a) BOD5, b) COD and c) TSS of input GW (dashed lines) and at the outlet of all filter media mixes (bars). Filter medium mixtures are denoted as (see text for further details) BM: base medium; 10GAC: granular activated carbon; 20CO: compost; 20BC: biochar; 20 PA: polyacrylate; 20PA20BC: polyacrylate and biochar; 20 PA+: polyacrylate (old configuration).

TKN removal efficiency significantly improved over time for all filter medium mixtures except for 20BC20PA (Table 3.4.1, Figure 3.4.11-a), possibly due to biofilm growth and progressive development of biological processes, as reported in previous studies (Pradhan et al., 2019). Average TKN output concentration ranged between 2.04±0.10 mg/L and 2.78±0.15 mg/L (in 10GAC and 20PA+ respectively) and average removal efficiency varied between 29.9±33.8% and 46.8±24.8% (20 PA+ and 20BC, respectively). These values are in line with the median TKN removal efficiencies (34–55%) observed in winter by Dal Ferro et al. (2021) for a vertical flow system treating kitchen GW, suggesting that the low temperatures may have limited TKN removal. Both 20CO and 20BC (41.3±24.4% and 46.8±24.8% respectively) performed significantly better than BM (34.6±29.7%) in removing TKN (Table 3.4.1). The low values of ammonia nitrogen NH_4^+-N concentrations (usually below 1 mg/L) indicate that organic nitrogen was the main component of TKN. Analysis of nitric nitrogen NO_3^--N concentrations did not reveal any significant temporal trend in removal efficiency (Table 3.4.1, Figure 3.4.11-b) even though GW concentration increased over time (Table 3.4.1), indicating that removal processes in the green wall were able to compensate for variations in input concentration. For all mixes, NO_3^--N concentration decreased from the GW value of 3.39±1.43 mg/L to output values between 1.82±0.14 mg/L and 2.61±0.16 mg/L for

20BC and 20PA+, respectively. Removal efficiencies of 20PA and 20PA+ were slightly (but not significantly) lower than the one of BM (25.6±28.8%), while all other filter medium mixtures performed significantly better than BM (Table 3.4.1). These findings agree with the previous results reporting improvements in nitrogen removal using GAC compared to more inert filter media (Dalahmeh et al., 2012).

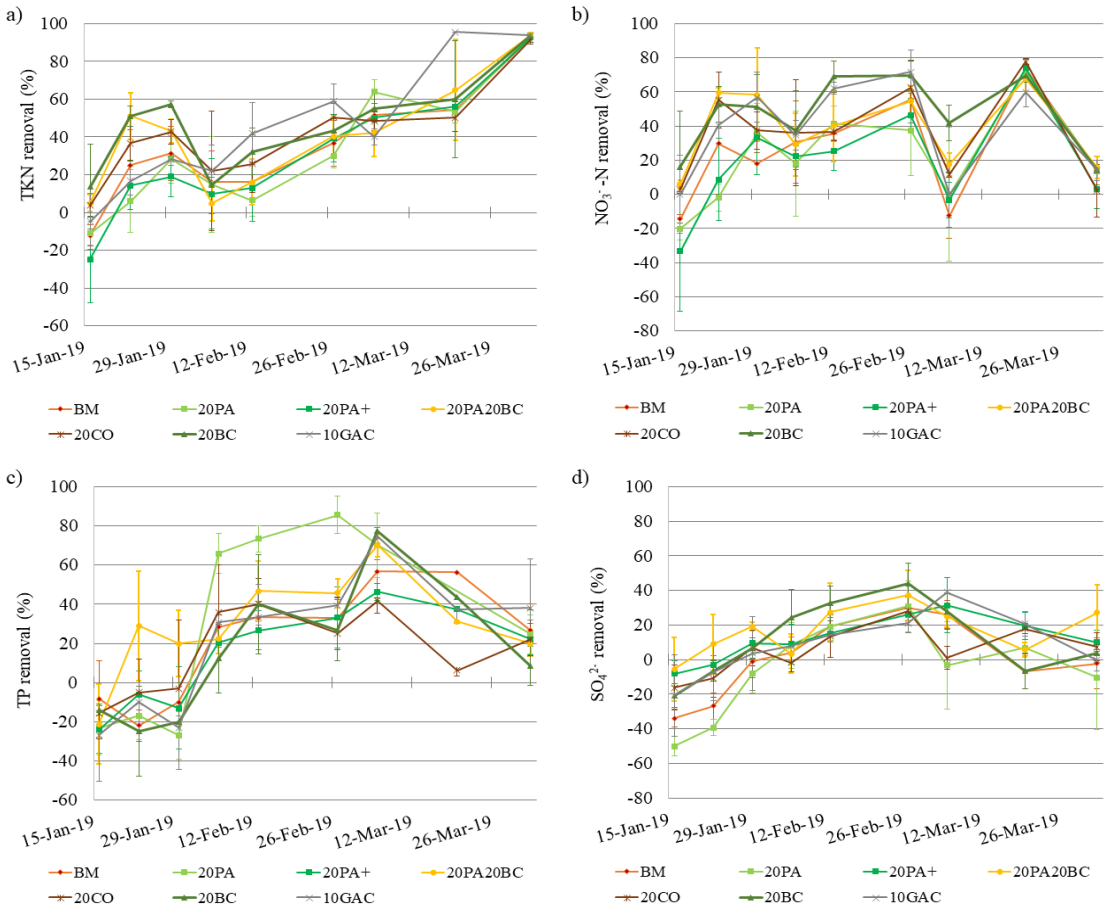

Figure 3.4.11. Removal efficiency of a) TKN, b) NO_3^--N, c) TP, d) SO_4^{2-} over the monitoring period. Filter medium mixtures are denoted as (see text for further details) BM: base medium; 10GAC: granular activated carbon; 20CO: compost; 20BC: biochar; 20PA: polyacrylate; 20PA20BC: polyacrylate and biochar; 20PA+: polyacrylate (old configuration).

TP concentration was low for most samples, both for GW (4.36±6.33 mg/L) and output water (between 2.05±0.19 mg/L and 3.71±0.30 mg/L for 20PA and 20CO, respectively). No significant temporal trend was identified for any filter medium mixture (Table 3.4.1), which may indicate the contribution of physicochemical processes (e.g., sorption) that were relatively constant over time (Pradhan et al., 2020). Net TP removal was observed for all filter medium mixtures (Figure 3.4.11-c), and the statistical tests showed that no additive significantly improved TP removal efficiency when added to the base medium (21.6±28.7%) (Table 3.4.1). In general, the average removal efficiency was coherent with studies employing ornamental plants (11–20%) (Kotsia et al., 2020), and in line with the very wide range of literature results on TP removal (Boano et al., 2020) which reflects the diverse rates of TP removal by plant uptake and microbial activity in green walls (Prodanovic et al., 2019a). Input SO_4^{2-} concentration in GW (88±21 mg/L)

was similar to concentrations in output samples (Figure 3.4.11-d). Average removal efficiency of BM (0.9±22%) indicates that SO_4^{2-} behaved quite conservatively in the green wall, as expected for aerobic conditions. Even though some mixtures (20BC: 11.7±21.5%; 20PA+: 12.2±17.2%; 20PA20BC: 16.5±14.1%) removed significantly more SO_4^{2-} than BM (Table 3.4.1), it is clear from the removal efficiency values that this removal is minimal. As expected, a similarly conservative behaviour was also found for Cl^- (data not shown), with concentrations in GW equal to 7.0±3.1 mg/L and in output water between 6.2±0.4 mg/L (BM) and 7.2±0.5 mg/L (20CO).

E. coli removal had excellent performances since the beginning of the monitoring period, and the Mann-Kendall test further identified an increasing trend in removal efficiency for all mixtures except 20BC (Table 3.4.1, Figure 3.4.12-a). Average removal efficiency was over 98% (>2.9 log units) for all mixtures, and the Student's t-test did not find a significant improvement compared to BM (98.9±1.8%, 3.1±1.8 log units) (Table 3.4.1). The inclusion of additives hence did not result in statistically significant improvements compared to the already high removal performance of the base medium mix. These performances are similar to the highest values reported in previous green wall studies for GW treatment (Bakheet et al., 2020; Boano et al., 2020; Pradhan et al., 2020; Prodanovic et al., 2020). MBAS concentration in output water exceeded two-fold reduction for all mixtures compared to GW (Figure 3.4.12-b), with no temporal trend during the observation period (Table 3.4.1). No mixture performed significantly better than BM (Table 3.4.1), even if 20BC showed a slightly higher average removal efficiency (71.4±21.7%).

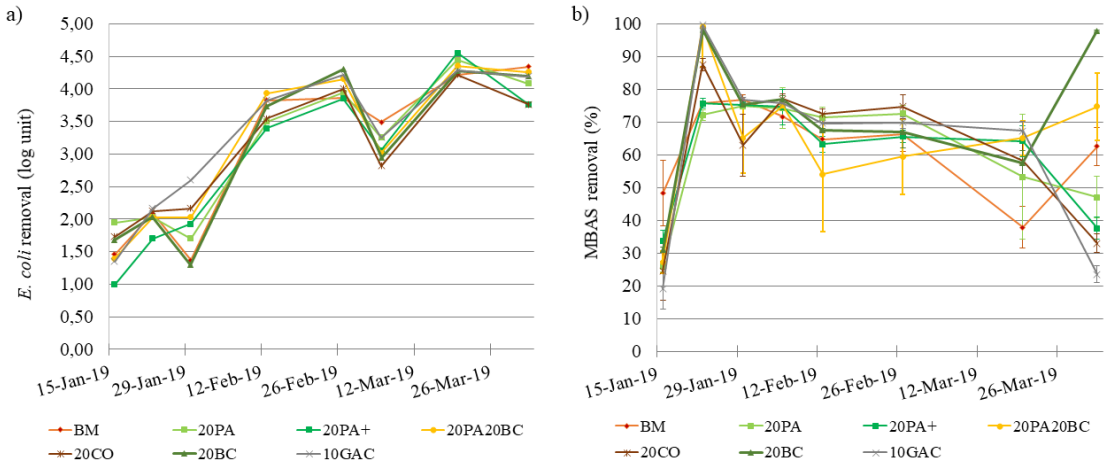

Figure 3.4.12. Removal efficiency of a) *E. coli*, b) MBAS over the monitoring period. Filter medium mixtures are denoted as (see text for further details) BM: base medium; 10GAC: granular activated carbon; 20CO: compost; 20BC: biochar; 20PA: polyacrylate; 20PA20BC: polyacrylate and biochar; 20PA+: polyacrylate (old configuration).

3.4.3 Phase 2

Effect of filter medium on possible release

The release of compounds from the base medium has been evaluated in phase 1 (Boano et al., 2021a) but a further preliminary analysis was performed in this phase to verify the impact of graphene on the possible release. Thus, the output of the BC+GR* control configuration was compared with input TW for the considered physical-chemical parameters.

Input and output water temperatures (Figure 3.4.13-top right) were mainly influenced by temperature of the distribution system and external temperature respectively. Temperature ranged between 12.5-24.8 °C for input TW and 11.8-24.0 °C for output TW, thus not significant difference was found for this parameter. pH (Figure 3.4.13-top left) increased from 7.16±0.23 in TW to 7.40±0.10 in output TW, with a slight but significant alkalinisation. No significant variation was found comparing input and output samples for EC (Figure 3.4.13-bottom left) and DO (Figure 3.4.13-bottom right), and no temporal trend was observed for these parameters (Table 3.4.2). The limited reduction in average DO concentration (input: 7.7±1.4 mg/L; output: 6.9±0.9 mg/L) showed the good oxygenation of the vertical unsaturated system.

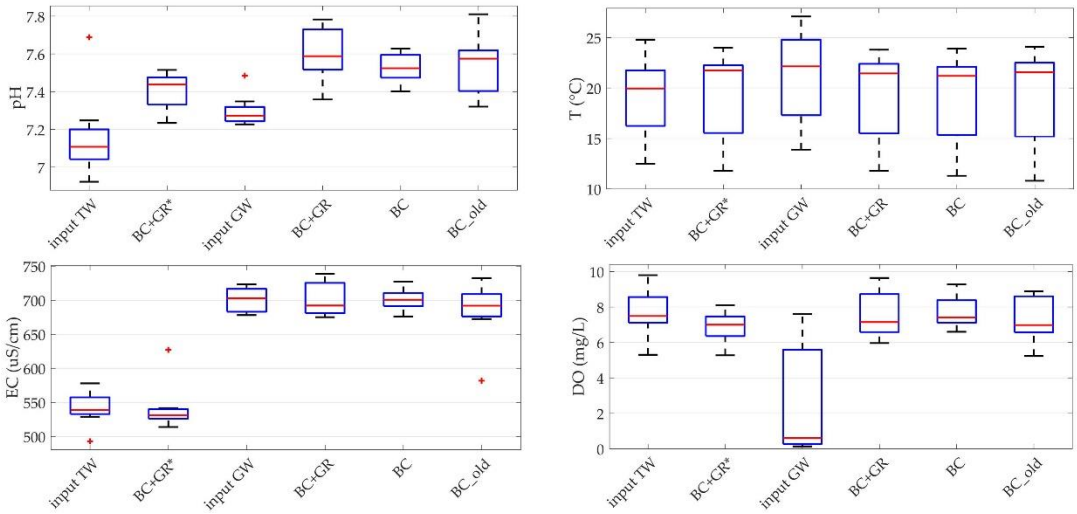

Figure 3.4.13. Boxplot of time series values for input water (TW and GW) and output water from all configurations for parameters measured on site with the multiparametric probe (Temperature: top left, pH: top right, EC: bottom left, DO: bottom right). Median value (red line), 25th and 75th percentiles (blue box), range (black whiskers) and outliers (red cross) are shown.

Table 3.4.2. p-values of Mann-Kendall test on all parameter removal efficiency. Bold numbers indicate an increasing trend ($p<0.05$) in temporal series; asterisks confirm the trend after false discovery rate adjustment. NaN occurs when all value in a data set are below the detection limit.

	Parameters													
Mix	**pH**	**T**	**EC**	**DO**	**BOD_5**	**COD**	**TSS**	**TKN**	**NO_3^--N**	**NH_4^+-N**	**TP**	**SO_4**	**Cl^-**	**MBAS**
BC	0.71	0.11	1.00	0.11	0.45	1.00	0.27	0.45	1.00	1.00	0.71	0.71	**0.02**	0.37
BC_old	0.17	0.11	0.71	0.23	0.26	0.88	0.06	1.00	0.54	0.29	0.90	0.71	0.90	0.76
BC+GR	0.04	0.11	1.00	0.04	0.18	1.00	0.39	0.39	0.21	1.00	0.17	1.00	0.27	0.76
BC+GR*	0.71	0.04	0.39	0.06	1.00	NaN	0.71	0.06	0.45	1.00	0.59	0.17	0.71	1.00

Table 3.4.3. p-values of the t-Student test comparing removal efficiency of each configuration. Bold numbers indicate that the tested configuration performed significantly better that the reference one. Asterisks confirm the test significance after false discovery rate adjustment. NaN occurs when all values were below the detection limit.

Does BC configuration perform significantly better than the others? (on removal efficiency)										
	BOD_5	**COD**	**TSS**	**TKN**	**NO_3^--N**	**NH_4^+-N**	**TP**	**SO_4**	**Cl^-**	**MBAS**
BC_old	0.973	NaN	0.243	0.094	0.092	**0.048***	**0.007***	**0.003***	0.830	0.391
BC+GR	0.498	NaN	0.955	0.177	0.798	NaN	0.123	0.139	0.842	0.846
Does BC_old configuration perform significantly better than the others? (on removal efficiency)										
	BOD_5	**COD**	**TSS**	**TKN**	**NO_3^--N**	**NH_4^+-N**	**TP**	**SO_4**	**Cl^-**	**MBAS**
BC	0.027	NaN	0.757	0.906	0.908	0.952	0.993	0.997	0.170	0.609
BC+GR	0.241	NaN	0.975	0.917	0.987	0.952	0.509	0.864	0.238	0.818
Does BC+GR configuration perform significantly better than the others? (on removal efficiency)										
	BOD_5	**COD**	**TSS**	**TKN**	**NO_3^--N**	**NH_4^+-N**	**TP**	**SO_4**	**Cl^-**	**MBAS**
BC	0.502	NaN	**0.045***	0.823	0.202	NaN	0.877	0.861	0.158	0.154
BC_old	0.759	NaN	**0.025***	0.083	**0.013***	**0.048***	0.491	0.136	0.762	0.182
Is the output concentration of BC+GR* significantly higher than input TW? (on concentrations)										
	BOD_5	**COD**	**TSS**	**TKN**	**NO_3^--N**	**NH_4^+-N**	**TP**	**SO_4**	**Cl^-**	**MBAS**
	0.110	NaN	0.069	0.929	0.066	0.361	0.099	0.096	0.092	**0.000**

Outflow water from the control configuration did not present a significant difference in BOD_5 (7.3±6.0 mg/L) compared to tap water (6.4±5.8 mg/L) in input (Figure 3.4.14-top left, Table 3.4.3). COD concentration was also not relevantly affected by the porous medium, since both input and output samples were always below the detection limit (20 mg/L, data not shown). TSS concentration in tap water was very low (0.98±1.23 mg/L) and showed a small but not significant release along the columns (output 1.38±1.65 mg/L) (Figure 3.4.14-top right, Table 3.4.3). Considering nitrogen compounds, TKN (Figure 3.4.14-bottom left) showed a non-significant removal (from 6.43±2.08 mg/L in input tap water to 4.22±2.29 mg/L in output BC+GR* water. Moreover, NO_3^--N (Figure 3.4.14-bottom right) and NH_4^+-N (data not shown) did not exhibit any significant difference (Table 3.4.3) between input (4.19±1.45 mg/L and 0.04±0.01 mg/L, respectively) and output (5.01±0.35 mg/L and 0.05±0.01 mg/L, respectively), despite the very small increase in the concentrations of both compounds.

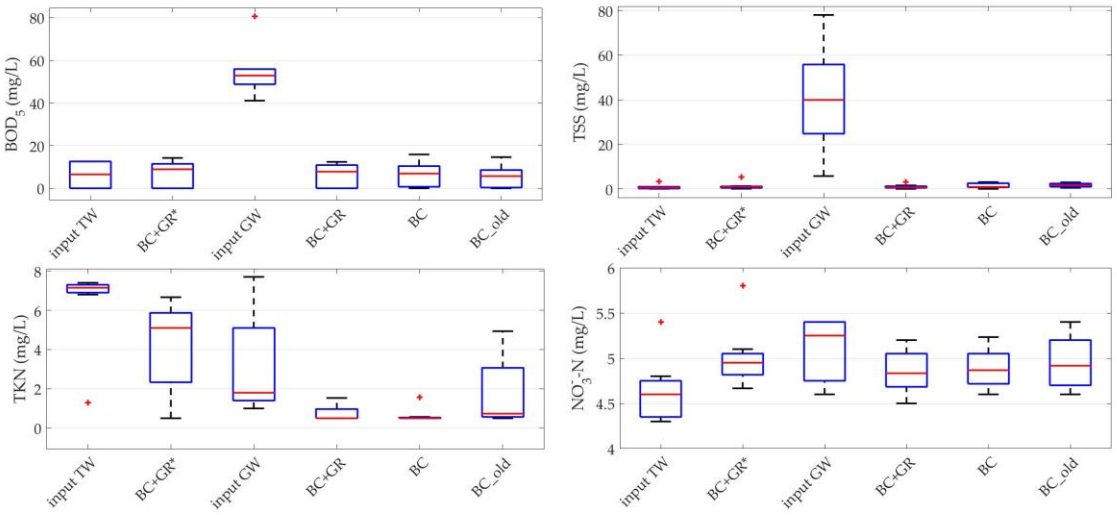

Figure 3.4.14. Boxplot of time series values for input water (TW and GW) and output water from all configurations for bio-chemical parameters (BOD_5 top left, TKN top right, NO_3^--N bottom left, NO_3^--N bottom right). Median value (red line), 25th and 75th percentiles (blue box), range (black whiskers) and outliers (red cross) are shown.

The filter medium BC+GR* released small but non-significant amounts of TP (input 2.14±2.37 mg/L; output 2.15±2.36 mg/L; Figure 3.4.15-top left), Cl^- (input 3.46±1.26 mg/L; output 4.39±0.78 mg/L, Figure 3.4.15-bottom left), and SO_4^{2-} (input 66.88±9.79 mg/L, output 74.29±12.18 mg/L, Figure 3.4.15-top right). On the other hand, a significant difference (Table 3.4.3) was observed between MBAS input and output concentration (0.64±0.35 mg/L and 603.13±290.53 mg/L, respectively), in agreement with previous results with BM only (Boano et al., 2021a), suggesting that MBAS release was due to base medium regardless of graphene (Figure 3.4.15-bottom right).

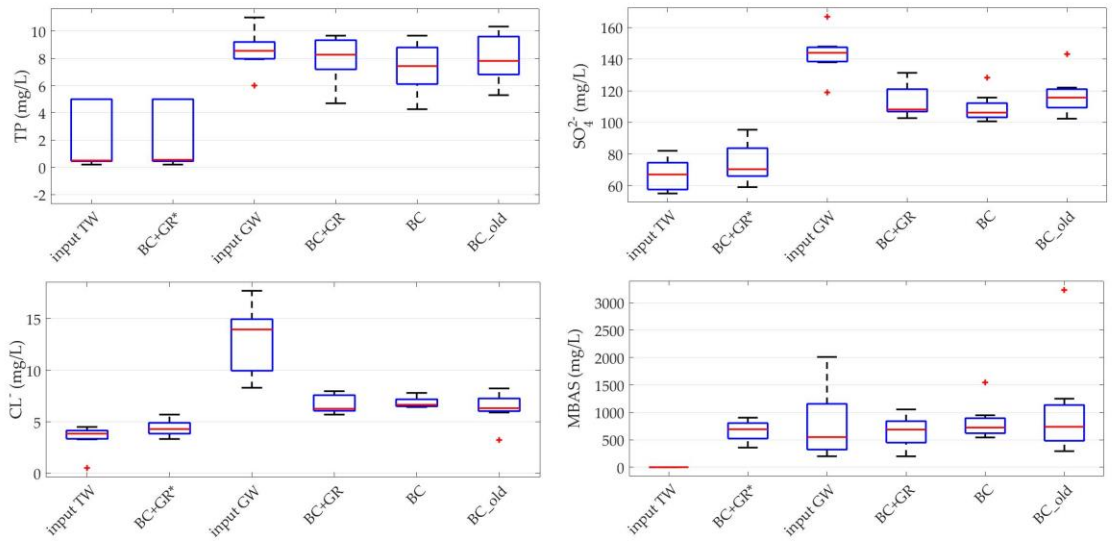

Figure 3.4.15. . Boxplot of time series values for input water (TW and GW) and output water from all configurations for bio-chemical parameters (TP top left, SO_4^{2-} top right, Cl^- bottom left, MBAS bottom right). Median value (red line), 25th and 75th percentiles (blue box), range (black whiskers) and outliers (red cross) are shown.

The analysis of the configuration fed with tap water (BC+GR*) revealed that the addition of graphene did not cause any significant release of contaminants. The only relevant exception was the limited release of MBAS, which was however similar to the release observed in a previous system without graphene (Boano et al., 2021a), and was hence not related to it. In general, the output values of the analysed parameters are coherent with a previous study based on coconut fibre and perlite fed with TW (Boano et al., 2021a).

Impact of graphene on GW-fed column performances

The impact of graphene on green wall performances has been evaluated comparing output concentrations and removal efficiencies of the BC+GR configuration with those of the control BC configuration installed at the same time.

The parameters measured on site did not exhibit any temporal trend for both configurations (Table 3.4.2). The slight increase in pH was similar for both BC and BC+GR configurations (input GW 7.30±0.08, BC 7.53±0.08, BC+GR 7.60±0.14) and coherent with literature values (Boano et al., 2021b; Gattringer et al., 2016; Prodanovic et al., 2020). EC was not influenced by the addition of graphene, and no relevant difference was found between input GW values (701±18 µS/cm) and the two considered configurations (BC 701±16 µS/cm and BC+GR 701±25 µS/cm). (Figure 3.4.13-bottom left). For both BC and BC+GR configurations, the DO content increased (Figure 3.4.13-bottom right) from anaerobic condition in input (2.58±3.14 mg/L) to aerobic conditions characterised by similar values in output (BC: 7.7±0.9 and BC+GR: 7.6±1.3 mg/L), as expected considering the vertical flow system characteristics (Boano et al., 2021a, 2021b; Kotsia et al., 2020).

Both configurations exhibited high BOD_5 removal performances (87.0±11.8% for BC and 87.0±10.6% for BCGR) that remained constant over time (Table 3.4.2). The BOD_5 range was 41.1-80.1 mg/L for input GW and decreased to 0-15.9 mg/L and 0-12.4 mg/L for BC and BC+GR, respectively (Figure 3.4.14-top left). COD concentration was 70.9±16.4 mg/L in GW and output concentrations were always below the detection limit of 20.0 mg/L for both BC and BC+GR, reaching a removal efficiency around 70.6% for both mixes. BOD_5 and COD removal performances were satisfactory for both configurations, even if lower than literature values that usually report performances over 90% (Gattringer et al., 2016; Kotsia et al., 2020; Prodanovic et al., 2020). Even if TSS removal was significantly better for BC+GR than BC mix (Table 3.4.3), TSS removal was excellent for both configurations (around 94%), and concentrations decreased from 40.6±22.7 mg/L in GW to 1.45±1.14 mg/L in BC and 1.03±0.96 mg/L in BC+GR (Figure 3.4.14-top right). This performance was coherent with literature evidences (Fowdar et al., 2017; Gattringer et al., 2016; Kotsia et al., 2020; Prodanovic et al., 2020). Considering nitrogen compounds, neither temporal trends (Table 3.4.2) nor significant differences (Table 3.4.3) were found for removal performances of BC and BC+GR configurations. The removal was higher than previous studies (Boano et al., 2021a, 2021b) on the same system but lower than some literature cases (Gattringer et al., 2016; Prodanovic et al., 2020), possibly because of the relatively low nitrogen concentrations of the current phase.

TKN removal was high (71.2±14.6% and 64.7±24.0%, respectively), starting from a range of 1.00-7.70 mg/L in input GW and often decreasing below the detection limit (0.5 mg/L) in both configurations). Removal of NO_3^--N and NH_4^+-N were respectively around 12% and 26% for both configurations. The moderate removal performances were probably due to the low concentrations in input GW (NO_3^--N: 7.18±6.00 mg/L, NH_4^+-N: 0.06±0.03 mg/L) and, for NO_3^--N, to the aerobic conditions that prevented denitrification.

The addition of graphene did not significantly influence the removal performances of TP, SO_4^{2-}, Cl^- and MBAS compared to the BC configuration (Table 3.4.3). Removal performances were quite low for these parameters for both configurations (TP 15.2±11.6%|6.8±13.0%, SO_4^{2-} 23.7±5.7%|20.6±8.07%, Cl^- 43.3±18.1%|44.8±18.9% for BC|BC+GR respectively). Input values of TP was within the literature range (Kotsia et al., 2020; Prodanovic et al., 2020) while removal efficiency resulted lower compared to literature evidences (Boano et al., 2021b; Prodanovic et al., 2020), even if TP removal varies widely among studies (Boano et al., 2021b; Fowdar et al., 2017; Prodanovic et al., 2020). TP removal was found to be lower for BC+GR than for BC, but the difference was not statistically significant. An average release was observed for MBAS (-111±258% for BC and -22±77% for BC+GR) because concentrations in output fluctuated considerably among sampling dates, as reflected by the high standard deviation values of removal efficiency. No temporal trend was found for any configuration (Table 3.4.2).

Impact of system age on performances of biochar columns

The age of the system did not significantly affect the behaviour of on-site parameters, according to the comparison between the newer (BC) and the older (BC_old, pots set up and already sampled during phase 1) biochar configurations. Both cases showed similar ranges for pH (7.40-7.63 for BC and 7.32-7.81 for BC_old) and EC values (701±16 BC and 683±46 BC_old). The BC_old configuration was characterised by a wider range in output DO concentration (5.2-8.9 mg/L) compared to BC (6.6-9.3 mg/L).

Both BC and BC_old showed very good removal performances for BOD_5 (87.0±11.8% and 88.8±10.4% respectively), and BC_old performed significantly better than BC (Table 3.4.3). The impact of age was not significant for COD removal performances (70.6±5.8% for BC and 71.1±6.1% for BC_old, data not shown), with output concentrations often reaching the detection limit for both configurations. TSS removal efficiency was excellent and statistically similar for both configurations (94.0±6.1% for BC and 93.2±6.8% for BC_old). Among nitrogen compounds, only NH_4^+-N removal was significantly affected by system age (Table 3.4.3) as BC performance significantly better than BC_old, which released small amounts of NH_4^+-N (BC_old: 0.15±0.19 mg/L; GW: 0.06±0.03 mg/L). The BC_old configuration also showed a higher variability in output concentrations for TKN (1.77±1.95 mg/L), while BC had a lower variability (NH_4^+-N: 0.04±0.00 mg/L, TKN: 0.64±0.37 mg/L). The average removal performance of TKN was high for BC (71.2±14.6%) but scarce for BC_old (22.8±95.9%); low performances were also found for NO_3^--N, as expected in a vertical flow system (12.3±26.9% for BC and 11.3±27.1% for BC_old).

The BC configuration performed significantly better (Table 3.4.3) for TP and SO_4^{2-} removal (15.2±11.6% and 23.7±5.7%) compared to BC_old (6.6±11.8% and 18.1±6.1%, respectively). Both configurations had similarly good performances for Cl^- removal (43.3±18.1% for BC and 50.1±11.1% for BC_old), although Cl^- was present in very low amounts. Age did not significantly impact on system performances in MBAS removal (Table 3.4.3), and release of MBAS was predominant for both configurations.

3.4.4 Phase 3

During this phase, the performances of GW treatment for the different levels of the green wall were analysed. Moreover, the same levels were compared between a new panel (P1) and a two-year-old panel (P2).

In the whole sampling period, water temperature was strongly influenced by air temperature in outdoor conditions (Figure 3.4.16). Starting from 9.0±3.2 °C in the input GW, the values slightly decreased along the columns, reaching similar values for both panels (P1: 7.9±3.4 | 7.0±3.1 | 7.3±3.1°C; P2: 8.4±3.3 | 7.3±3.2 | 7.0±2.8°C), coherently with previous studies (Boano et al., 2021a).

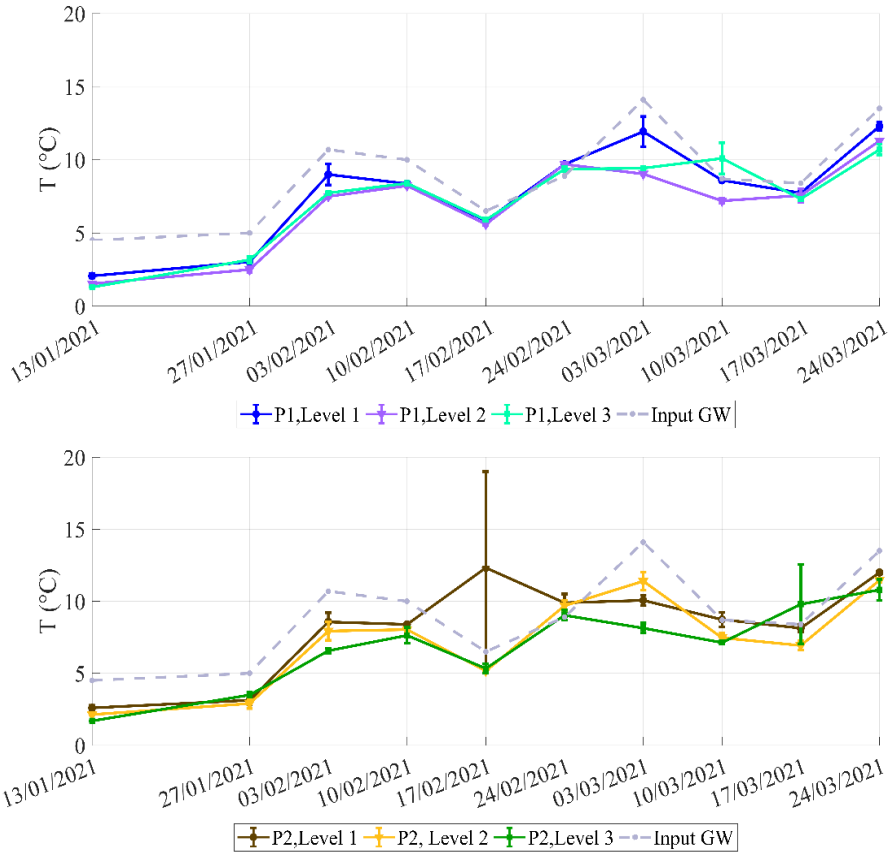

Figure 3.4.16. Temperature values measured in the outflows of the different levels (L1, L2, and L3) of panels P1 (top) and P2 (bottom) and in input greywater (GW).

Input GW showed pH between 6.91 and 7.50 (average value 7.34±0.17) (Figure 3.4.17), and analogous values were observed along the columns (average values per level, P1: 7.31±0.12 | 7.39±0.19 | 7.73±0.16; P2: 7.48±0.11 | 7.46±0.12 | 7.76±0.17). All pH

values were suitable for plant growing (Prodanovic et al., 2020) and were in the optimal range for nitrogen removal (Yin et al., 2016).

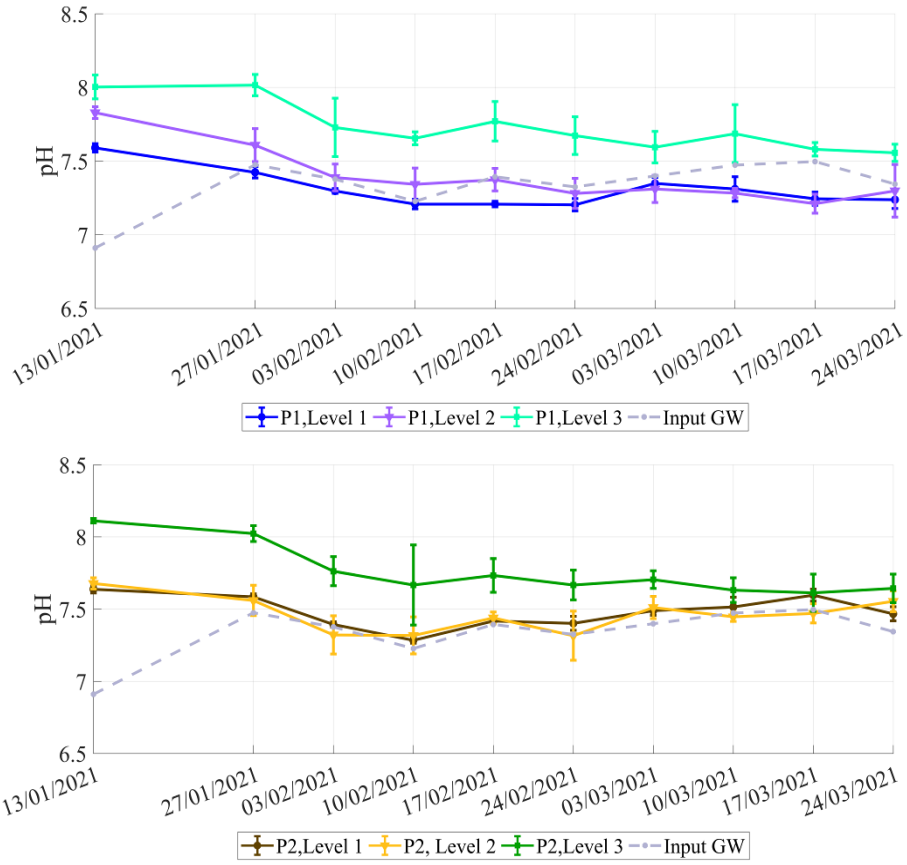

Figure 3.4.17. pH values measured in the outflows of the different levels (L1, L2, and L3) of panels P1 (top) and P2 (bottom) and in input greywater (GW).

DO showed strong variations (Figure 3.4.18), as it increased from anoxic values in input GW (0.93-3.36 mg/L, average 2.09±0.73 mg/L) to 10.82±0.91 mg/L and 10.48±1.30 mg/L in P1 and P2 outflow respectively. These input values were probably caused by aerobic reactions in the GW tank that lowered DO concentration. P1 showed a gradual increase in DO between the first and second levels (5.06±1.29 | 8.44±2.06 | 10.82±0.91 mg/L). P2 reached similar output values but after three levels (5.17±0.83 | 5.80±1.68 | 10.48±1.30 mg/L).

EC did not exhibit relevant variations between the input GW (675-713 µS/cm) and the outflow of the two panels (Figure 3.4.19) even if a slight increase was observed along the columns, similarly to Prodanovic et al. (2020). The outflow from each level ranged 700-722 µS/cm for P1 and 677-721 for P2. Literature values reported a wide range, between 147 and 274 µS/cm (Fowdar et al., 2017; Prodanovic et al., 2020), and also 640-774 µS/cm (Boano et al., 2021a; Gattringer et al., 2016), depending on many factors such as the EC of the tap water used to prepare synthetic GW and the release of soluble compounds from the porous medium. Considering that a washing procedure was performed before the sampling, the observed values were probably mostly influenced by the high EC of the tap water (Figure 3.4.3).

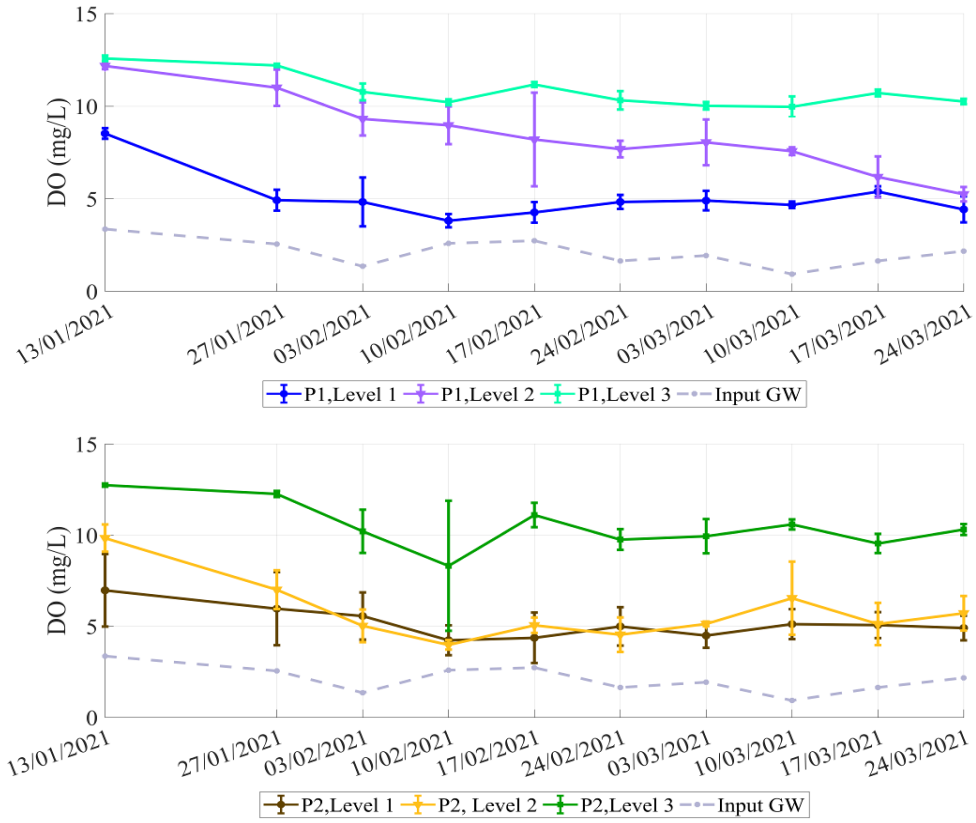

Figure 3.4.18. . Dissolved Oxygen (DO) concentration values measured in the outflows of the different levels (L1, L2, and L3) of panels P1 (top) and P2 (bottom) and in input greywater (GW).

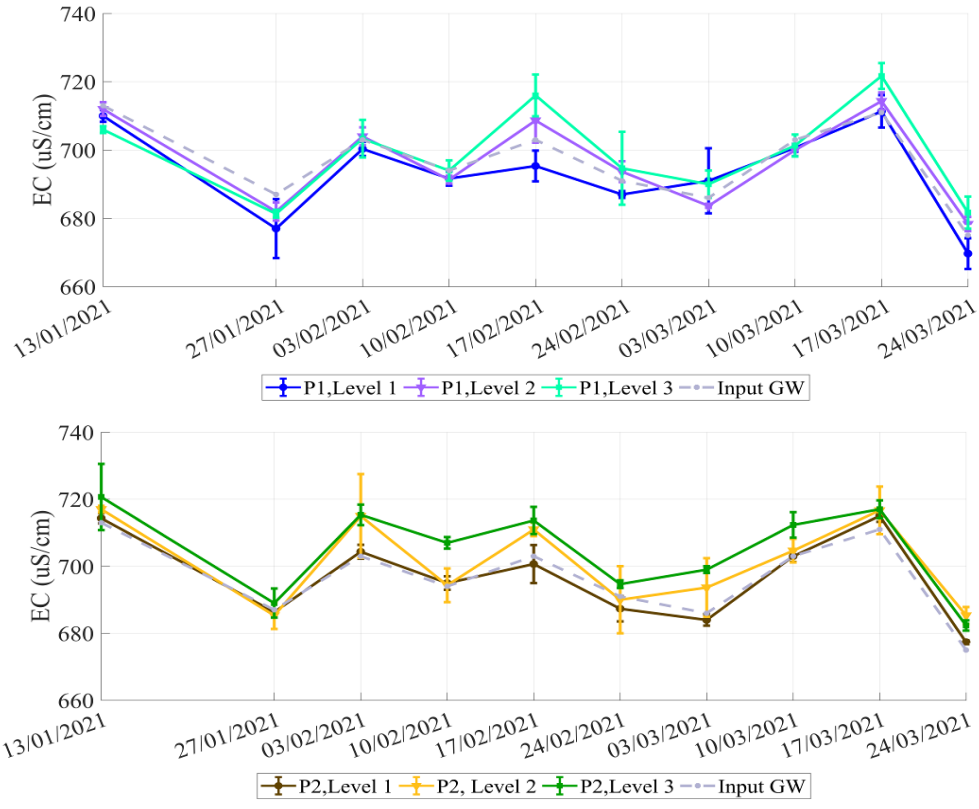

Figure 3.4.19. Electrical Conductivity (EC) values measured in the outflows of the different levels (L1, L2, and L3) of panels P1 (top) and P2 (bottom) and in input greywater (GW).

Both panels showed good performances in removing TSS from input GW (range 22.7-82.0 mg/L, average 41.1±17.3 mg/L) (Figure 3.4.20), even if occasional clogging events were observed when sampling the outflows of P2. The decrease of TSS concentration along the columns was as follows: P1 reached 2.7±3.5 mg/L after two levels of treatment (19.8±18.1|2.7±3.5|1.1±2.0 mg/L), while P2 required three levels to reach a similar result (43.3±20.7|16.7±10.4| 3.8±3.6 mg/L), with some episodes of TSS release from the first level of treatment. The removal efficiency was higher after the first level in P1 than in P2, that also featured a high TSS release on 03/03/2021 after a strong clogging event. Similarly to other studies (Fowdar et al., 2017; Gattringer et al., 2016; Prodanovic et al., 2020), overall removal efficiency reached 97.4±4.6% for P1 and 89.1±13.8% for P2 (Figure 3.4.21). No temporal trend was found in the removal efficiency, but a significant difference was found between P1 and P2 after all treatment levels (p = 0.016 | 0.004 | 0.033).

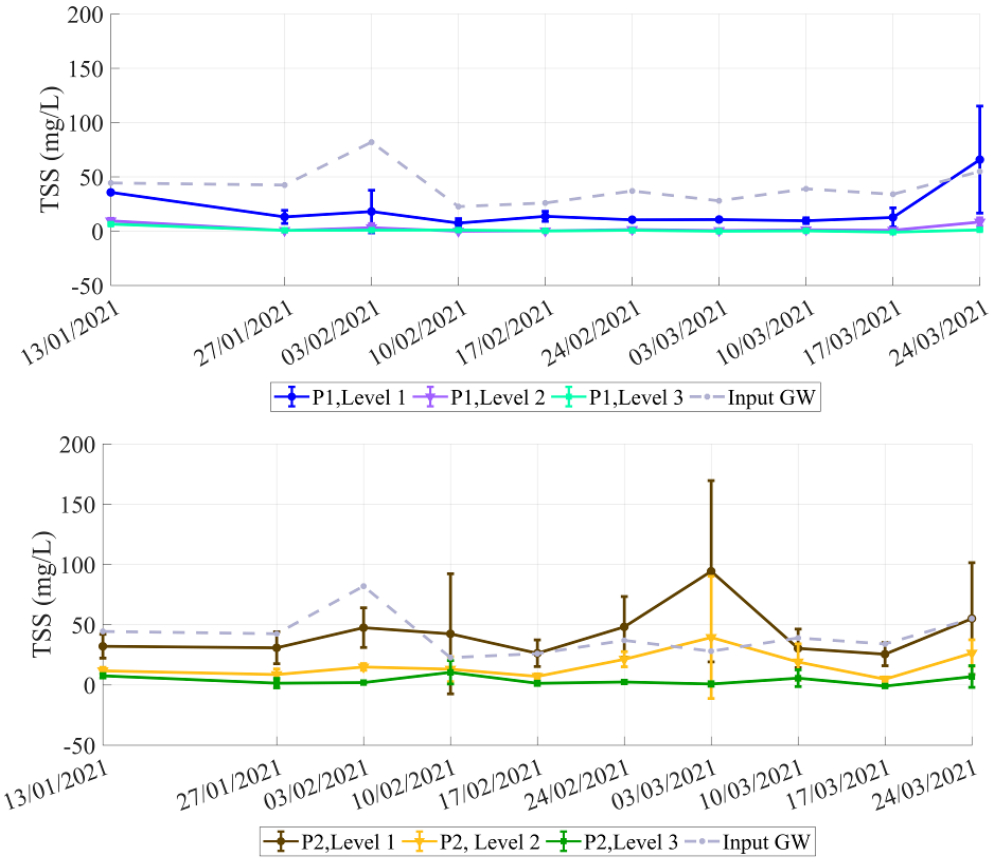

Figure 3.4.20. Concentration of total suspended solids (TSS) in output water samples and input GW for all the levels in P1 (top) and P2 (bottom).

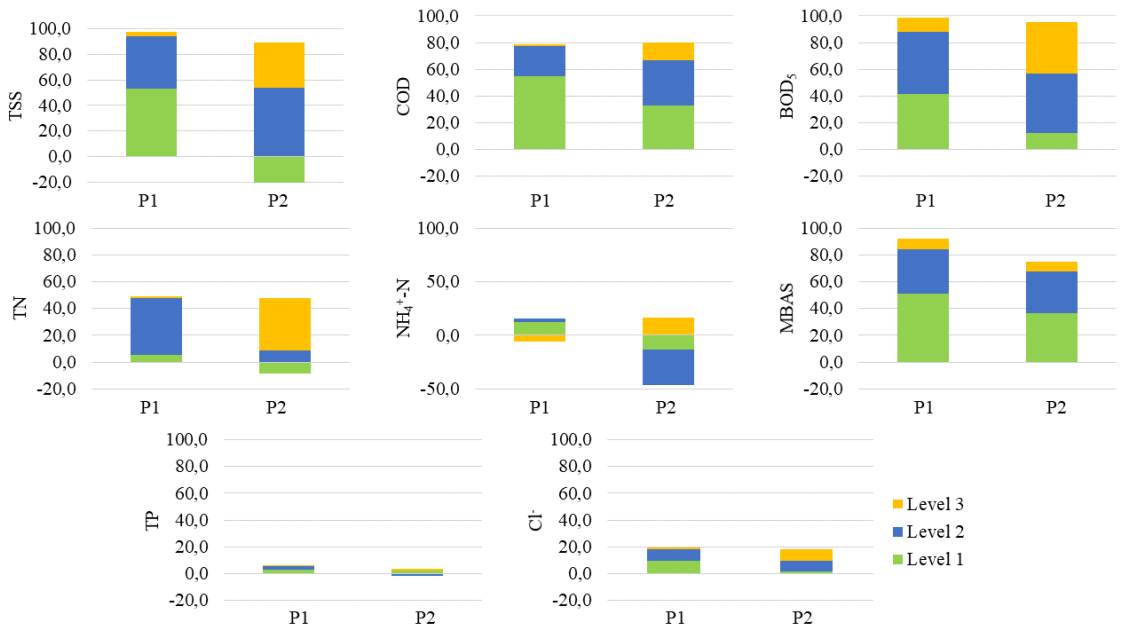

Figure 3.4.21. Average cumulative removal efficiency (%) obtained at the different levels of panels P1 (newer) and P2 (older) for total suspended solids (TSS), chemical oxygen demand (COD), biochemical oxygen demand (BOD_5), total nitrogen (TN), ammonia nitrogen (NH_4^+-N), methylene blue active substances (MBAS), total phosphorous (TP), chloride (Cl^-).

COD concentration decreased along the columns in both panels and no temporal trend was observed (Figure 3.4.22). P1 worked significantly better than P2 in the first and second levels, but the final output did not show any statistical difference between the two panels (average output of P1: 47.2±19.8 | 24.2±5.4 | 22.6±4.5 mg/L, P2: 70.8±19.3 | 35.3±12.1 | 20.8±1.4 mg/L). The input GW ranged between 74 and 153 mg/L, thus the overall removal efficiency reached 78.5±5.2% for P1 and 80.1±4.2% for P2 (Figure 3.4.21). These values are higher than the average values observed in the same system in a previous study (Boano et al., 2021a) and close to literature values (Kotsia et al., 2020; Prodanovic et al., 2020).

BOD_5 removal efficiency (Figure 3.4.21) was similar to literature values (Bakheet et al., 2020; Boano et al., 2021a; Fowdar et al., 2017; Gattringer et al., 2016; Kotsia et al., 2020) and both panels showed very good performances (45.2±36.2% | 86.5±14.8% | 98.8±2.4% in P1; 16.5±20.8% | 51.8±32.3% | 94.5±9.2% in P2), even though P1 performed significantly better than P2 for almost all levels ($p = 0.000 | 0.001 | 0.051$ for the three levels) (Figure 3.4.23). Only the second level of both panels showed an increasing BOD_5 removal over time, possibly due to the fast plant growth. Input GW ranged between 41.1 and 70.7 mg/L (the first sampled value of 10.4 mg/L was underestimated due to technical issues), with an average of 53.2±8.0 mg/L.

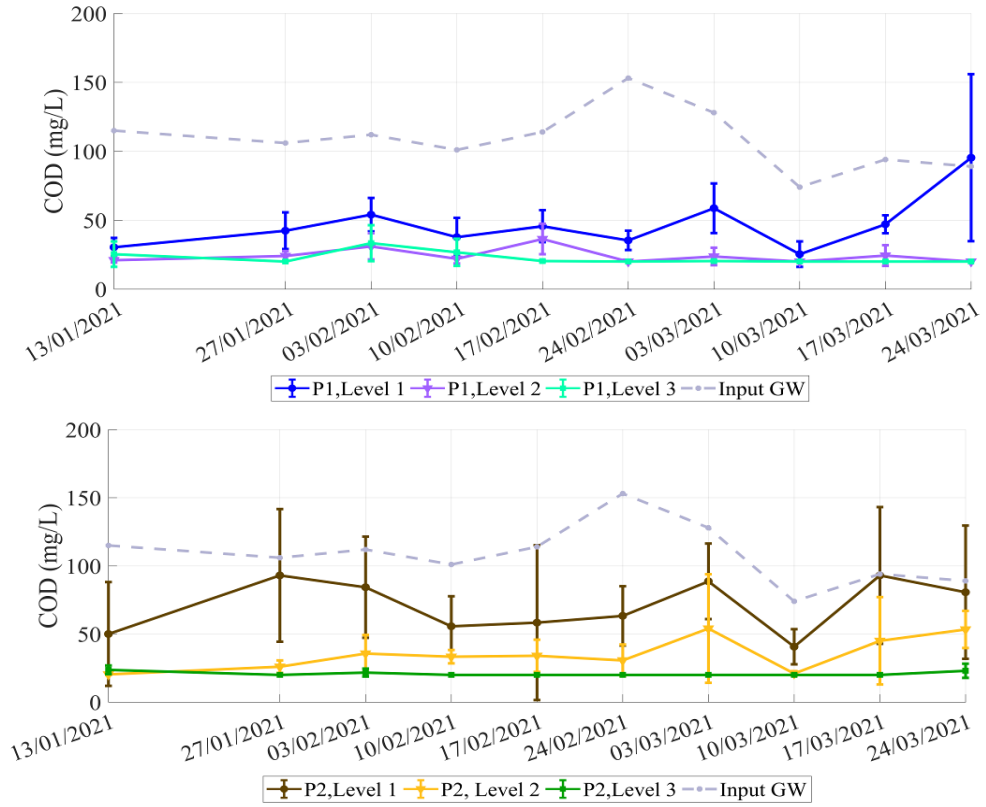

Figure 3.4.22. Concentration of COD in output water samples and input GW for all the levels in P1 (top) and P2 (bottom).

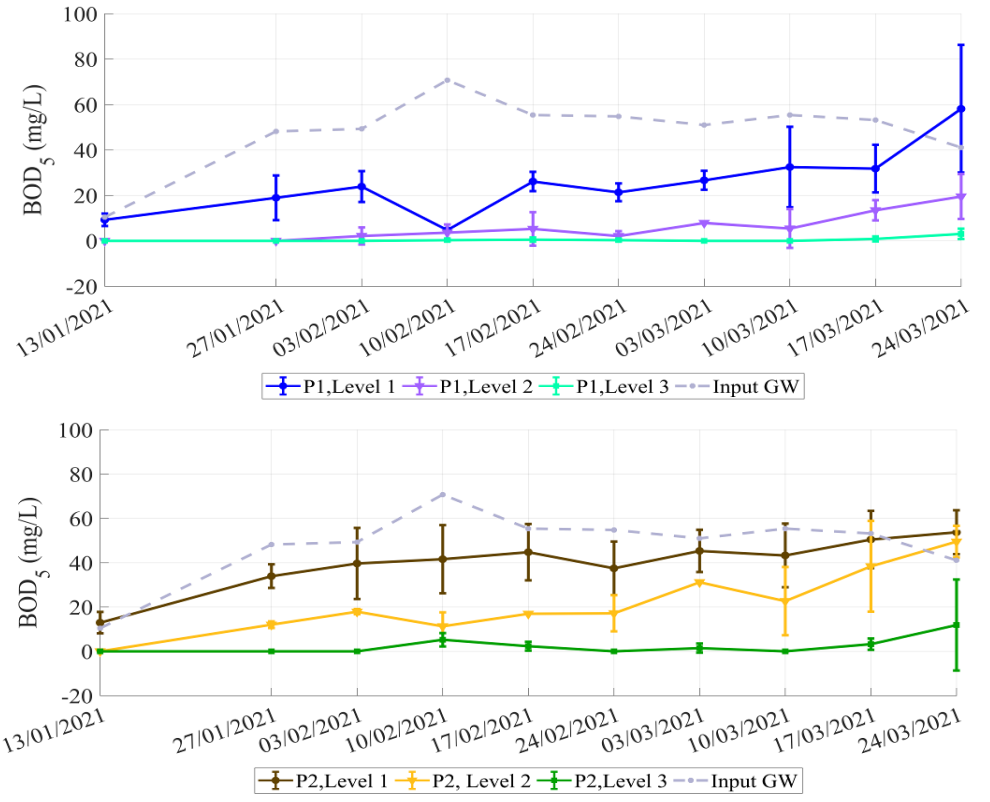

Figure 3.4.23. Concentration of BOD_5 in output water samples and input GW for all the levels in P1 (top) and P2 (bottom).

TN concentration ranged between 0.5 and 2.8 mg/L in input GW (average 1.57±0.66 mg/L) and decreased around 0.73 mg/L in output for both panels (Figure 3.4.24). TN removal did not show a temporal trend over time and both panels removed almost 50% (Figure 3.4.21), with no statistical difference in their total removal efficiency (average 49.2±30.4% P1, 48.0±23.3% P2). However, most removal in P1 occurred at the second level of treatment (5.5±75.2% | 47.9±25.9% | 49.2±30.4%) and the second level also performed significantly better in P1 than in P2 (-8.3±27.3% | 8.9±47.3% | 48±23.3%). P2 showed release of TN from the first level of pots, possibly due to releases of organic particles following some clogging events. NH_4^+-N had low input concentrations ranging between 0.30 and 0.37 mg/L, but they were often below the detection limit. Eventually, both panels reached concentrations below the detection limit. NO_3^--N concentration was almost always below the detection limit both in input and output of both panels, and hence provided no relevant contribution to TN concentration. All nitrogen compounds were characterised by very low values both in input GW and output treated water compared with literature results (Boano et al., 2021a; Fowdar et al., 2018, 2017; Jin et al., 2018; Prodanovic et al., 2020, 2018, 2017), possibly because the anoxic conditions in the GW storage tank enhanced nitrogen removal from GW.

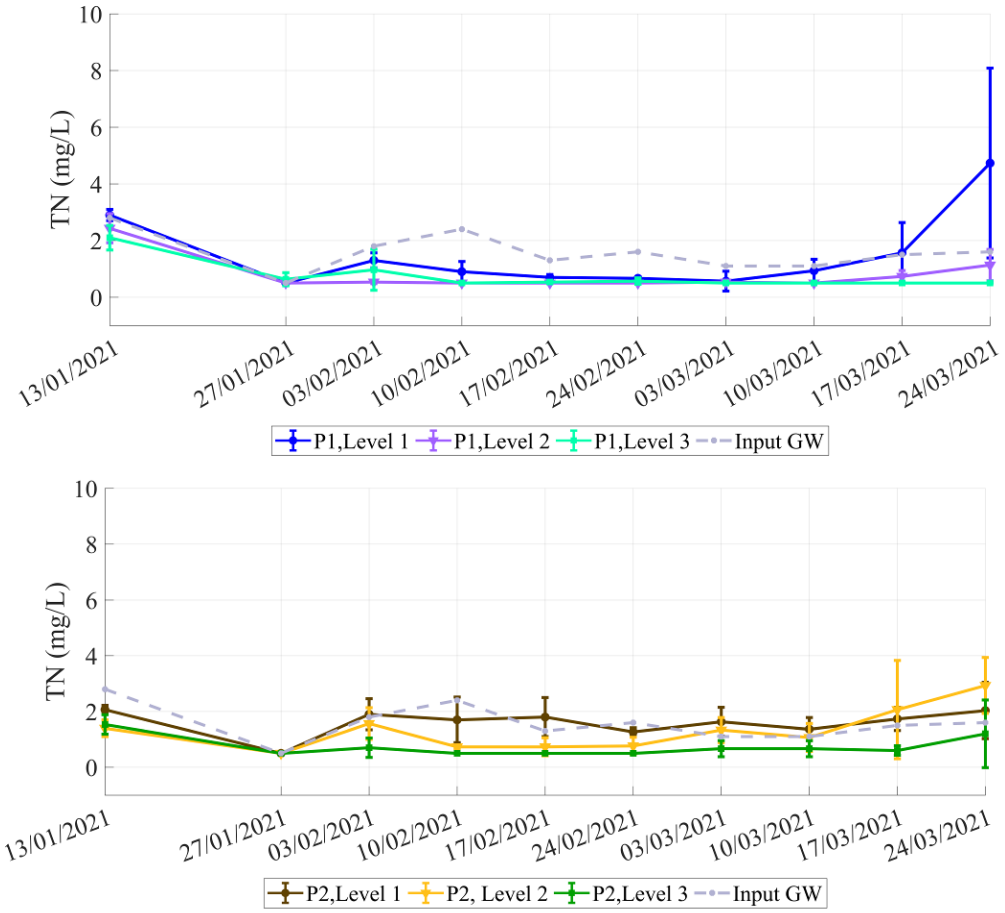

Figure 3.4.24. Concentration of total nitrogen (TN) in output water samples and input GW for all the levels in P1 (top) and P2 (bottom).

TP concentration ranged between 7.20 and 9.20 mg/L for input GW and the concentration was quite constant within the two panels (data not shown), as expected from literature (Prodanovic et al., 2020). Both panels kept their performances stable over time. P1 performed significantly better than P2 (P1: 3.1±5.5% | 5.7±3.5% | 5.8±2.8%; P2: 2.0±4.7% | 0.5±6.9% | 1.7±7.5%), especially in the second and third levels, even if the overall removal was moderate in both cases (Figure 3.4.21).

Chloride concentration was relatively stable from input GW (43.34±3.52 mg/L) to output (P1: 39.23±5.87 | 35.56±4.09 | 34.84±3.42 mg/L; P2: 42.67±4.45 | 39.38±5.60 | 35.61±3.80 mg/L), as expected from previous studies (e.g., Bakheet et al., 2020). Although a very low removal of Cl^- was observed, P1 removed significantly better than P2 in all levels (P1: 9.8±8.0% | 18.4±3.9% | 19.6±3.6%; P2: 1.6±5.1% | 9.4±7.5% | 17.9±3.4%) (Figure 3.4.21).

MBAS values in GW (10.50±6.27 mg/L, range 4.80-22.20 mg/L) were lower compared to previous studies (Hourlier et al., 2010) (Figure 3.4.25). The overall removal efficiency was excellent (92.7±3.8% and 75.3±8.0% for P1 and P2 respectively (Figure 3.4.21). No temporal trend was found for both panels, and P1 removed MBAS significantly better than P2 in all three levels, excluding the first sample that was not analyzed due to technical issues (P1: 51.0±23.2% | 84.6±12.3% | 92.7±3.8%; P2: 36.7±22.9% | 68.0±10.4% | 75.3±8.0%). Qualitatively, P1 and P2 showed a similar behaviour, with decreasing concentrations along the levels (P1: 4.36±2.64 | 1.76±2.35 | 0.81±0.74 mg/L; P2: 5.64±3.35 | 2.88±1.53 | 2.23±1.18 mg/L).

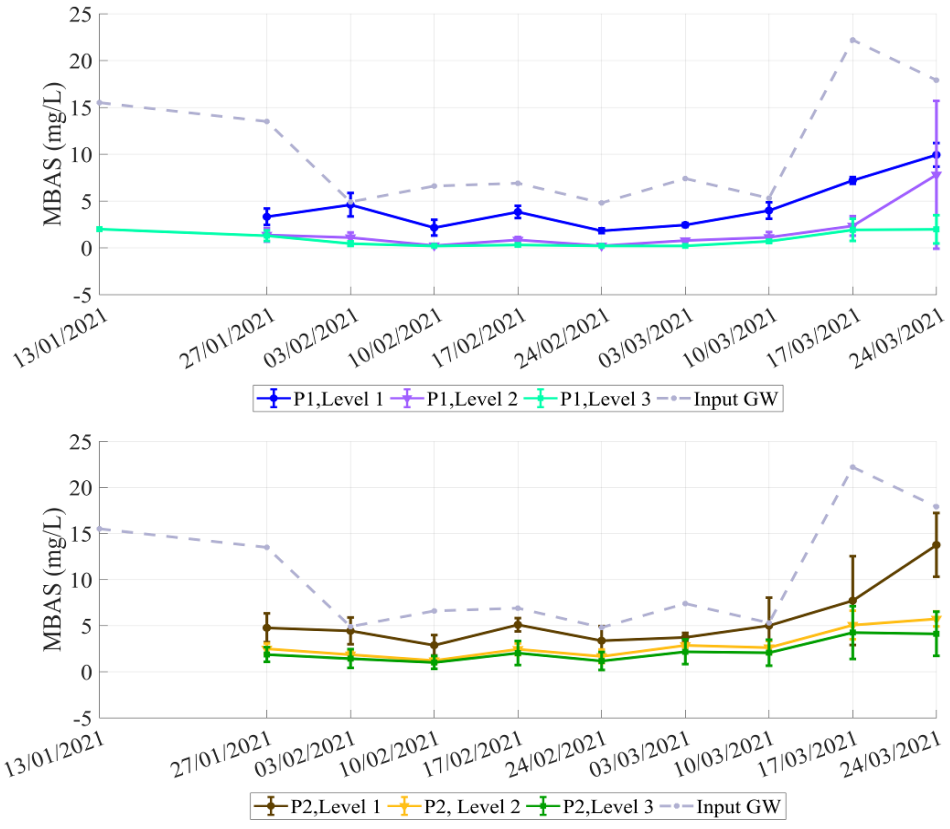

Figure 3.4.25. Concentration of methylene blue active substances (MBAS) in output water samples and input GW for all the levels in P1 (top) and P2 (bottom).

3.4.5 Phase 4

Results of phase 4 are still under analysis, but some preliminary consideration can be provided. This phase aimed to test the resilience of each level of the green wall to variable hydraulic loads due to different amount of people producing GW.

In general, all parameters confirm that the concentrations decrease along the columns, as in phase 3. Both panels reach a good oxygenation in all levels of outflow water (Table 3.4.4) regardless the feeding load. Also pH and EC did not show any dependency on the feeding load. pH stabilized at a slightly alkaline value along the column, while average EC remained almost constant (Table 3.4.4).

Table 3.4.4. Average and standard deviation (in parenthesis) over time of on-site parameters of input GW and outflow from each level.

Parameter	Input GW	Variable load panel			Constant load panel		
		Level 1	Level 2	Level 3	Level 1	Level 2	Level 3
T (°C)	19.29 (5.94)	17.04 (5.70)	16.26 (5.72)	16.26 (5.64)	16.98 (5.58)	16.27 (5.58)	16.22 (5.57)
DO (mg/L)	2.29 (1.71)	7.95 (0.90)	9.22 (1.09)	9.51 (1.17)	7.59 (0.96)	9.25 (1.07)	9.53 (1.18)
pH	7.09 (0.14)	7.31 (0.07)	7.63 (0.02)	7.87 (0.04)	7.20 (0.03)	7.50 (0.03)	7.76 (0.12)
EC (uS/cm)	702.40 (20.72)	700.51 (1.68)	697.27 (1.57)	693.69 (1.73)	707.49 (12.41)	705.56 (2.32)	701.16 (2.24)

Also the laboratory parameters confirm the trend seen in phase 3, with a strong reduction of concentration for TSS, BOD5, COD and MBAS along the columns (Table 3.4.5 The concentration of nitrogen compounds was in general quite low, and the outlet values reached the detection limit both for NO_3^--N and NH_4^+-N in most of the sampling dates.

Table 3.4.5. Average and standard deviation (in parenthesis) over time of laboratory parameters of input GW and outflow from each level.

Parameter (mg/L)	Input GW	Variable load panel			Constant load panel		
		Level 1	Level 2	Level 3	Level 1	Level 2	Level 3
TSS	54.25 (54.12)	8.77 (1.91)	2.18 (1.86)	1.20 (1.99)	10.30 (4.92)	1.38 (0.80)	1.03 (0.96)
BOD5	59.29 (17.15)	24.66 (5.51)	7.47 (3.06)	3.92 (1.57)	24.54 (5.38)	5.26 (1.57)	3.09 (2.16)
COD	120.07 (34.92)	41.69 (6.98)	23.82 (6.84)	20.82 (2.30)	40.00 (10.96)	20.31 (2.09)	20.11 (0.75)
TP	8.82 (1.80)	7.79 (1.24)	7.77 (0.44)	7.69 (0.16)	8.22 (0.53)	8.18 (0.59)	8.10 (0.24)
TN	1.75 (0.93)	0.84 (0.21)	0.53 (0.11)	0.59 (0.33)	0.87 (0.20)	0.63 (0.41)	0.54 (0.25)
NO_3^--N	0.30 (0.93)	0.30 (0.02)	0.30 (0.00)	0.30 (0.00)	0.30 (0.00)	0.30 (0.00)	0.30 (0.00)
NH_4^+-N	0.08 (0.08)	0.04 (0.00)	0.04 (0.00)	0.04 (0.00)	0.05 (0.03)	0.04 (0.02)	0.04 (0.00)
MBAS	24.07 (8.46)	8.89 (2.30)	3.19 (1.06)	1.54 (0.30)	8.44 (2.73)	2.08 (1.62)	1.32 (1.49)
Cl^-	51.31 (11.58)	40.43 (0.99)	38.20 (0.72)	37.93 (0.47)	40.49 (0.85)	37.96 (0.40)	37.98 (0.93)

The variable load did not show any impact when underload (HLR=395 $Lm^{-2}d^{-1}$) was performed. No particular differences in concentration decreasing patterns were observed neither during nor after this period. On the other hand, the overflow (with HLR=1136 $Lm^{-2}d^{-1}$) impacted negatively on treatment performances in the first and second levels in important parameters such as TSS, BOD_5 and COD. Figure 3.4.26,Figure 3.4.27 and Figure 3.4.28 show the comparison between the variable load panel and the constant panel over time for these three parameters. Furthermore, plants started to suffer due to excessive moisture caused by the overload but they completely recovered after two weeks of standard load. However, it is important to highlight that the overload was tested to simulate an anomalous volume of greywater (36.8 $Lcol^{-1}d^{-1}$) that represent a very large amount of water that could depend on particular events in the buildings. Furthermore, the overload HLR was very high because of the high standard HLR that was chosen in the experiments.

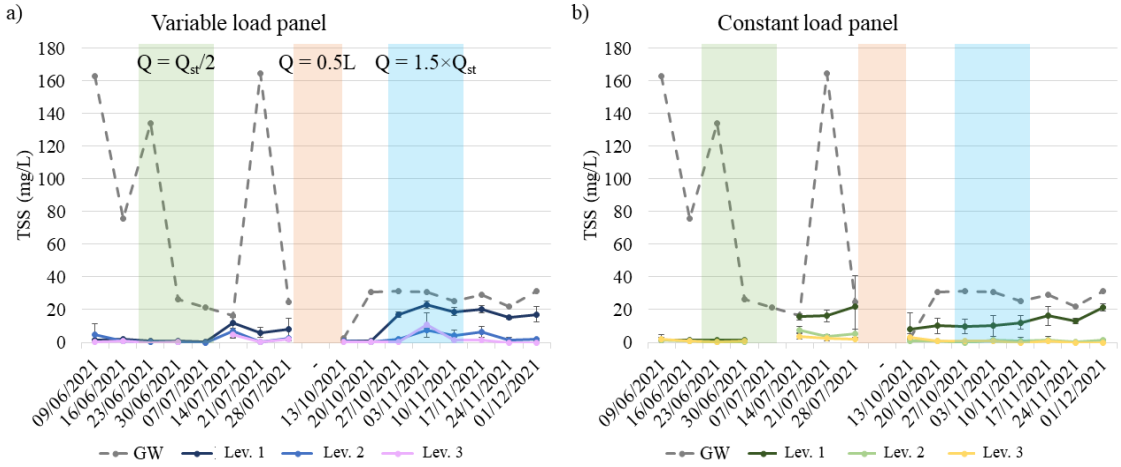

Figure 3.4.26. Comparison between outflow of variable load panel (left column) and constant load panel (right column) for TSS. Highlighted areas show help the visual comparison of the two panel during the different loading rate.

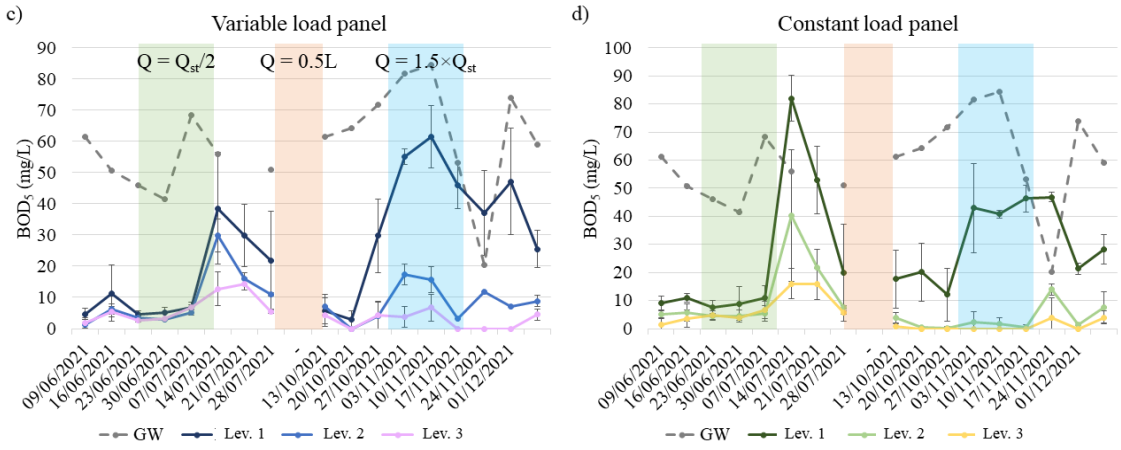

Figure 3.4.27 Comparison between outflow of variable load panel (left column) and constant load panel (right column) for BOD_5. Highlighted areas show help the visual comparison of the two panel during the different loading rate.

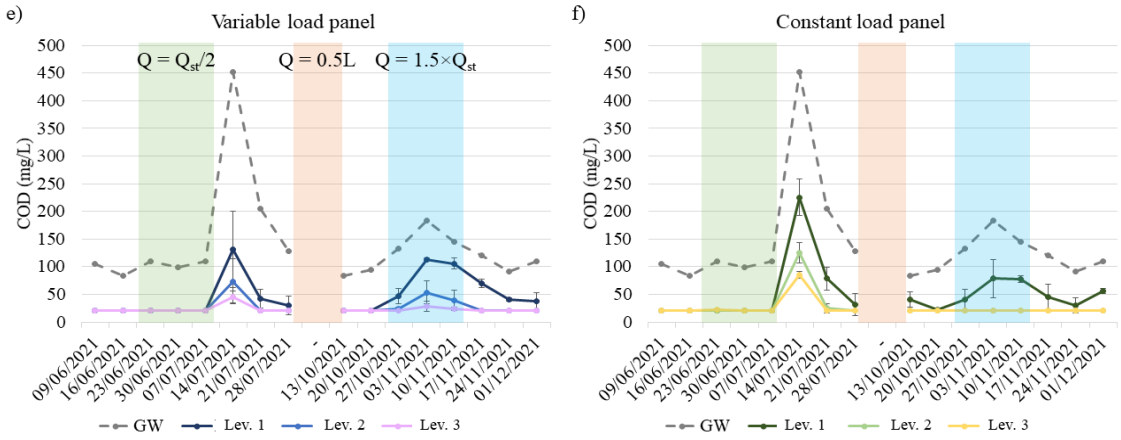

Figure 3.4.28. Comparison between outflow of variable load panel (left column) and constant load panel (right column) for COD. Highlighted areas show help the visual comparison of the two panel during the different loading rate.

Input and output concentrations of all the four experimental campaigns are available in table format in Appendix B.

♦ Photographical method

This part of the work was developed in collaboration with Dr. Vincent Gagnon and Dr. Florent Chazarenc. During their years at École Polytechnique de l'Université de Nantes, they developed an innovative photographical method to reach a better understanding of the biological processes into CWs at mesocosm scale.

4.1 Mesocosms set up

The experiment was conducted in Nantes in 12 transparent HSSF CWs (56.5 x 19.5 x 74.5 cm) made of 1 cm thick acrylic sheet. The HSSF CWs were filled with 60 cm of transparent 1-4 mm glass sand (Ovive SA – Sable de verre cristal) and with 5 cm of 1.0-2.5 mm white sand (Ovive SA – Sable Quartz) at the surface to prevent algae development. The exterior of the CWs was covered with black plastic and insulation (5 cm polystyrene foam) to prevent algae and heating. The feeding tube consisted of a 10 cm PVC pipe installed vertically which had horizontal slits (about 1 mm) every 5 cm that permitted the wastewater to flow horizontally through the CWs. The outlet was located at the bottom on the other side of the CWs and connected to an over flow, keeping the CWs saturated at 60 cm Figure 4.1.1.

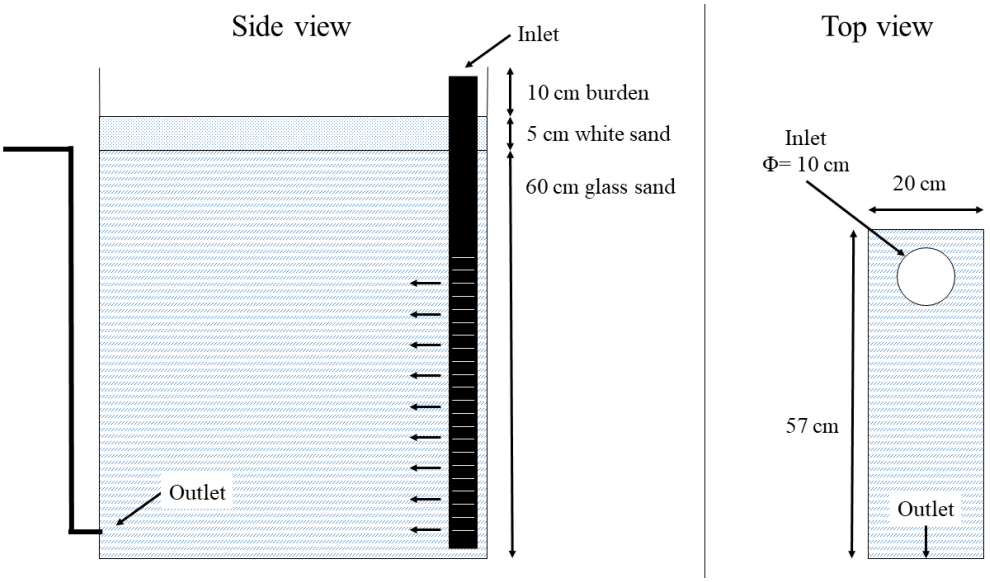

Figure 4.1.1. Scheme of the mesocosm, side and top view.

The CWs were fed with 5 Ld^{-1} of synthetic wastewater (OECD 303) for 5 days per week with a loading rate of 16 g COD $m^{-2}d^{-1}$ and a theoretical hydraulic retention time of 7 days. The CWs were planted in triplicates with *Phragmites australis*, *Typha angustifolia*, *Phalaris arundinacea,* and three were left unplanted as a control. The CWs were planted in March 2014 on the roof of the university (École des Mines de Nantes, Nantes, France) and the microbial enzymatic activities were measured in July-August 2014 and in June-July 2015.

In order to allow a following phase of validation, two types of elements were added to the systems: 25 metallic mesh cylinders (Φ=2 cm, depth 4 cm, white back) were placed as targets on the CWs surface; six small tubes (Φ=1 cm) were also placed at different depth in the middle of the CWs and in the front corner to collect water samples.

4.2 Collection of the pictures

This innovative photographical method uses the properties of fluorescein diacetate (FDA) to measure enzymatic activity inside the CWs, along space and time. FDA (3'6'-diacetyl-fuorescein) is a transparent molecule containing a fluorescein flank by two acetates. Microbial enzymes, free and bound to cell membrane, hydrolyse the transparent FDA into bright fluorescein, whose fluorescence can be measured and correlated to the enzyme activity (Adam and Duncan, 2001). At neutral pH in water, fluorescein has absorption peaks in the UV (239, 283, 322 nm) in addition to blue spectrum (475 and 490 nm) and emission peak in the green spectrum (515 nm; Sjoback et al. 1995).

A black box made of metal scaffolding (140 x 74 x 115 cm) covered by two layer of corrugated black plastic sheets (4 mm thick each) was built, to be able to measure the fluorescence with a digital camera in the outdoor setting. The black box was pushed against one of the transparent side of the CWs. A thick black blanket was used to cover the box and filled the gap between the CW mesocosm to prevent light to enter the box. The interior of the box could be illuminated with white light (using two neon tubes) or with UV light (mercury vapor light bulbs 300–400 nm). All lights were placed on each side of the box in order to avoid or minimize the reflection of light on the CW (Figure 4.2.1).

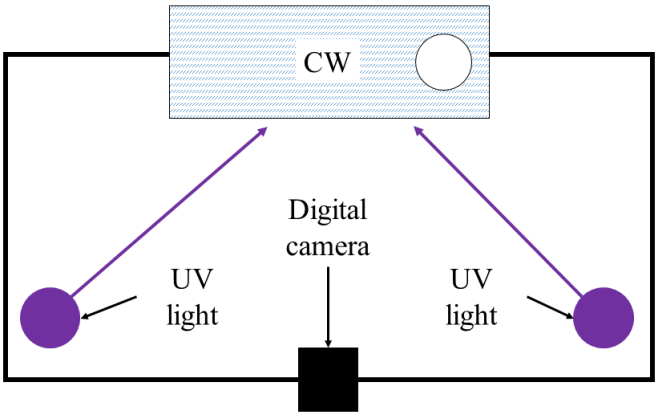

Figure 4.2.1. Schematic top view of the black box around the wetland, location of camera and UV-light.

On the opposite side of the black box a digital camera (Canon EOS 400D Digital Rebel XTi) was set on a tripod at 72 cm from the CW aiming directly at the centre of the CW with a 35 mm lens (no zoom). The digital camera was set to manual, 100 ISO, f-stop 7.1 and the exposition time was of 1/3 s for the pictures taken under white light and 13 s for the images taken under UV-A light. A UV filter (Amber C, Solar Screen) was placed in front of the lens during the enzymatic measurement under UV-A light to filter out any dark purple colour coming from the UV lamp. Photos were taken every 15 to 30 seconds under UV-A light for about one hour using Canon EOS DIGITAL camera software. The pictures were saved in the camera RAW format (.CR2) in order to avoid compression. The group of pictures of a CW collected in the same hour will be hereafter named as *series*.

During this thesis work, the pictures were converted in 16-bit .TIFF using an automatized procedure in ImageJ software, with no white balance correction. All the further analyses on the images have been digitally performed using a Matlab script specifically developed for this study.

4.3 Calibration

The aim of the calibration process is to find the equation to convert the green fluorescent intensity present in the image under UV-A light to a concentration of fluorescein produced with time. Since the production of fluorescein results from the degradation of FDA by enzymes, the correlation rising from the calibration will transform the CWs image into a high resolution 2D map (width and depth) of the enzymatic activity within the CW.

Some preliminary tests were conducted in Nantes performed in unplanted pots at small scale to define the design of the mesocosm systems observing the fluorescein response to UV-A light. Different types of sands (crable white, fine white, black, impure glass and pure glass) were tested to choose the one with a better optical response, resulting in the pure glass sand. Furthermore, the range of pH in which CWs operate was tested to verify the influence of fluorescein responsivity to small pH variations (Sjoback et al., 1995), resulting in no relevant impact within this range. Then, the presence of a black precipitate in the CWs was revealed. This substance was supposed to be iron sulfide (FeS) due to its colour, presence at low redox locations and the typical smell of HS precursor. This precipitate partly covered the transparent glass sand and was spatially heterogeneous within the CWs. This changed the optical properties of the substrate from transparent to different shades of grey and quenched the green fluorescence intensity according to the localised precipitate concentration. Therefore, the calibration needed to take into account the optical response of different concentration of FeS precipitate within the CWs to convert the green fluorescent intensity from the CW image to fluorescein concentration.

4.3.1 Calibration of FeS optical effects in white light

The aim of the FeS calibration process is to find an equation correlating the greyscale light intensity present in the image to a concentration of precipitate in the CWs. This will

allow to make a 2D map of the CW (width and depth) of the FeS concentration and correct for quenching of the fluorescence by FeS (see fluorescein calibration). The calibration is done by imaging a series of small acrylic containers (4.5 x 4.5 x 8 cm) filled with transparent glass sand (1-4 mm Ovive SA – Sable de verre cristal) and containing a known concentration of FeS (0.00, 0.81, 1.61, 4.82, 8.04 and 16.07 mg/L). Each container was filled from the bottom to prevent trapping of air bubbles, using a 4 mm tube placed vertically. The image of the calibration container (Figure 4.3.1) was taken using the photographic method stated previously under white light (WL). Image of the FeS calibration container was processed in Matlab with the following steps:

1) The 16-bit .TIFF image was converted in greyscale

2) For each FeS concentration a representative area of the image was selected (excluding region of light aberration or anomalous FeS precipitate)

3) The average and standard deviation of the grey scale intensity of this area was calculated, with the Digital Number (DN in each pixel, where 0 is black and 65535 is white).

The relation between DN under white light (I_{WL}) and FeS concentration was interpolated with a two parameters exponential curve (eq. 1), due to the observed non-linear response of intensity to FeS concentration:

$$I_{WL} = a \times e^{b[FeS]} \qquad (1)$$

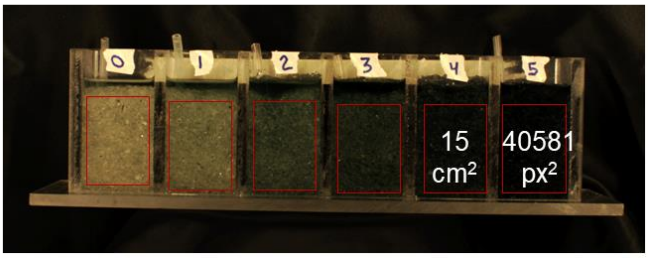

Figure 4.3.1. Picture for the calibration in white light. Each box contains glass sand saturated with different concentrations of FeS. Image in greyscale at +70% brightness.

4.3.2 Fluorescein optical response

The fluorescein calibration was done with the same small containers as before, but the images were taken under UV-A light condition (Figure 4.3.2). This calibration aims to provide an equation to correlate the intensity of the green band to the concentration of fluorescein at different FeS concentrations. Thus calibration curves were made with fluorescein concentration of: 0 mg/L, 1 mg/L, 2 mg/L, 3 mg/L, 4 mg/L, 5 mg/L at the following FeS concentration: 0 mg/L, 0.81 mg/L, 1.61 mg/L, 4.82 mg/L, 8.04 mg/L, 16.07 mg/L. Higher concentrations of FeS (i.e. 24.11 and 40.65 mg/L) were also tested, but the images were too dark to obtain any reliable information. The calibration images were analysed following the same procedure of the FeS calibration (paragraph 4.3.1), but

the green DN of the RGB image was used instead of greyscale, in order to consider only the wavelength emitted by the fluorescein.

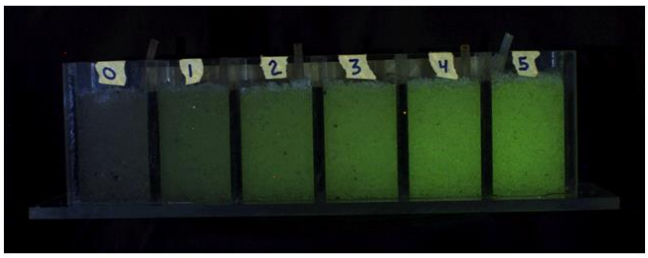

Figure 4.3.2. Picture for the calibration in UV-light. Each box contains glass sand saturated with different concentrations of fluorescein. Image in greyscale at +80% brightness.

This analysis highlighted the linear correlation between the light intensity (measured as average DN) and the fluorescein concentration. The presence of FeS gave a non-linear contribution to the correlation, affecting the slope of the correlation lines. In order to consider both contributions in the following CWs mapping, a 3D non-linear equation has been proposed in this thesis to relate the concentration of the two compounds (Eq. 2).

$$I_{UV} = c \times e^{d[FeS]} \times [f] \quad (2)$$

Occasional outliers have been ignored during the fitting procedure when evident and recognizable errors were visible in the corresponding picture (e.g. wrong dilution, external light intrusion).

4.4 CW's picture processing

A minimum of three images were needed for the analysis of each CW: 1) the image of the rhizosphere taken under white light (WL), which was used to map the distribution of the FeS and the roots, 2) the UV image taken at time 0 (UV_0), when the CW was just filled up with FDA solution and 3) at least one UV image of the sampling *series* taken at any moment after time 0 (UV_N). In this thesis, a manual selection was firstly done to exclude all pictures accidentally affected by external sunlight. The selected pictures were then converted in 16-bit .TIFF format with an automatic procedure in ImageJ. The following steps were performed using a customised Matlab script.

UV_N were compared with the UV_0 by subtraction to better recognise aberrations on some images that were not identified with the previous selection, thus the affected images were discarded. Furthermore, the subtraction highlighted that many pictures were not perfectly aligned (Figure 4.4.1), probably due to windy conditions during the shooting. Thus, UV_0 was aligned to WL picture by manually selecting matching points, then an automatic script was prepared to align all UV_N pictures to the UV_0 picture. In this way, the image treatment in the following steps was correctly performed in the same area of the CW, for all the N images without further manual intervention. In few cases the original pictures were already aligned, thus they were chosen for the following processing instead of the treated one.

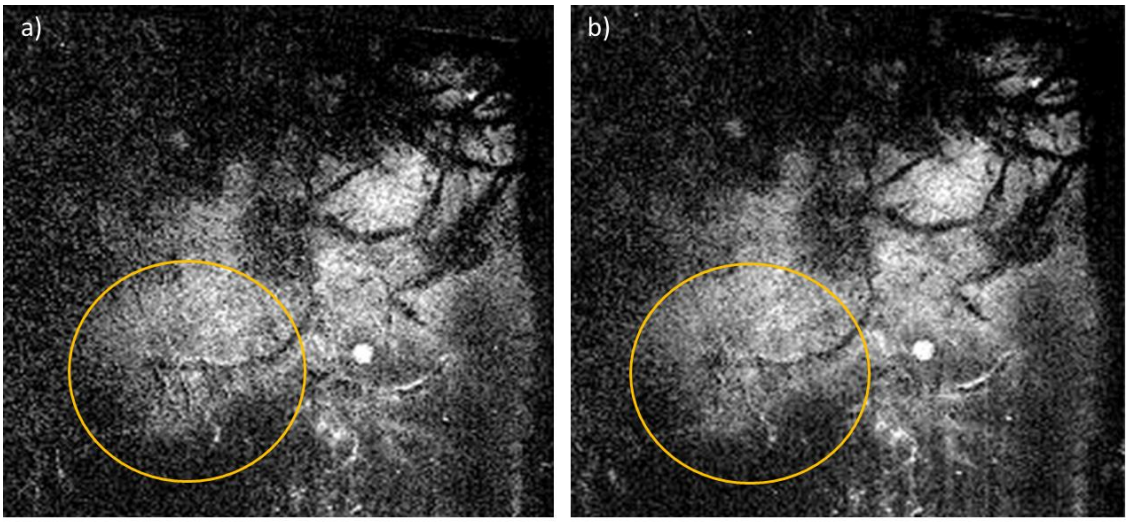

Figure 4.4.1. a) subtraction of UV_0 from a non-aligned UV_N. b) subtraction of UV_0 from the same UV_N after alignment.

The WL image was converted in a grey scale image and the green band of the UV-light images were extracted. The interested area was selected into a frame (Figure 4.4.2) and UV_0 was subtracted to all UV_N, in order to remove the background (roots, sand, etc.) and only show the fluorescence emitted at time N.

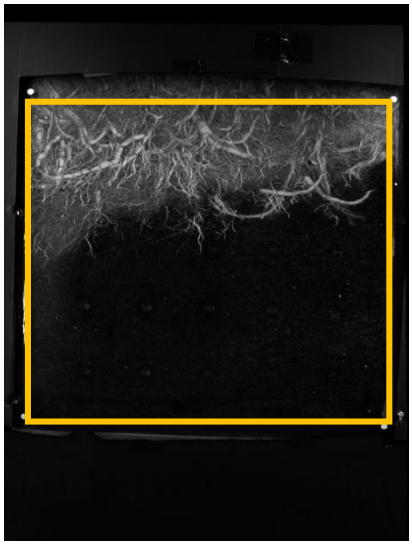

Figure 4.4.2. Selecting frame to cut the area of interest.

A pixel-by-pixel analysis would have not been significant due to the digital process of picture acquisition: the sensor of the camera is made up of a matrix of pixel that are sensitive to light, and each pixel collects the information of a specific band colour (Red, Green, or Blue - RGB) to allow the interpolation in each band when the whole picture is digitally developed. For this reason, the spatial resolution of the analysed area was decreased of 5%: the area has been divided in regular squares in a grid by 20x20 pixels and the average DN of each square has been calculated; this value was then assigned to all the pixels in the corresponding square (Figure 4.4.3).

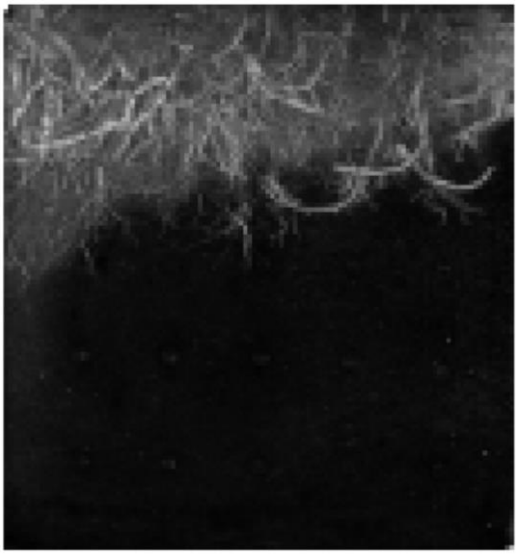

Figure 4.4.3. White light image after resolution decreasing. The image has been brightened to favour the visualisation of this step.

From the WL image of the CW, FeS concentration was determined in each pixel using the non-linear calibration equation (1). Because Eq. (1) relies on average values of light intensity, negative values of FeS concentration were occasionally found and have been set to [FeS] = 0 mg/L (Figure 4.4.4-a). Eq. (2) was applied to the resulting matrix of digital numbers and adjusted according to the FeS concentration to build enzymatic activity maps from each UV_N image (Figure 4.4.4-b).

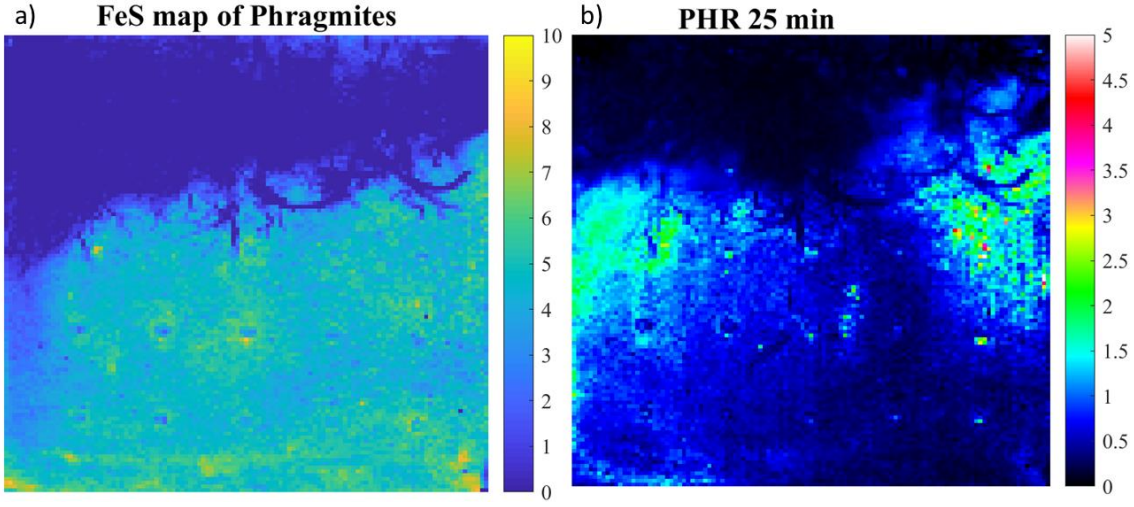

Figure 4.4.4. a) FeS concentration map from WL image in grey scale. b) Fluorescein concentration map from UV-A image at 25 minutes.

The flow chart in Figure 4.4.5 summarises the picture processing.

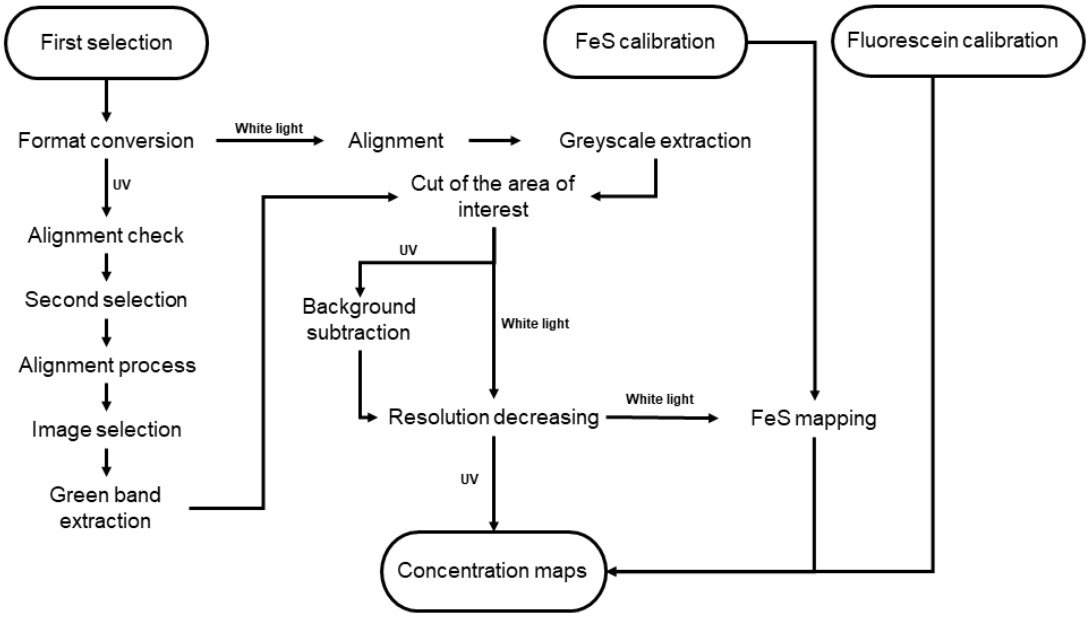

Figure 4.4.5. Flow chart that summarizes the picture processing to build concentration maps.

♦ Results of photographical method

5.1 Calibration

5.1.1 Influence of FeS

Data interpolation allows to set the coefficients for the calibration curve that relates light intensity in greyscale images to the concentration of FeS (Eq. 3).

$$I_{WL} = 5176.9 \times e^{-0.3632[FeS]} \quad (3)$$

The highest concentrations result in more uncertainties due to the higher degree of overlapping between standard deviations, thus the optimal range to evaluate FeS concentration remains between 0 and 8 mg/L (Figure 5.1.1). This calibration curve is preliminary use to build a 2D map of FeS concentration in the CWs before collecting the pictures under UV light.

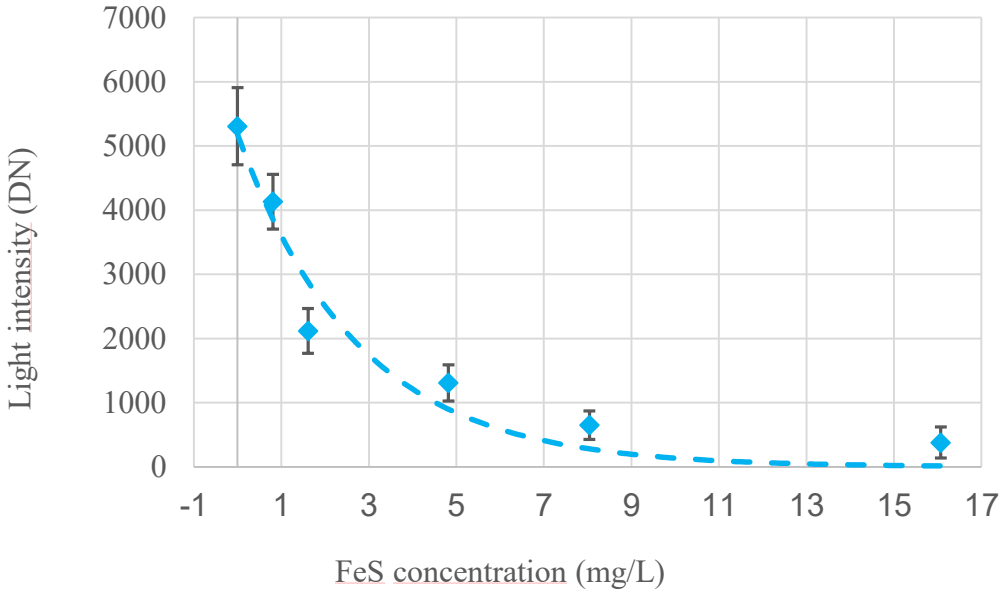

Figure 5.1.1. Correlation curve of FeS concentration in white light.

5.1.2 Fluorescein

The light intensity response to fluorescein under UV light follows a linear relationship with the fluorescein concentration (Figure 5.1.2), but the slope of this correlation varies with the interference of FeS concentration. Thus, Eq (4) takes into account both linear and non-linear relations. In order to build an equation with physically based coefficients, the 0 mg/L fluorescein concentration must correspond to $I_{UV} = 0$, since during picture processing the background light of mesocosms (e.g. roots, sand) is digitally removed by subtraction (see paragraph 4.4).

$$I_{UV} = 481.8 \times e^{-0,3473[FeS]} \times [f] \qquad (4)$$

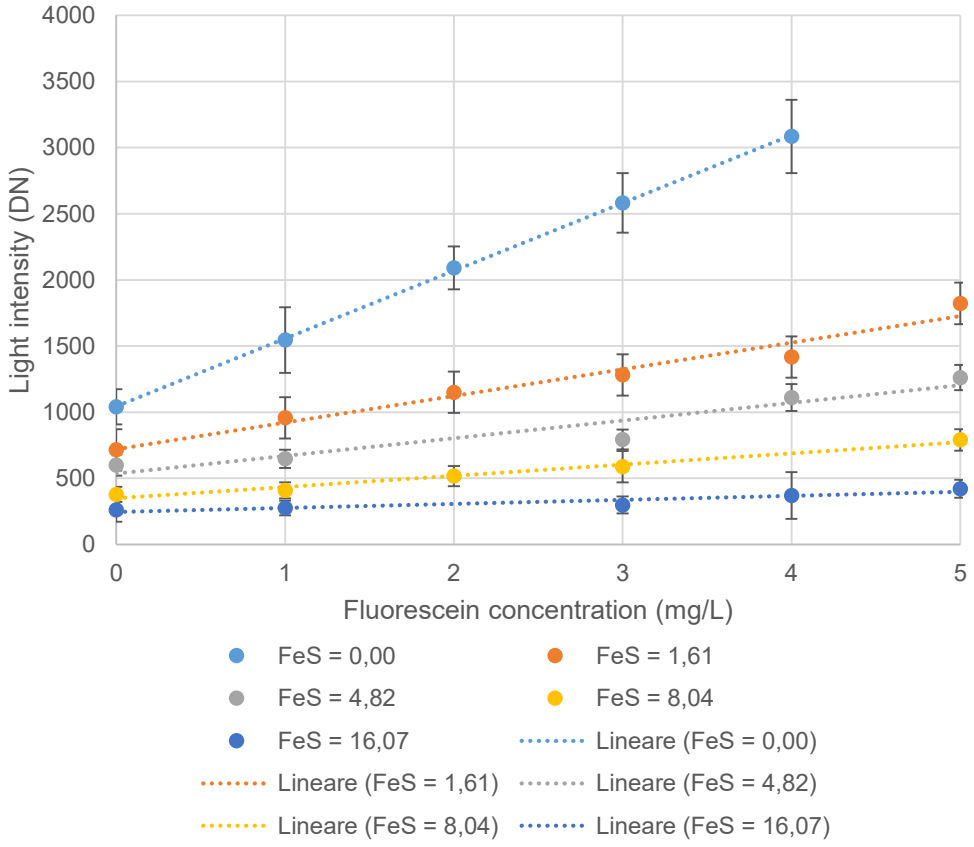

Figure 5.1.2. Correlation curve of fluorescein light emission at different concentration in UV light.

5.2 Picture selection and alignment

The sampling campaign was performed twice (in 2014 and in 2015) but not all CWs were pictured in both times nor the images had enough quality to be analysed. All available images were checked and three series of the 2014 campaign, one replicate per plant species, were chosen for further processing.

The multiple steps of selection and alignment of pictures lead to analyse 25%, 15% and 72% of the collected pictures for the *Phragmites*, *Phalaris* and *Typha* series,

respectively. Figure 5.2.1shows the distribution of analysed picture over time for the three mesocosms after picture selection with the quality criteria explained in chapter 4.4.

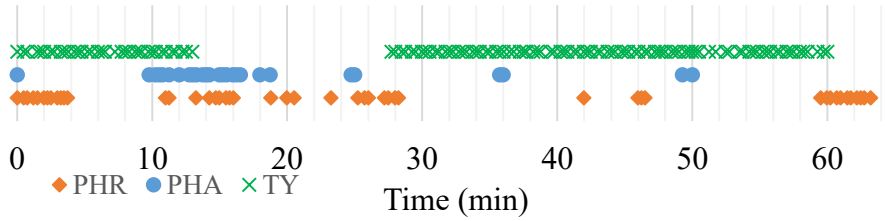

Figure 5.2.1. Timeline of the analysed picture per each series.

5.3 FeS maps

Figure 5.3.1 shows the concentration maps for FeS precipitate in the three analysed mesocosms. The distribution of FeS at higher concentrations is not uniform, but it is instead located differently in the three systems: at the bottom in the *Phragmites* mesocosm, mainly in the centre in the *Phalaris* mesocosms and following a diagonal from input (on the right) to output (on the left) in the *Typha* mesocosms.

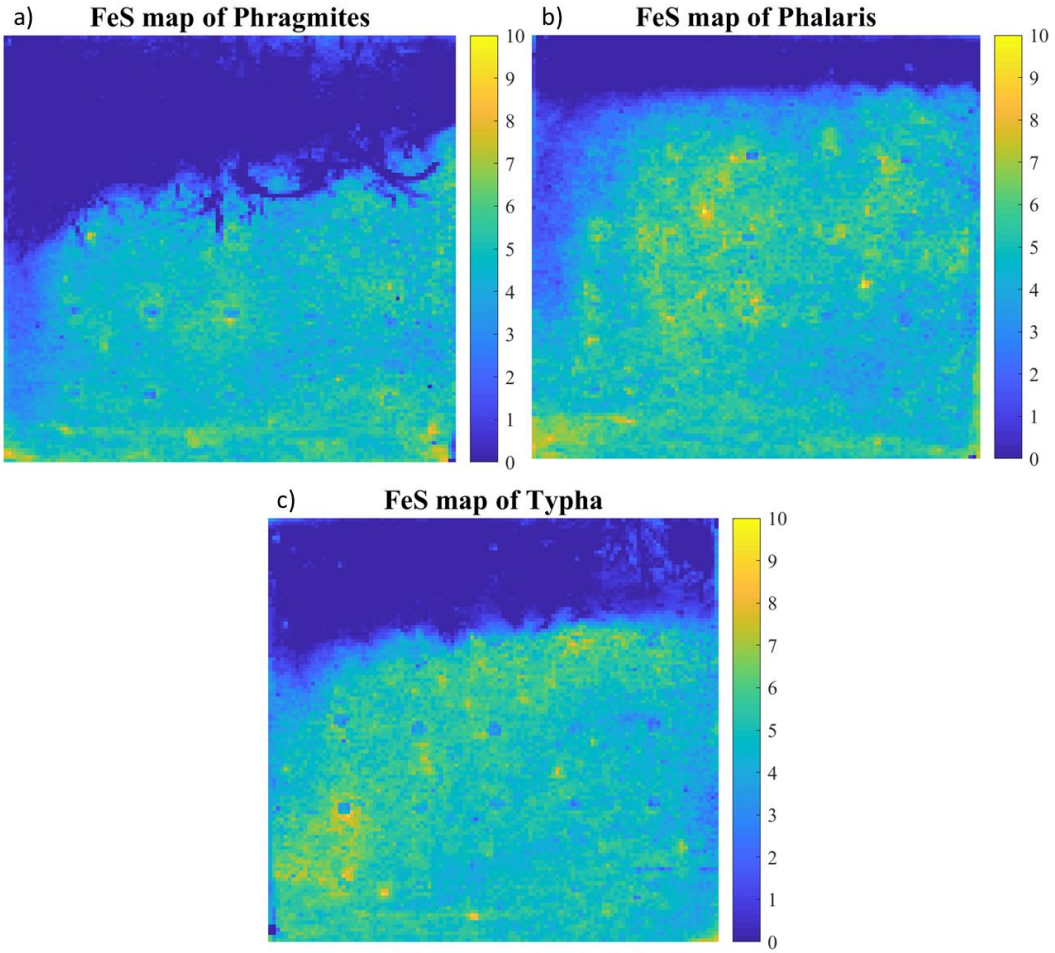

Figure 5.3.1 Examples of maps of FeS concentration for a) *Phragmites australis,* b) *Phalaris arundinacea* and c) *Typha angustifolia.*

5.4 Enzymatic activity maps

The enzymatic activity maps are represented as a proxy by the spatial distribution of fluorescein development along time. The method correlates the light emission with the fluorescein concentration. In the following paragraphs the fluorescein concentration maps are qualitatively presented and some examples of possible further analysis are provided.

Figure 5.4.1 shows an extract of the time series of one analysed mesocosm planted with *Phragmites australis*. After picture selection, 46 pictures were analysed, covering one hour in non-regular intervals. The first analysed picture was 0.5 min after shooting started and the last one was 63 minutes after its conclusion. Most of the activity is located close to the roots and develops quite fast, as indicated by the variation in fluorescein concentration within a few tens of minutes. A zone of intense reaction can also be observed close to the outflow (clearly visible from minute 42; Figure 5.4.1.d in the bottom left area).

Figure 5.4.2 shows a part of the time series of one analysed mesocosm planted with *Phalaris arundinacea*. After picture selection, 26 pictures were analysed in the time interval of 40 minutes, beginning with the first after 10 minutes of shooting start and ending at the 50th-minute shot. The quality of these pictures produced a few light aberrations in some pixels (visible as small green and yellow points in the concentration maps), and the dark area in the right portion of each map could be a shadow due to imperfect coverage of the external light. However, it is clear that most of the reaction (thus the most of enzymatic activity) is found close to the root zone and close to the outflow on the left.

Figure 5.4.3 shows an extract of the time series of one analysed mesocosm planted with *Typha angustifolia*. After picture selection, 125 pictures were analysed, covering one hour in non-regular intervals. Also in this case, most of the activity develops close to the roots, mostly at the inlet side (on the right).

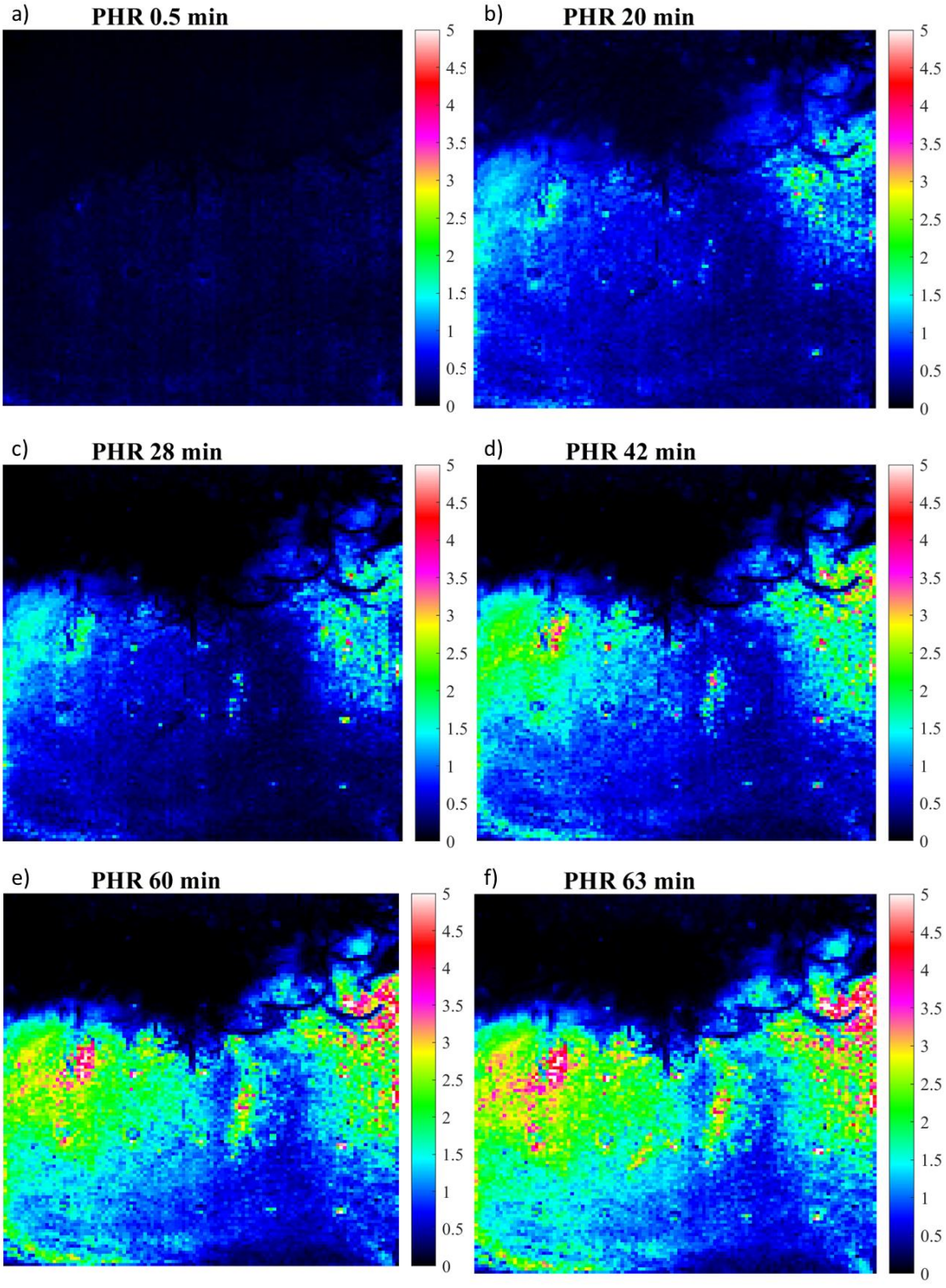

Figure 5.4.1. Extract of time series of fluorescein concentration maps for *Phragmites Australis*, from the first to the last available UV-light pictures.

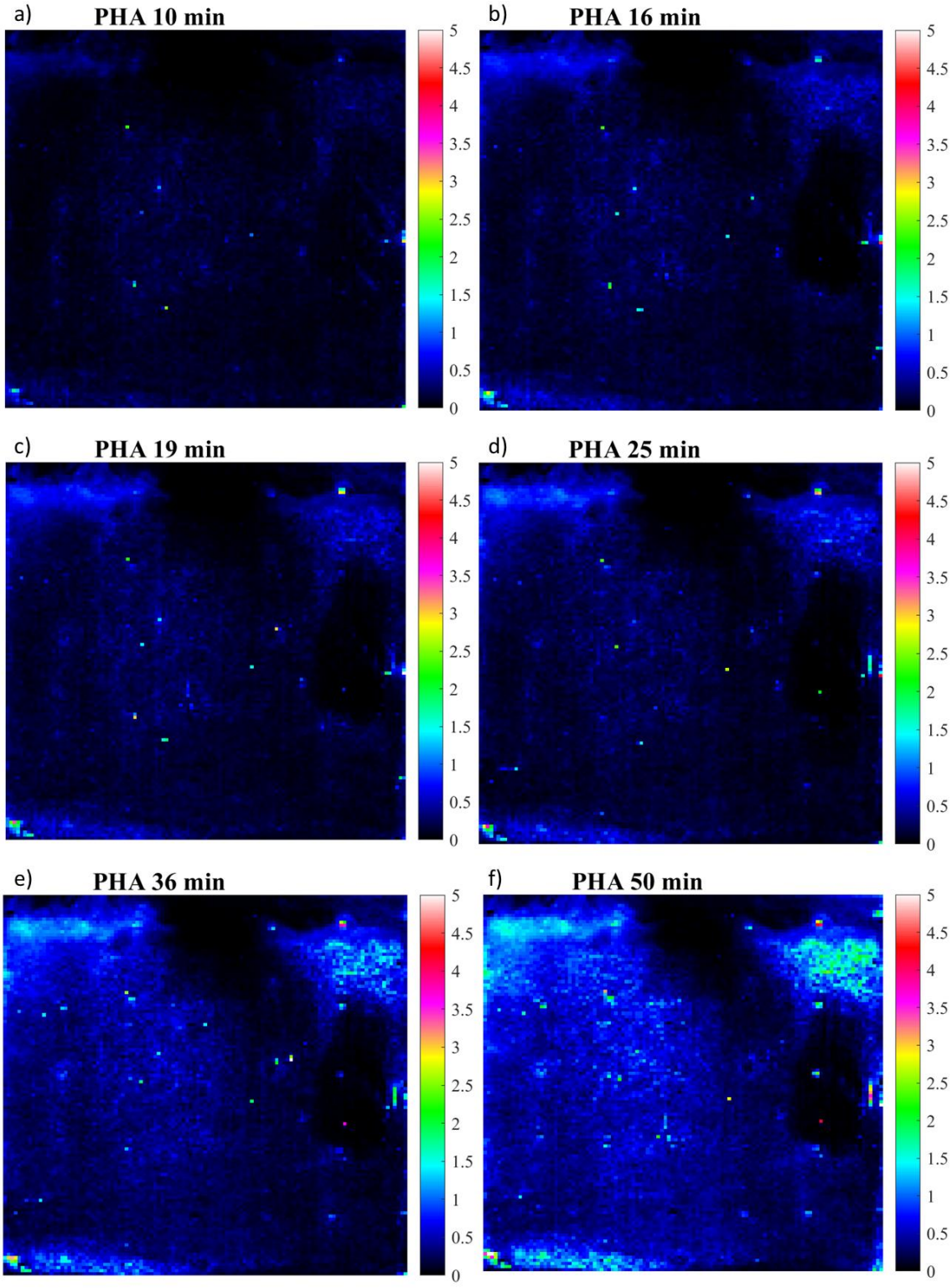

Figure 5.4.2. Extract of the time series of fluorescein concentration maps for *Phalaris Arundinacea*, from the first to the last available UV-light pictures.

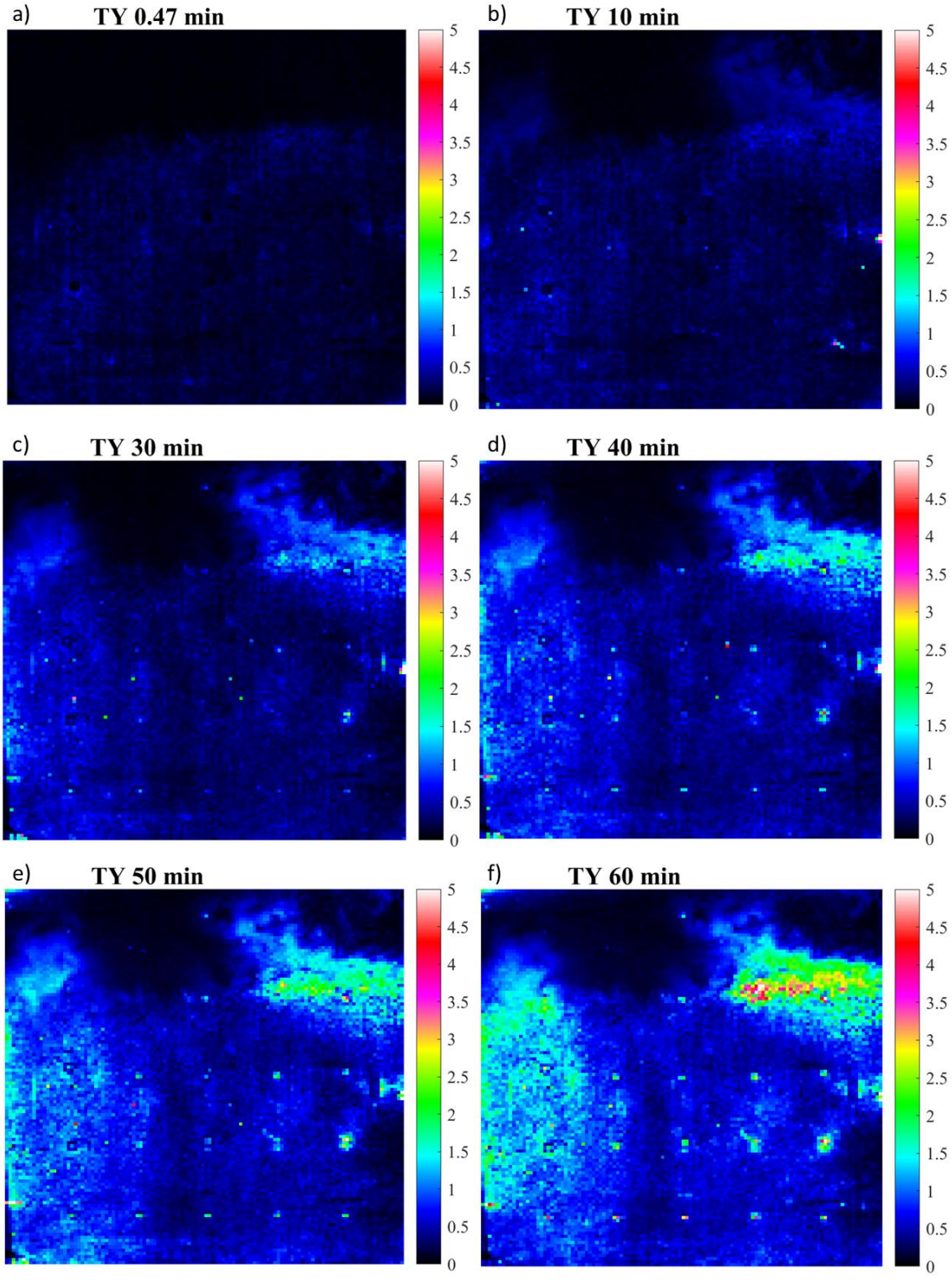

Figure 5.4.3. Extract of the time series of fluorescein concentration maps for *Typha angustifolia*, from the first to the last available UV-light pictures.

Figure 5.4.4 shows the last activity map of each mesocosm and the corresponding white light images that reveal the plants root systems. The enzymatic activity is mostly developed close to the root system, probably due to better oxygenation and support for biofilm growth. The enzymatic activity is not distributed uniformly near the root zone,

thus suggesting that a relation between root dimension or density and enzymatic activity should be further investigated.

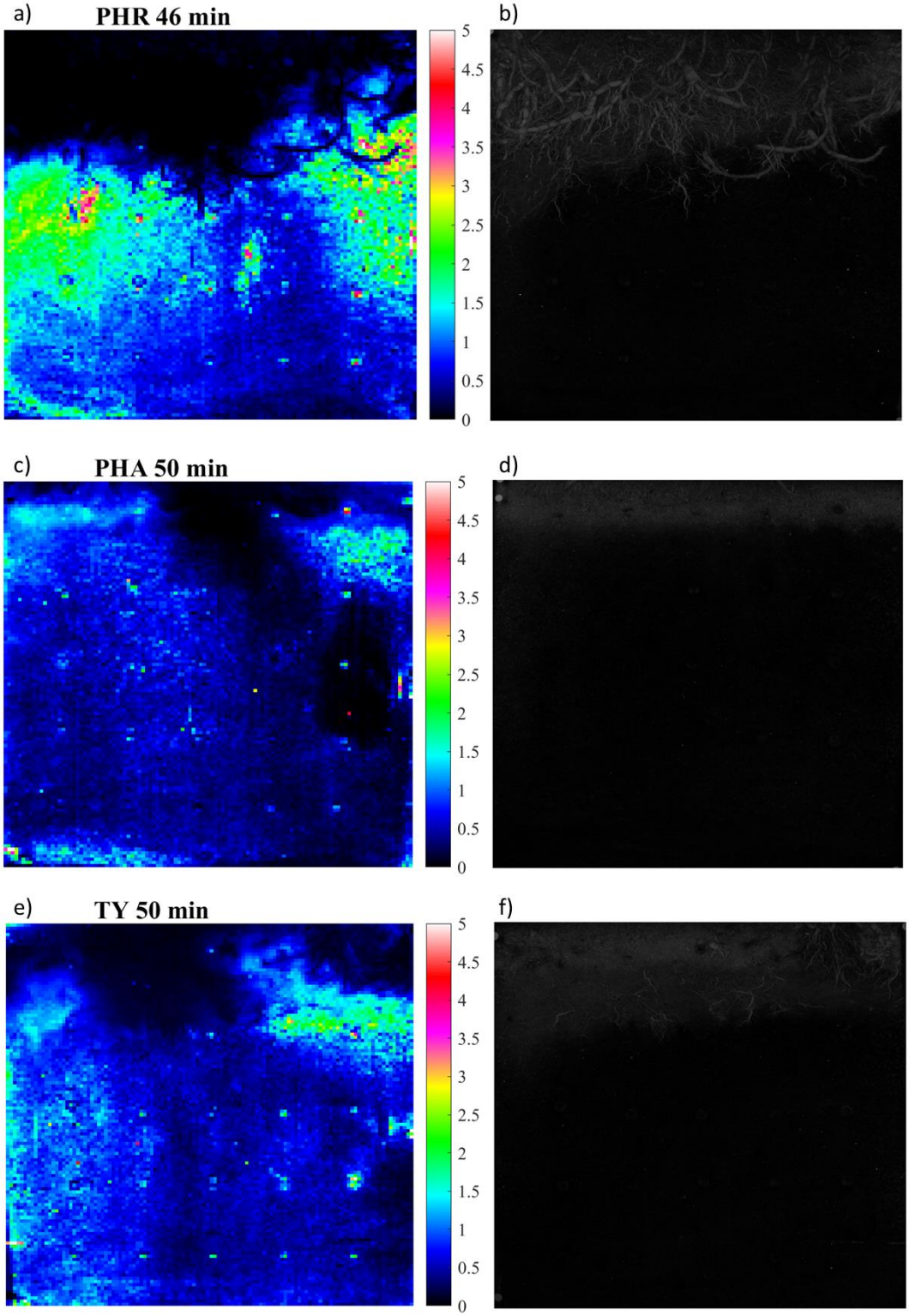

Figure 5.4.4. Concentration maps (left) and white light picture (right) of a-b) *Phragmites australis,* c-d) *Phalaris arundinacea* and e-f) *Typha angustifolia.*

The concentration of fluorescein inside the mesocosms can be evaluated for all available instants, revealing the general activity of the microbial community that

progressively metabolises FDA releasing fluorescein. Figure 5.4.5 shows the build-up of fluorescein concentration over time. In general, the curves display an expected increasing trend, but some parts of the curves highlight the necessity to improve the picture collecting system to avoid anomalies possibly due to external light infiltration. It should be noticed that the concentrations calculated with the photographical method could be influenced by the possible absorption of the tracer on the porous medium or by its subsequent release. However, the average concentration calculated with the photographical method for the final picture of each mesocosm is comparable with the values in the samples collected at the outlet of the mesocosms after one hour (Table 5.4.1).

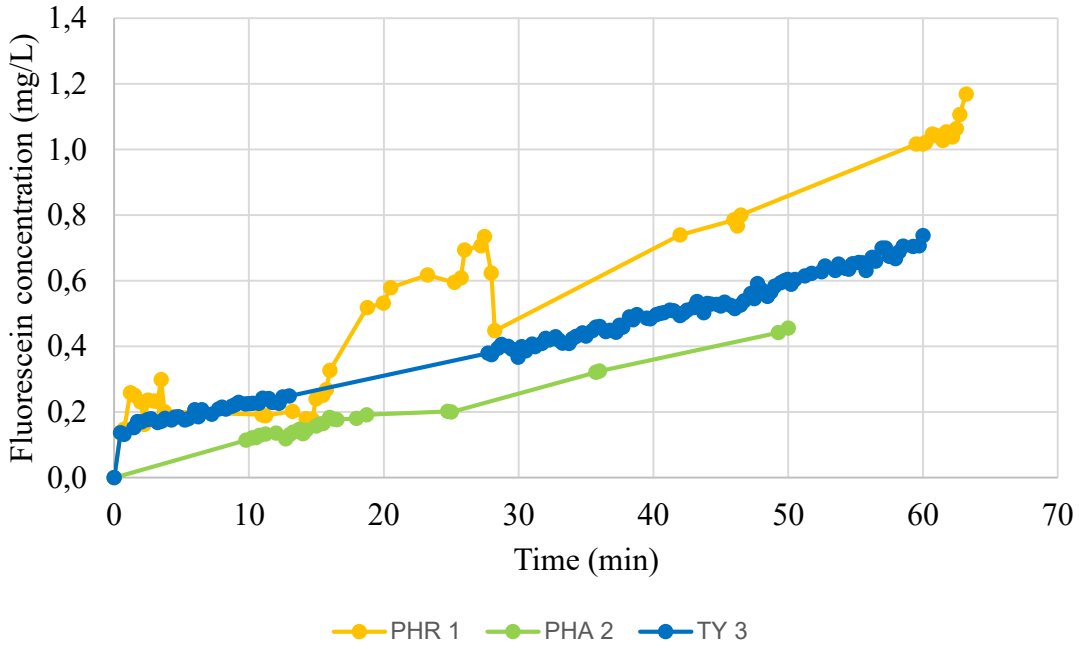

Figure 5.4.5. Complete time series of the average concentration of fluorescein calculated for all available pictures.

Table 5.4.1. Average concentration of fluorescein (mg/L) for the last available image and at the outlet sample of each mesocosm.

Plant species	**Average concentration of fluorescein in each mesocosm for the last available image (mg/L)**	**Time of last available image (min)**	**Sampled concentration at the outlet after 60 min (mg/L)**
Phragmites australis	1.02	60	0.95
Phalaris arundinacea	0.46	50	0.73
Typha angustifolia	0.74	60	0.75

Further analysis on the concentration maps should be done in future to provide aggregated data that relate the enzymatic activity with the depth or the distance from the root system.

♦ Conclusions

6.1 Green wall design for GW treatment

This thesis evaluated the treatment performance of an outdoor green wall with ornamental plants, treating synthetic domestic greywater for non-potable reuse. The four phases of this study allowed to test different condition (e.g. drainage system, filter medium composition, flow rate variability) with a high HLR and in outdoor conditions. Following four consecutive phases, the system design was progressively improved with know-how arisen from the previous ones. Preliminary tests on filter media firstly led to choose a mixture of coconut fibre and perlite (80:20) for the base medium and to identify ornamental plants resistant to GW and high moisture.

During the first phase, the green wall showed excellent removal performances for BOD_5 (>95% for all mixtures) and *E. coli* (>98% for all mixtures); while the removal efficiencies of these contaminants were very high, the adoption of the additives resulted in not significant improvement compared to BM. Good performances were also observed for COD and nitrogen removals; biochar significantly increased removal performances for TKN (46.8±24.8%) and NO_3^--N (46.9±21.5%) compared to BM (TKN: 34.6±29.7%, NO_3^--N: 25.7±28.8%), and removal efficiency for COD (50.7±28.5%) was also high but not significantly better than BM (63.0±13.6%). These results demonstrate the potential benefit of using biochar as an additive in GW treatment with green walls. Among other additives, compost performed better than BM in removing TKN and NO_3^--N, but its use is not recommended because this advantage was largely outweighed by frequent clogging issues that increased the need for maintenance of the green wall. Clogging was likely favoured by the low effective porosity of the compost mixture. Significant improvements compared to BM were also observed for granular activated carbon and the combined biochar and polyacrylate mixture, but only for removal of NO_3^--N. Apparently, the combination of biochar and polyacrylate, which had the highest amount (40%) of additives, reduced the advantage provided by the addition of biochar alone, suggesting that the type of additive may be as important, if not more, as the amount of base filter medium. No evident difference was noticed between the two polyacrylate mixes, suggesting that the higher age of the old mix did not affect the removal performances.

The second phase started from the best configuration identified during the previous phase (i.e. 65% coconut fibre, 16% perlite and 20% biochar). 5% of graphene was added to the selected mix, evaluating possible release and improvement in treatment

performances. The analysis of the configuration fed with tap water (BC+GR*) revealed that the addition of graphene did not cause any significant release of contaminants related to the additive itself. The removal of BOD_5, COD, TSS and nitrogen compounds was satisfactory; *E. coli* removal efficiency was excellent. However, no evidence was found in the present study that the addition of graphene significantly improves the system performances compared to the other configurations. Apparently, the benefits provided by the inclusion of graphene were marginal (and limited to the first level of the system) compared to the already high treatment performance of the other materials (e.g., biochar) used as filter media. In terms of removal efficiency, the operational time showed slight performance decrease in some parameters such as TP, SO_4^{2-} and NH_4^+-N. However, both these aspects were deeply investigated during the third phase.

The third phase evaluated the effect of operational time on the removal performances comparing two identical modules set up at two-year distance and the contribution of each level of treatment. Both panels showed excellent removal performances for TSS, BOD_5, COD and MBAS, even if operational age significantly impacted on removal efficiency of TSS (P1: 97.4±4.6%, P2: 89.1±13.8%) and MBAS (P1: 92.7±3.8%, P2: 75.3±8.0%). The third level of treatment was essential to eliminate any statistical difference in the overall removal efficiency for COD (P1: 78.5±5.2%, P2: 80.1±4.2%), TN (P1: 49.2±30.4%, P2: 48.0±23.31%) and BOD_5, even when differences were observed for previous levels (e.g. BOD_5, P1: 45.2±36.2 | 86.5±14.8 | 98.8±2.4%; P2: 16.5±20.8 | 51.8±32.3 | 94.5±9.2%). Empirical observation of clogging events (particularly for the old panel) suggested the opportunity of enhancing system drainage in the following phase.

The fourth phase aimed to test the resilience of the green wall to variable hydraulic loads due to different amount of people producing GW. Results are still under analysis, but some preliminary consideration can be provided. In general, all parameters confirm that the concentrations decrease along the columns, with a strong reduction of concentration for TSS, BOD_5, COD and MBAS, and a good oxygenation of the system. The variable load didn't show any impact during nor after underload ($HLR=395 Lm^{-2}d^{-1}$). On the other hand, the overflow ($HLR = 1136\ Lm^{-2}d^{-1}$) impacted negatively on treatment performances in the first and second levels in important parameters such as TSS, BOD_5 and COD. Furthermore, plants started to suffer due to excessive moisture caused by the overload but they completely recovered after two weeks of standard load. However, it is important to highlight that the overload HLR was very high because of the high standard HLR that was chosen in the experiments.

The design tested during this thesis is only one of the possible green wall systems, and it was mainly focused on filter media performances, comparing different mixes and evaluating operational time effects. However, it is important to remind that the choice of filter medium in a green wall should consider other factors besides removal efficiency such as cost evaluation. In fact, the inclusion of an additive with a slightly lower efficiency could be acceptable if it allows for substantial cost reductions. As an example, in remote areas where transportation costs are significant, dry polyacrylate could be inexpensively transported and hydrated on site to entail significant savings compared to

conventional filter media. On the other hand, the use of more expensive materials with higher removal efficiency could reduce the wall size per unit volume of treated greywater (e.g., installing two-row panels) and potentially compensate their higher material cost. For example, the use of graphene is not recommended in routine application of green wall for GW treatment, with the possible exception of very compact systems with a single level of pots.

While resilience to feeding volume variations was proven, further studies will be necessary to test the impact on GW composition, considering more aggressive compounds such as disinfectant that could stress the system. More interdisciplinary studies will be also necessary to integrate the treating green wall in buildings, considering both the design phase of new buildings and the retrofitting of existing real estates.

6.2 Photographical method

The photographical method proposed by Dr. Gagnon and Dr. Chazarenc allows to visualize the enzymatic activity inside a CW mesocosm. This approach produces a huge number of data that require an automatic process to be thoroughly analysed. During this thesis, the photographical method was improved and automatized. The optimization of the calibration curve between fluorescence intensity and fluorescein concentration allowed to obtain more precise information on fluorescein distribution, despite the interference of FeS precipitate. Furthermore, the automation of the image processing procedure allowed for the quick creation of concentration maps to better understand the activity of the bacterial community within the system. From preliminary observations, it was observed that the root zone and inlet/outlet areas are the most active zones, possibly due to higher oxygen concentration.

The following steps to develop the method will require a validation by comparing the results of the analysis with the actual fluorescein concentrations sampled during 2014 experiments. After that, the development of a numerical model will allow to improve the understanding of microbial processes within CWs, in term of spatial and temporal distributions. This knowledge is expected to help the development of design indications of CWs.

♦ References

Abed, S.N., Almuktar, S.A., Scholz, M., 2020. Impact of Storage Time on Characteristics of Synthetic Greywater for Two Different Pollutant Strengths to Be Treated or Recycled. Water. Air. Soil Pollut. 231, 1–18. https://doi.org/10.1007/s11270-020-04602-1

Abed, S.N., Scholz, M., 2016. Chemical simulation of greywater Chemical simulation of greywater. Environ. Technol. 37, 1631–1646. https://doi.org/10.1080/09593330.2015.1123301

Abu Ghunmi, L., Zeeman, G., Fayyad, M., van Lier, J.B., 2011. Grey Water Treatment Systems : A Review. Crit. Rev. Environ. Sci. Technol. 41, 657–698. https://doi.org/10.1080/10643380903048443

Adam, G., Duncan, H., 2001. Development of a sensitive and rapid method for the measurement of total microbial activity using fluorescein diacetate (FDA) in a range of soils. Soil Biol. Biochem. 33, 943–951. https://doi.org/https://doi.org/10.1016/S0038-0717(00)00244-3

Al-ismaili, A.M., Ahmed, M., Al-busaidi, A., Al-adawi, S., Tandlich, R., Al-amri, M., 2017. Extended use of grey water for irrigating home gardens in an arid environment. Environ. Sci. Pollut. Res. 24, 13650–13658. https://doi.org/10.1007/s11356-017-8963-z

Al-jayyousi, O.R., 2003. Greywater reuse : towards sustainable water management. Desalination 156, 181–192.

Alexandri, E., Jones, P., 2008. Temperature decreases in an urban canyon due to green walls and green roofs in diverse climates. Build. Environ. 43, 480–493. https://doi.org/10.1016/j.buildenv.2006.10.055

Alfiya, Y., Gross, A., Sklarz, M., Friedler, E., 2013. Reliability of on-site greywater treatment systems in Mediterranean and arid environments - A case study. Water Sci. Technol. 67, 1389–1395. https://doi.org/10.2166/wst.2013.687

Allen, L., Christian-Smith, J., Palaniappan, M., 2010. Overview of Greywater Reuse: The Potential of Greywater Systems to Aid Sustainable Water Management, Pacific Institute. Pacific Institute.

Arden, S., Ma, X., 2018. Constructed wetlands for greywater recycle and reuse: A review. Sci. Total Environ. 630, 587–599. https://doi.org/10.1016/j.scitotenv.2018.02.218

Avery, L.M., Frazer-Williams, R.A.D., Winward, G., Shirley-Smith, C., Liu, S., Memon, F.A., Jefferson, B., 2007. Constructed wetlands for grey water treatment. Ecohydrol. Hydrobiol. 7, 191–200. https://doi.org/10.1016/S1642-3593(07)70101-5

Bakheet, B., Prodanovic, V., Deletic, A., McCarthy, D., 2020. Effective treatment of greywater via green wall biofiltration and electrochemical disinfection. Water Res. 185, 116228. https://doi.org/10.1016/j.watres.2020.116228

Bauduceau, N., Berry, P., Cecchi, C., Elmqvist, T., Fernandez, M., Hartig, T., Krull, W., Mayerhofer, E., N, S., Noring, L., Raskin-Delisle, K., Roozen, E., Sutherland, W., Tack, J., 2015. Towards an EU Research and Innovation Policy Agenda for Nature-based Solutions & Re-naturing Cities: Final Report of the Horizon 2020 Expert Group on "Nature-based Solutions and Re-naturing Cities". Publications Office of the European Union. https://doi.org/doi.org/10.2777/765301

Benami, M., Gillor, O., Gross, A., 2016. Potential microbial hazards from graywater reuse and associated matrices : A review. Water Res. 106, 183–195. https://doi.org/10.1016/j.watres.2016.09.058

Benjamini, Y., Hochberg, Y., 1995. Controlling the false discovery rate: a practical and powerful approach to multiple testing. J. R. Stat. Soc. Ser. B 57, 289–300. https://doi.org/10.1111/j.2517-6161.1995.tb02031.x

Boano, F., Caruso, A., Costamagna, E., Fiore, S., Demichelis, F., Galvão, A., Pisoeiro, J., Rizzo, A., Masi, F., 2021a. Assessment of the Treatment Performance of an Open-Air Green Wall Fed with Graywater under Winter Conditions. ACS ES&T Water 1, 595–602. https://doi.org/10.1021/acsestwater.0c00117

Boano, F., Caruso, A., Costamagna, E., Ridolfi, L., Fiore, S., Demichelis, F., Galvão, A., Pisoeiro, J., Rizzo, A., Masi, F., 2020. A review of nature-based solutions for greywater treatment : Applications , hydraulic design , and environmental benefits. Sci. Total Environ. 711, 134731. https://doi.org/10.1016/j.scitotenv.2019.134731

Boano, F., Costamagna, E., Caruso, A., Fiore, S., Chiappero, M., Pisoeiro, J., Rizzo, A., Masi, F., Galv, A., 2021b. Evaluation of the influence of filter medium composition on treatment performances in an open-air green wall fed with greywater. J. Environ. Manage. 300. https://doi.org/10.1016/j.jenvman.2021.113646

Boyjoo, Y., Pareek, V.K., Ang, M., 2013. A review of greywater characteristics and treatment processes. Water Sci. Technol. 67, 1403–1424. https://doi.org/10.2166/wst.2013.675

BSI, 2011. Greywater systems. Domestic greywater treatment equipment. Requirements and test methods. s.l.:BS 8525-2:2011.

Burek, P., Satoh, Y., Fischer, G., Kahil, M.T., Scherzer, A., Tramberend, S., Nava, L.F., Wada, Y., Eisner, S., Flörke, M., Hanasaki, N., Magnuszewski, P., Cosgrove, B., Wiberg, D., 2016. Water Futures and Solution. Fast Track Initiative, International Institute for Applied Systems Analysis.

Bustami, R.A., Belusko, M., Ward, J., Beecham, S., 2018. Vertical greenery systems : A systematic review of research trends. Build. Environ. 146, 226–237.

https://doi.org/10.1016/j.buildenv.2018.09.045

Cameron, R.W.F., Taylor, J.E., Emmett, M.R., 2014. What's "cool" in the world of green façades? How plant choice influences the cooling properties of green walls. Build. Environ. 73, 198–207. https://doi.org/10.1016/j.buildenv.2013.12.005

Castellar da Cunha, J.A., Arias, C.A., Carvalho, P., Rysulova, M., Canals, J.M., Pérez, G., Bosch, M.G., Morató, J.F., 2018. "WETWALL" — an innovative design concept for the treatment of wastewater at an urban scale. Desalin. Water Treat. 109, 205–220. https://doi.org/10.5004/dwt.2018.22143

Castleton, H.F., Stovin, V., Beck, S.B.M., Davison, J.B., 2010. Green roofs; Building energy savings and the potential for retrofit. Energy Build. 42, 1582–1591. https://doi.org/10.1016/j.enbuild.2010.05.004

Chaillou, K., Gérente, C., Andrès, Y., Wolbert, D., 2011. Bathroom Greywater Characterization and Potential Treatments for Reuse. Water Air Soil Pollut. 215, 31–42. https://doi.org/10.1007/s11270-010-0454-5

Charchalac Ochoa, S.I., Ushijima, K., Hijikata, N., Funamizu, N., 2015. Treatment of domestic greywater by geotextile filter and intermittent sand filtration bioreactor. J. Water Reuse Desalin. 39–49. https://doi.org/10.2166/wrd.2014.042

Chrispim, M.C., Nolasco, M.A., 2017. Greywater treatment using a moving bed biofilm reactor at a university campus in Brazil. J. Clean. Prod. 142, 290–296.

Climate System Analysis Group, 2020. Big Six Monitor [WWW Document]. URL http://cip.csag.uct.ac.za/monitoring/bigsix.html (accessed 10.2.20).

Cohen-Shacham, E., Walters, G., Janzen, C., Maginnis, S., 2016. Nature-based solutions to address global societal challenges. Gland, Switzerland: IUCN. xiii + 97pp., Nature-based solutions to address global societal challenges. IUCN, Gland, Switzerland.

Costamagna, E., Caruso, A., Galvão, A., Rizzo, A., Masi, F., Fiore, S., Boano, F., n.d. Impact of biochar and graphene additives on the treatment performances of an open-air green wall fed with greywater. Submitted.

Costamagna, E., Fiore, S., Boano, F., 2022. Influence of the number of levels and system age on greywater treatment in a green wall. Ecol. Eng. 183, 106755. https://doi.org/https://doi.org/10.1016/j.ecoleng.2022.106755

Costamagna, E., Raffaelli, B., Fiore, S., Boano, F., 2021. Studio sperimentale della depurazione di acque grigie mediante muri verdi. Geoing. Ambient. e Mineraria LVIII, 5–9.

Council of the European Communities, 1991. Directive 91/271/EEC concerning urban waste water treatment. Off. J. Eur. Communities.

D.M. 185, 2003. Gazzetta Ufficiale della Repubblica Italiana - 23 luglio 2003, n. 169.

Dal Ferro, N., De Mattia, C., Gandini, M.A., Maucieri, C., Stevanato, P., Squartini, A., Borin, M., 2021. Green walls to treat kitchen greywater in urban areas: Performance

from a pilot-scale experiment. Sci. Total Environ. 757, 144189. https://doi.org/10.1016/j.scitotenv.2020.144189

Dalahmeh, S.S., Pell, M., Vinnerås, B., Hylander, L.D., Öborn, I., Jönsson, H., 2012. Efficiency of bark, activated charcoal, foam and sand filters in reducing pollutants from greywater. Water. Air. Soil Pollut. 223, 3657–3671. https://doi.org/10.1007/s11270-012-1139-z

De Gisi, S., Casella, P., Notarnicola, M., Farina, R., 2016. Grey water in buildings: a mini-review of guidelines, technologies and case studies. Civ. Eng. Environ. Syst. 33:1, 35–54.

Deska, I., Mrowiec, M., Ociepa, E., Lewandowska, A., 2020. Influence of the hydrogel amendment on the water retention capacity of extensive green roof models. J. Ecol. Eng. 21, 195–204. https://doi.org/10.12911/22998993/112763

Diaper, C., Toifl, M., Storey, M.V., 2008. Greywater Technology Testing Protocol, CSIRO Water for a Healthy Country Flagship.

Dixon, M., Butler, D., Fewkes, A., 1999. Guidelines for Greywater Re-Use: Health Issues. Water Environ. J. 13, 322–326.

Dotro, G., Langergraber, G., Molle, P., Nivala, J., Puigagut, J., Stein, O., vo Sperling, M., 2017. Treatment wetlands. IWA publishing.

Edwin, G.A., Gopalsamy, P., Muthu, N., 2014. Characterization of domestic gray water from point source to determine the potential for urban residential reuse: a short review. Appl. Water Sci. 4, 39.49.

EPA, 2016. Guidelines on Integrating Water Reuse into Water Planning and Management in the context of the WFD (Water Frame work Directive), s.l.: Environmental Protection Agency.

EPA Victoria, 2016. Code of practice – onsite wastewater management, s.l.: Environmental Protection Authority Victoria.

EPHC NRMMC AHMC, 2006. Australian guidelines for water recycling: managing health and environmental risks (Phase 1), s.l.: s.n.

Eregno, F.E., Moges, M.E., Heistad, A., 2017. Treated Greywater Reuse for Hydroponic Lettuce Production in a Green Wall System : Quantitative Health Risk Assessment. water 9. https://doi.org/10.3390/w9070454

Eriksson, E., Auffarth, K., Henze, M., Ledin, A., 2002. Characteristics of grey wastewater. Urban Water 4, 85–104.

Estelrich, M., Vosse, J., Comas, J., Atanasova, N., Costa, J.C., Gattringer, H., Buttiglieri, G., 2021. Feasibility of vertical ecosystem for sustainable water treatment and reuse in touristic resorts. J. Environ. Manage. 294. https://doi.org/10.1016/j.jenvman.2021.112968

European, Commission, 2015. Towards an EU Research and Innovation policy agenda for Nature-Based Solutions & Re-Naturing Cities. https://doi.org/10.2777/479582

European Commission, 2012. Proposal for a Directive of the European Parliament and of the Council Amending Directives 2000/60/EC and 2008/105/EC as Regards Priority Substances in the Field of Water Policy, s.l.: European Commission.

Fowdar, H.S., Deletic, A., Hatt, B.E., Cook, P.L.M., 2018. Nitrogen Removal in Greywater Living Walls : Insights into the Governing Mechanisms. Water 10, 1–13. https://doi.org/10.3390/w10040527

Fowdar, H.S., Hatt, B.E., Breen, P., Cook, P.L.M., Deletic, A., 2017. Designing living walls for greywater treatment. Water Res. 110, 218–232. https://doi.org/10.1016/j.watres.2016.12.018

Francis, R.A., Lorimer, J., 2011. Urban reconciliation ecology: The potential of living roofs and walls. J. Environ. Manage. 92, 1429–1437. https://doi.org/10.1016/j.jenvman.2011.01.012

Friedler, E., Hadari, M., 2006. Economic feasibility of on-site greywater reuse in multi-storey buildings. Desalination 190, 221–234. https://doi.org/10.1016/j.desal.2005.10.007

Gattringer, H., Claret, A., Radtke, M., Kisser, J., Zraunig, A., Rodriguez-Roda, I., Buttiglieri, G., 2016. Novel vertical ecosystem for sustainable water treatment and reuse in tourist resorts. Int. J. Sustain. Dev. Plan. 11, 263–274. https://doi.org/10.2495/SDP-V11-N3-263-274

Ghaitidak, D.M., Yadav, K.D., 2013. Characteristics and treatment of greywater — a review 2795–2809. https://doi.org/10.1007/s11356-013-1533-0

Grant, S.B., Saphores, J.D., Feldman, D.L., Hamilton, A.J., Fletcher, T.D., Cook, P.L.M., Stewardson, M., Sanders, B.F., Levin, L.A., Ambrose, R.F., Deletic, A., Brown, R., Jiang, S.C., Rosso, D., Cooper, W.J., Marusic, I., 2012. Taking the "waste" out of "wastewater" for human water security and ecosystem sustainability. Science (80-.). 337, 681–686. https://doi.org/10.1126/science.1216852

Hosseinzadeh, M., Bidhendi, G.N., Torabian, A., Mehrdadi, N., Pourabdullah, M., 2015. A new flat sheet membrane bioreactor hybrid system for advanced treatment of effluent, reverse osmosis pretreatment and fouling mitigation. Bioresour. Technol. 192, 177–184. https://doi.org/10.1016/j.biortech.2015.05.066

Hourlier, F., Masse, A., Jaouen, P., Lakel, A., Gerente, C., Faur, C., Le Cloirec, P., 2010. Formulation of synthetic greywater as an evaluation tool for wastewater recycling technologies. Environ. Technol. 31, 215–223. https://doi.org/10.1080/09593330903431547

Jin, Z., Xie, X., Zhou, J., Bei, K., Zhang, Y., Huang, X., Zhao, M., Kong, H., Zheng, X., 2018. Blackwater treatment using vertical greening: Efficiency and microbial community structure. Bioresour. Technol. 249, 175–181. https://doi.org/10.1016/j.biortech.2017.09.176

Jokerst, A., Sharvelle, S.E., Hollowed, M.E., Roesner, L.A., 2011. Seasonal Performance of an Outdoor Constructed Wetland for Graywater Treatment in a Temperate Climate. Water Environ. Res. 83, 2187–2198.

https://doi.org/10.2175/106143011x12989211841412

JSWA, 2016. Management of Wastewater in Japan, s.l.: Japan sewage sludge work association.

Kadlec, R.H., Wallace, S.D., 2009. Treatment Wetlands, Treatment Wetlands. CRC Press. https://doi.org/10.1201/9781420012514

Kotsia, D., Deligianni, A., Fyllas, N.M., Stasinakis, A.S., Fountoulakis, M.S., 2020. Converting treatment wetlands into "treatment gardens": Use of ornamental plants for greywater treatment. Sci. Total Environ. 744, 140889. https://doi.org/10.1016/j.scitotenv.2020.140889

Kotsiris, G., Nektarios, P.A., Ntoulas, N., Kargas, G., 2013. An adaptive approach to intensive green roofs in the Mediterranean climatic region. Urban For. Urban Green. 12, 380–392. https://doi.org/10.1016/j.ufug.2013.05.001

Kummu, M., Ward, P.J., De Moel, H., Varis, O., 2010. Is physical water scarcity a new phenomenon? Global assessment of water shortage over the last two millennia. Environ. Res. Lett. 5. https://doi.org/10.1088/1748-9326/5/3/034006

Lakho, F.H., Qureshi, A., Novelli, L.D.D., Depuydt, V., Depreeuw, T., Van Hulle, S.W.H., Rousseau, D.P.L., 2022. Performance of a green wall (Total Value Wall^{TM}) at high greywater loading rates and Life Cycle Impact Assessment. Sci. Total Environ. 821, 153470. https://doi.org/10.1016/j.scitotenv.2022.153470

Lakho, F.H., Vergote, J., Ihsan-Ul-Haq Khan, H., Depuydt, V., Depreeuw, T., Van Hulle, S.W.H., Rousseau, D.P.L., 2021. Total value wall: Full scale demonstration of a green wall for grey water treatment and recycling. J. Environ. Manage. 298, 113489. https://doi.org/10.1016/j.jenvman.2021.113489

Larsen, T.A., Alder, A.C., Eggen, R.I.L., Maurer, M., Lienert, J., 2009. Source Separation: Will We See a Paradigm Shift in Wastewater Handling? Environ. Sci. Technol. 43, 6126–6130. https://doi.org/10.1021/es9010515

Leonard, M., Gilpin, B., Robson, B., Wall, K., 2016. Field study of the composition of greywater and comparison of microbiological indicators of water quality in on-site systems. Environ. Monit. Assess. 188. https://doi.org/10.1007/s10661-016-5442-9

Leong, J.Y.C., Oh, K.S., Poh, P.E., Chong, M.N., 2017. Prospects of hybrid rainwater-greywater decentralised system for water recycling and reuse: A review. J. Clean. Prod. 142, 3014–3027. https://doi.org/10.1016/j.jclepro.2016.10.167

Li, Z., Boyle, F., Reynolds, A., 2010. Rainwater harvesting and greywater treatment systems for domestic application in Ireland. DES 260, 1–8. https://doi.org/10.1016/j.desal.2010.05.035

Ling, T.Y., Chiang, Y.C., 2018. Well-being, health and urban coherence-advancing vertical greening approach toward resilience: A design practice consideration. J. Clean. Prod. 182, 187–197. https://doi.org/10.1016/j.jclepro.2017.12.207

Liu, S., Butler, D., Memon, F.A., Makropoulos, C., Avery, L., Jefferson, B., 2010.

Impacts of residence time during storage on potential of water saving for grey water recycling system. Water Res. 44, 267–277. https://doi.org/10.1016/j.watres.2009.09.023

Maes, J., Jacobs, S., 2017. Nature-Based Solutions for Europe's Sustainable Development. Conserv. Lett. 10, 121–124. https://doi.org/10.1111/conl.12216

Maiga, Y., Moyenga, D., Ushijima, K., Sou, M., Maiga, A.H., 2014. Greywater Characteristics In Rural Areas of the Sahelian Region for Reuse Purposes : The Case of Burkina Faso. Rev. des Sci. l'eau 27, 39–54. https://doi.org/doi.org/10.7202/1021981ar

Manso, M., Castro-gomes, J., 2015. Green wall systems : A review of their characteristics. Renew. Sustain. Energy Rev. 41, 863–871. https://doi.org/10.1016/j.rser.2014.07.203

Masi, F., Bresciani, R., Rizzo, A., Edathoot, A., Patwardhan, N., Panse, D., Langergraber, G., 2016. Green walls for greywater treatment and recycling in dense urban areas: A case-study in Pune. J. Water Sanit. Hyg. Dev. 6, 342–347. https://doi.org/10.2166/washdev.2016.019

Medl, A., Stangl, R., Florineth, F., 2017. Vertical greening systems – A review on recent technologies and research advancement. Build. Environ. 125, 227–239. https://doi.org/10.1016/j.buildenv.2017.08.054

Mekonnen, M.M., Hoekstra, A.Y., 2016. Sustainability: Four billion people facing severe water scarcity. Sci. Adv. 2, 1–7. https://doi.org/10.1126/sciadv.1500323

Milano, M., Ruelland, D., Fernandez, S., Dezetter, A., Fabre, J., Servat, E., 2012. Facing climatic and anthropogenic changes in the Mediterranean basin: What will be the medium-term impact on water stress? Comptes Rendus - Geosci. 344, 432–440. https://doi.org/10.1016/j.crte.2012.07.006

Moges, M.E., Eregno, F.E., Heistad, A., 2015. Performance of biochar and filtralite as polishing step for on-site greywater treatment plant. Manag. Environ. Qual. An Int. J. 26, 607–625. https://doi.org/10.1108/MEQ-07-2014-0101

Morel, A., Diener, S., 2006. Greywater Management.

Noah, M., 2002. Graywater Use Still a Gray Area. J. Environ. Health 64, 22.

Noutsopoulos, C., Andreadakis, A., Kouris, N., Charchousi, D., Mendrinou, P., Galani, A., Mantziaras, I., Koumaki, E., 2018. Greywater characterization and loadings e Physicochemical treatment to promote onsite reuse. J. Environ. Manage. 216, 337–346. https://doi.org/10.1016/j.jenvman.2017.05.094

NSF/ANSI, 2011. NSF/ANSI 350 – 2011. On-site residential and commercial water reuse treatment systems, s.l.: s.n.

NSW-DEUS, 2007. NSW guidelines for greywater reuse in sewered single household residential premises, s.l.: s.n.

ONU, 2018. Sustainable Development Goal 6: Synthesis Report on Water and Sanitation,

United Nations. https://doi.org/10.1126/science.278.5339.827

Oron, G., Adel, M., Agmon, V., Friedler, E., Halperin, R., Leshem, E., Weinberg, D., Consulting, A., Yaakov, Z., 2014. Greywater use in Israel and worldwide : Standards and prospects. Water Res. 58, 92–101. https://doi.org/10.1016/j.watres.2014.03.032

Oteng-Peprah, M., Acheampong, M.A., de Vries, N.K., 2018. Greywater Characteristics, Treatment systems, Reuse strategies and User Perception - a Review. Water Air Soil Pollut. 229:255.

Otterpohl, R., Braun, U., Oldenburg, M., 2002. Innovative technologies for decentralised wastewater management in urban and peri-urban areas. Berichte-Wassergute und Abf All Wirtschaft Tech. Univ. Berichtsh. 173, 109–126.

Pérez, G., Rincón, L., Vila, A., González, J.M., Cabeza, L.F., 2011. Behaviour of green facades in Mediterranean Continental climate. Energy Convers. Manag. 52, 1861–1867. https://doi.org/10.1016/j.enconman.2010.11.008

Pradhan, S., Al-ghamdi, S.G., Mackey, H.R., 2019a. Greywater recycling in buildings using living walls and green roofs: A review of the applicability and challenges. Sci. Total Environ. 652, 330–344. https://doi.org/10.1016/j.scitotenv.2018.10.226

Pradhan, S., Al-Ghamdi, S.G., Mackey, H.R., 2019b. Greywater treatment by ornamental plants and media for an integrated green wall system. Int. Biodeterior. Biodegrad. 145, 104792. https://doi.org/10.1016/j.ibiod.2019.104792

Pradhan, S., Helal, M.I., Al-Ghamdi, S.G., Mackey, H.R., 2020. Performance evaluation of various individual and mixed media for greywater treatment in vertical nature-based systems. Chemosphere 245, 125564. https://doi.org/10.1016/j.chemosphere.2019.125564

Prodanovic, V., Hatt, B., Mccarthy, D., Deletic, A., 2020. Green wall height and design optimisation for effective greywater pollution treatment and reuse. J. Environ. Manage. 261, 110173. https://doi.org/10.1016/j.jenvman.2020.110173

Prodanovic, V., Hatt, B., McCarthy, D., Zhang, K., Deletic, A., 2017. Green walls for greywater reuse: Understanding the role of media on pollutant removal. Ecol. Eng. 102, 625–635. https://doi.org/10.1016/j.ecoleng.2017.02.045

Prodanovic, V., McCarthy, D., Hatt, B., Deletic, A., 2019a. Designing green walls for greywater treatment : The role of plants and operational factors on nutrient removal. Ecol. Eng. 130, 184–195. https://doi.org/10.1016/j.ecoleng.2019.02.019

Prodanovic, V., Wang, A., Deletic, A., 2019b. Assessing water retention and correlation to climate conditions of fi ve plant species in greywater treating green walls. Water Res. 167, 115092. https://doi.org/10.1016/j.watres.2019.115092

Prodanovic, V., Zhang, K., Hatt, B., McCarthy, D., Deletic, A., 2018. Optimisation of lightweight green wall media for greywater treatment and reuse. Build. Environ. 131, 99–107. https://doi.org/10.1016/j.buildenv.2018.01.015

Pruss-Ustun, A., World Health Organization, 2008. Safer water, better health: costs,

benefits and sustainability of interventions to protect and promote health.

PUB, 2014. Technical Guide for Greywater recycling systems, s.l.: s.n.

Pucher, B., Zluwa, I., Spörl, P., Pitha, U., Langergraber, G., 2022. Evaluation of the multifunctionality of a vertical greening system using different irrigation strategies on cooling, plant development and greywater use. Sci. Total Environ. 849, 157842. https://doi.org/10.1016/j.scitotenv.2022.157842

Ramprasad, C., Smith, C.S., Memon, F.A., Philip, L., 2017. Removal of chemical and microbial contaminants from greywater using a novel constructed wetland: GROW. Ecol. Eng. 106, 55–65. https://doi.org/10.1016/j.ecoleng.2017.05.022

Remy, C., Jekel, M., 2008. Sustainable wastewater management: life cycle assessment of conventional and source-separating urban sanitation systems. Water Sci. Technol. 58, 1555–1562. https://doi.org/doi.org/10.2166/wst.2008.533

Rizzo, A., Bresciani, R., Masi, F., Boano, F., Revelli, R., Ridolfi, L., 2018. Flood reduction as an ecosystem service of constructed wetlands for combined sewer overflow. J. Hydrol. 560, 150–159. https://doi.org/10.1016/j.jhydrol.2018.03.020

Rodriguez-Chueca, J., Polo-Lopez, M.I., Mostero, R., Ormad, M.P., Fernandez-Ibañez, P., 2014. Disinfection of real and simulated urban wastewater effluents using a mild solar photo-Fenton. Appl. Catal. B Environ. 150–151, 619–629. https://doi.org/10.1016/j.apcatb.2013.12.027

Rysulova, M., Kaposztasova, D., Vranayova, Z., 2017. Green Walls as an Approach in Grey Water Treatment Green Walls as an Approach in Grey Water Treatment, in: IOP Publishing (Ed.), IOP Conference Series: Materials Science and Engineering. p. 072049. https://doi.org/10.1088/1757-899X/245/7/072049

Serra, V., Bianco, L., Candelari, E., Giordano, R., Montacchini, E., Tedesco, S., Larcher, F., Schiavi, A., 2017. A novel vertical greenery module system for building envelopes: The results and outcomes of a multidisciplinary research project. Energy Build. 146, 333–352. https://doi.org/10.1016/j.enbuild.2017.04.046

Seyam, S., 2019. The impact of greenery systems on building energy: Systematic review. J. Build. Eng. 26, 100887. https://doi.org/10.1016/j.jobe.2019.100887

Sjoback, R., Nygren, J., Kubista, M., 1995. Absorption and fluorescence properties of fluorescein. Spectrochim. Acta Part A L7–L21.

Šostar-Turk, S., Petrinić, I., Simonič, M., 2005. Laundry wastewater treatment using coagulation and membrane filtration. Resour. Conserv. Recycl. 44, 185–196. https://doi.org/10.1016/j.resconrec.2004.11.002

South, E.C., Hohl, B.C., Kondo, M.C., MacDonald, J.M., Branas, C.C., 2018. Effect of Greening Vacant Land on Mental Health of Community-Dwelling Adults: A Cluster Randomized Trial. JAMA Netw. open 1, e180298. https://doi.org/10.1001/jamanetworkopen.2018.0298

Svete, L.E., 2012. Vegetated greywater treatment walls : Design modifications for

intermittent media filters. Norwegian University of Life Sciences.

Teotónio, I., Silva, C.M., Cruz, C.O., 2018. Eco-solutions for urban environments regeneration: The economic value of green roofs. J. Clean. Prod. 199, 121–135. https://doi.org/10.1016/j.jclepro.2018.07.084

Thompson, K.A., Valencia, E.W., Scott Summers, R., Cook, S.M., 2020. Sorption, coagulation, and biodegradation for graywater treatment. Water Sci. Technol. 81, 2152–2162. https://doi.org/10.2166/wst.2020.273

Tzoulas, K., Korpela, K., Venn, S., Yli-Pelkonen, V., Kaźmierczak, A., Niemela, J., James, P., 2007. Promoting ecosystem and human health in urban areas using Green Infrastructure: A literature review. Landsc. Urban Plan. 81, 167–178. https://doi.org/10.1016/j.landurbplan.2007.02.001

UK government, 1999. The Water Supply (Water Fittings) Regulations.

United Nations, 2017. World water development report, s.l.: s.n. USEPA, 2012. Guidelines for water reuse, Washington: U.S. Ageny for International Development.

USEPA, 2012. Guidelines for water reuse, Washington: U.S. Ageny for International Development.

Vakil, K.A., Sharma, M.K., Bhatia, A., Kazmi, A.A., Sarkar, S., 2014. Characterization of greywater in an Indian middle-class household and investigation of physicochemical treatment using electrocoagulation. Sep. Purif. Technol. 130, 160–166. https://doi.org/10.1016/j.seppur.2014.04.018

Vuppaladadiyam, A.K., Merayo, N., Prinsen, P., Luque, R., 2018. A review on greywater reuse : quality , risks , barriers and global scenarios. Rev. Environ. Sci. Bio/Technology 9. https://doi.org/10.1007/s11157-018-9487-9

Vymazal, J., 2002. The use of sub-surface constructed wetlands for wastewater treatment in the Czech Republic : 10 years experience. Ecol. Eng. 18, 633–646.

WHO, 2006. Guidelines for the safe use of wastewater, excreta and greywater. excreta and greywater use in agriculture volume IV, s.l.: World Health Organisation.

Wolcott, S., Martin, P., Goldowitz, J., Sadeghi, S., 2016. Performance of green wall treatment of brewery wastewater. Environ. Prot. Eng. 42, 137–149. https://doi.org/10.5277/epe160411

World Health Organization, 2017. Progress on Drinking Water, Sanitation and Hygiene: update and SDG baselines, s.l.: s.n.

Yin, Z., Santos, C.E.D. dos, Vilaplana, J.G., Sobotka, D., Czerwionka, K., Damianovic, M.H.R.Z., Xie, L., Morales, F.J.F., Makinia, J., 2016. Importance of the combined effects of dissolved oxygen and pH on optimization of nitrogen removal in anammox-enriched granular sludge. Process Biochem. 51, 1274–1282. https://doi.org/10.1016/j.procbio.2016.05.025

Zhu, J., Wagner, M., Cornel, P., Chen, H., Dai, X., 2018. Feasibility of on-site grey-water reuse for toilet flushing in China. J. Water Reuse Desalin. 8, 1–13.

https://doi.org/10.2166/wrd.2016.086

Zraunig, A., Estelrich, M., Gattringer, H., Kisser, J., Langergraber, G., Radtke, M., Rodriguez-Roda, I., Buttiglieri, G., 2019. Long term decentralized greywater treatment for water reuse purposes in a tourist facility by vertical ecosystem. Ecol. Eng. 138, 138–147. https://doi.org/10.1016/j.ecoleng.2019.07.003

♦ Appendix A

Table A.I. Synoptic view of the main design characteristics of green walls for greywater treatment in literature, limited to pilot and full scale studies.

	(Gattringer et al. 2016)	**(Masi et al. 2016)**	**(Zraunig et al. 2019)**	**(Prodanovic et al. 2019)**	**(Prodanovic et al. 2020)**	**(Bakheet et al. 2020)**	**(Dal Ferro et al. 2021)**	**(Estelrich et al. 2021)**	**(Lakho et al. 2021)**	**(Lakho et al. 2022)**	**(Pucher et al. 2022)**
Place	Lloret der Mar, Spain	Pune, India	Lloret der Mar, Spain	Melbourne, Australia	Melbourne, Australia	Melbourne, Australia	Padova, Italy	Lloret der Mar, Spain	Gent, Belgium	Gent, Belgium	Vienna (austria)
Scale and type	Full scale HF+VF+ aeration	Pilot VF	Full scale HF+aeration	Pilot VF	Pilot, pot VF	Pilot VF	Pilot VF	Full scale HF+VF+ aeration	Full scale VF	Full scale VF	Full scale VF (wall 4)
Exposition	Semi-indoor	Outdoor	Semi-indoor	Open-air greenhouse	Open-air greenhouse	Open-air greenhouse	Open-air	Semi-indoor	Open-air (S-W)	open-air (S-W)	Open air
Treatment surface per row (m^2)	1.75	0.01	1.58	0.04	0.04	0.04	0.16	1.8	0.78	0.36	0.3
Growing medium	Expanded clay	Exp. clay	Exp. clay &, CF (1:1)	Exp. clay &sand (1:1)	Expanded clay	PL and CF (1:1)	PL and CF (1:1)	PL and CF (1:1)	Expanded clay	Expanded clay	Lava, organic soil and biochar (2:1:1)	Lava, organic soil and biochar (2:1:1)	Expanded clay, zaolite, perlite, sand, crushed expanded clay
WW type	GW	GW		Real GW	SLGW	SLGW	SGW	kitchen GW	GW	GW	GW	GW	SGW
Inflow rate (m^3d^{-1})	1	0.01		1.008	0.004	0.004	0.004	0.023	2	0.1	0.06	0.09
HLR first row (Lm^2d^{-1})	250	1000		637.0	100	100	100	36.2-72.6	280	128	175	300
Plant species	Different species of marshplants (e.g. Typha, Iris), graminoids (Carex, Cyperus) tropical and subtropical plants (e.g. Ficus, Spathiphyllum, Epiprenum)	Abelia, Wedelia Portulaca, Alternenthera, Duranta and Hemigraphis		Cyperus alternifolius, Monstera deliciosa, Carex acutiformis, Ficus pumila, Juncus inflexus, Philodendron scandens, Juncus effusus, Philodendron erubescens, Equisetum hyemale, Syngonium podophyllum, Spathiphyllum Wallisii, Iris Laevigata, Spathiphyllum Wallisii, Mentha Aquatica, Calathea	Carex appressa	Carex appressa	Carex appressa	Mentha aquatica	Oenanthe javanica	Lysimachia	Iris sp, Juncus sp, Carex sp, Cyperus sp, Monstera sp…	Carex morrowii, Acorus gramineus, Mazus reptans, Ajuga reptans, Deschampsia cespitosa, Geum rivale, Heuchera hybrid, Houttuynia cordata, Campanula posharskyana, Geranium wlassovianum and Hemerocallis hybrid	Carex morrowii, Acorus gramineus, Mazus reptans, Ajuga reptans, Deschampsia cespitosa, Geum rivale, Heuchera hybrid, Houttuynia cordata, Campanula posharskyana, Geranium wlassovianum and Hemerocallis hybrid	Caltha Palustris, Carex Grayi, Eriophorum Vaginatum, Eupatorium Canabinum, Geranium Wallichianum, Iris Pseudocorus, Liriope Muscari, Lythrum Salicaria, Mentha Acquatica, Ophiopogon Planiscapus, Sedum Telephium, Thelypteris Palustris, Typha Minima, Valeriana Officinalis

Table A.II. Synoptic view of the inflow GW characteristics of green walls for treatment in literature, limited to pilot and full scale studies. Parameters in mg/L (other units for turbidity in NTU, E. coli in MPN/100mL, EC in µS/cm, pH).

	(Gattringer et al. 2016)		**(Masi et al. 2016)**		**(Zraunig et al. 2019)**	**(Prodanovic et al. 2019)**	**(Prodanovic et al. 2020)**	**(Bakheet et al. 2020)**	**(Dal Ferro et al. 2021)**	**(Estelrich et al. 2021)**	**(Lakho et al. 2021)**	**(Lakho et al. 2022)**	**(Pucher et al. 2022)**
pH	7.25				7.08±0.31		6.85	6.62±0.01	8.7		7.4±0.7	6.8±0.3	7.96±0.43
EC	817.61				767±108		163	173±2	992.0	752.1±48.1	793±146	748±109	750±55
Turbidity					68±39.8		42.1	54.9±7.2	139.0	24.8±8.5	73±95	286±119	26.82±5.8
TSS	336.09		58.8±12.9	53.8±18.4	63±114		71.5	90.7±1.1		42.5±25.8	40±30	153±115	
COD	409.11	84.9±2.5	48.8±24.6	43.9±22.6	158±112		317	322±6	855	130±73.4	160±103	483±166	382±59
BOD_5	130.32	39.7±3.2	17.1±7.9	18.6±10.2	116±67			140±0	200	110.5±48.3	31±12	307±51	
TN	16.17				10.4±9.3	5.2	5.1			6.8±8.7	12±11	13.8±5	11.74±2.2
TKN	27.03		4.6±0.8	4.6±1.2	10.3±9				28.05				
NO_3^--N	0.67				0.02±0.04				0.01	0.1±0.18	0.7±0.6	0.68±0.8	0.22±0.2
NH_4^+N	4.89		3.4±1.7	3.5±0.8	4.88±2.92				6.89	3.6±4	3±6	5.6±3.09	6.67±1.49
TP						3	2.97		15.7				
$P\text{-}PO_4$	1.26				0.34±0.76				6.4	0.3±0.62	1.1±2.3	0.91±0.36	
Cl^-								27.9±1.3					
MBAS									12.6				
E coli							21.7	29.1±12.4		1.1*10^6	5e2±1.51e3	2.78e2±2.29e-1	
TOC	50.76				39±25.6					29±14.8			88.9±25.4

Table A.III. Characteristics of the outflow treated GW of green walls for treatment in literature, limited to pilot and full scale studies. Parameters in mg/L (other units for turbidity in NTU, E. coli in MPN/100mL, EC in µS/cm, pH). Removal efficiency of each system (in percentage).

	(Gattringer et al. 2016)	(Masi et al. 2016)			(Zraunig et al. 2019)	(Prodanovic et al. 2019)	(Prodanovic et al. 2020)	(Bakheet et al. 2020)	(Dal Ferro et al. 2021)			(Estelrich et al. 2021)	(Lakho et al. 2021)	(Lakho et al. 2022)	(Pucher et al. 2022)
pH	7,43				7,36±0,29		7,25	7,18±0,21	7,81	7,93	7,92		7,5±0,5	8,8±0,6	7,63±0,15
EC	774,34				783±52		156	183±2	1338	1202	1074,00	795,6±77,1	919±209	602±191	770±72
Turbidity					1,8±1,5		1,47	2,52±0,53	16,1	14,25	17,10	1,0±0,2	10±10	11±15	5,62±6,91
TSS	3,98		45,6±20	48,1±20,1	3,±6		1,25	1,4±0,4				6,8±6,6	13±18	15±13	
COD	13,89	69,4±1,7	21,4±15,3	27,7±21,2	6±12		28,3	13,6±1,2	98,2	82,4	66	16,4±4,9	91±108	85±31	75±66
BOD_5	3,81	29,9±2,5	6,7±2,7	11±8,3	3±3			2±0	41,5	30	25	3,8±2	5±3	15±10	
TN	4,21				4,6±2,6	0,36±0,06	0,41					1,6±1,1	11±9	10±5,4	3,5±2,44
TKN	1,63		3,5±3,4	3,9±3	2,4±2,3				13,6	12,1	13,5				
NO_3^--N	3,61				2,31±1,80				0,04	0,07	0,08	1,3±1,0	5,9±6,8	7,3±4,2	0,41±0,45
NH_4^+N	0,17		1,7±0,7	1,1±0,5	1,55±1,37				3,18	2,52	2,53	0,04±0,09	0,08±0,07	0,07±0,05	1,27±1,12
TP						1,42±0,23	1,7		11,9	9,43	10,32				
P-PO_4	0,32				0,54±0,80				8,95	6,72	7,11	0,2±0,1	3,6±2,6	0,94±0,63	
Cl^-								28±0							
MBAS									2,13	2,28	2,70				
E coli							2,72	3,24±1,33				0		1,03e2±9,53e-1	
TOC	6,09											2,7+-0,7			22,8+-15,9
Removal efficiency (%)															
Turbidity					96±6		97,6	95,4	88,4	89,7	87,7	95,4±2,8	86	96	79
TSS	98,8				88±17		98,4	98,4				86,4±12,9	67	90	
COD	96,6	18,3±1,1	53,3±21,3	42±25,8	92±16		92,4	95,8	88,5	90,4	92,3	84±8,9	43	82	80
BOD_5	97,1	24,6±3,9	53,7±22	44,3±26,1	95±4			98,6	79,3	85,0	87,5	97,7±1,6	83	95	
TN	74				37±47	93±1	91,8					64,8±41,8	8	26	70
TKN	94				69±36				51,4	56,9	51,9				
NO_3^--N	-440,3								-300,0	-600,0	-700,0				
NH_4^+N	96,6				52±29				53,8	63,4	63,3	99,1±2,1	97	98	81
TP						53±8	46,0		24,2	39,9	34,3				
P-PO_4									-39,0	-4,3	-10,4				
Cl^-								-0,3							
MBAS									83,1	81,9	78,6				
E coli							86	88,9				> 4 CFU/L		log(0,4)	
TOC	88											88,9±5,6			74

♦ Appendix B

This appendix reports in table format the results already presented in the fourth chapter, related to inflow and outflow concentrations during the four experimental campaign on the green wall modules.

Phase 1

Table B.I. Average and standard deviation (in parenthesis) over time of on-site and laboratory parameters of input GW and outflow from each configuration.

Parameters	Input TW	Input GW	BM*	BM	GAC	CO	BC	PA	PABC	PA+
T (°C)	14.62 (2.27)	7.70 (4.59)	7.75 (0.29)	7.53 (0.15)	7.59 (0.12)	7.19 (0.07)	7.62 (0.08)	7.40 (0.16)	7.59 (0.24)	7.14 (0.10)
DO (mg/L)	9.18 (0.98)	9.25 (4.45)	10.69 (0.34)	11.02 (0.19)	11.06 (0.13)	10.23 (0.35)	10.76 (0.13)	11.10 (0.23)	10.80 (0.34)	11.13 (0.15)
pH	7.01 (0.30)	7.35 (0.31)	7.24 (0.09)	7.40 (0.04)	7.34 (0.09)	7.28 (0.14)	7.33 (0.05)	7.35 (0.08)	7.21 (0.08)	7.50 (0.14)
EC (uS/cm)	455 (87)	549 (107)	524 (6)	641 (7)	633 (5)	645 (8)	638 (3)	639 (8)	642 (5)	645 (8)
TSS (mg/L)	2.69 (3.34)	9.63 (2.94)	8.02 (0.87)	9.37 (0.96)	10.75 (1.18)	11.96 (2.29)	12.86 (1.81)	10.76 (2.47)	9.71 (1.14)	9.08 (0.70)
COD (mg/L)	67.67 (29.9)	274.22 (90.25)	122.0 (4.93)	171.55 (16.29)	159.90 (14.05)	190.89 (15.26)	147.0 (8.94)	158.1 (24.4)	163.3 (10.6)	163.5 (8.22)
BOD (mg/L)	0.43 (0.45)	52.37 (8.97)	1.18 (0.33)	1.17 (0.27)	1.97 (0.87)	3.06 (0.95)	1.76 (1.05)	1.84 (0.15)	2.08 (0.71)	1.31 (0.22)
TKN (mg/L)	2.42 (2.54)	5.01 (3.11)	4.34 (0.19)	2.66 (0.14)	2.04 (0.10)	2.51 (0.16)	2.22 (0.40)	2.69 (0.14)	2.43 (0.36)	2.78 (0.15)
NO_3^-N (mg/L)	1.94 (1.79)	3.39 (1.43)	2.19 (0.15)	2.43 (0.13)	2.14 (0.14)	2.19 (0.15)	1.82 (0.14)	2.50 (0.23)	2.10 (0.13)	2.61 (0.16)
NH_4^+-N (mg/L)	0.43 (0.93)	0.68 (1.00)	0.41 (0.06)	0.41 (0.06)	0.38 (0.04)	0.33 (0.07)	0.54 (0.08)	0.34 (0.07)	0.43 (0.07)	0.30 (0.04)
TP (mg/L)	0.69 (1.74)	4.36 (6.33)	1.23 (0.02)	2.76 (0.25)	2.90 (0.48)	3.71 (0.30)	3.31 (0.20)	2.05 (0.19)	3.20 (0.14)	3.21 (0.16)
SO_4^{2-} (mg/L)	35.33 (29.6)	87.78 (20.74)	54.65 (2.40)	85.33 (2.78)	77.96 (3.07)	81.59 (2.46)	76.85 (2.99)	89.70 (4.86)	72.67 (3.60)	75.41 (2.91)
Cl^- (mg/L)	2.34 (3.01)	6.96 (3.10)	4.90 (0.39)	6.20 (0.39)	6.45 (0.23)	7.21 (0.47)	6.88 (0.18)	6.55 (0.70)	6.06 (0.24)	6.41 (0.25)
MBAS (mg/L)	0.15 (0.09)	3645 (521)	1852 (172)	1318 (69)	1496 (38)	1621 (73)	1128 (25)	1417 (85)	1437 (129)	1427 (42)
E. coli (MPN/ 100mL)	-	79666 (98263)	-	24.75 (24.62)	16.88 (5.91)	17.88 (8.42)	23.13 (50.9)	16.50 (18.9)	18.00 (24.8)	37.75 (22.5)

Phase 2

Table B.II. Average and standard deviation over time of input GW and outflow GW.

Parameters	Input TW	Input GW	BC_old	BC	BC+GR	BC+GR*
T (°C)	19.15 (3.95)	21.19 (4.60)	19.16 (4.81)	19.06 (4.47)	19.29 (4.39)	19.36 (4.42)
DO (mg/L)	7.68 (1.36)	2.58 (3.14)	7.32 (1.35)	7.71 (0.89)	7.57 (1.30)	6.88 (0.89)
pH	7.16 (0.23)	7.30 (0.08)	7.54 (0.16)	7.53 (0.08)	7.60 (0.14)	7.40 (0.10)
EC (uS/cm)	541.25 (26.05)	700.63 (17.79)	683.46 (45.54)	700.96 (15.70)	701.25 (25.33)	541.96 (35.37)
TSS (mg/L)	0.98 (1.23)	40.60 (22.73)	1.73 (0.90)	1.45 (1.14)	1.03 (0.96)	1.38 (1.65)
COD (mg/L)	20.00 (0.00)	70.88 (16.39)	20.00 (0.00)	20.00 (0.00)	20.00 (0.00)	20.00 (0.00)
BOD (mg/L)	6.37 (5.81)	55.37 (13.44)	5.82 (5.71)	6.79 (6.37)	6.49 (5.33)	7.25 (6.02)
TKN (mg/L)	6.43 (2.08)	3.16 (2.76)	1.77 (1.95)	0.64 (0.37)	0.75 (0.43)	4.22 (2.29)
NO_3^--N (mg/L)	4.19 (1.45)	7.18 (6.00)	4.95 (0.29)	4.89 (0.22)	4.85 (0.24)	5.01 (0.35)
NH_4^+-N (mg/L)	0.04 (0.01)	0.06 (0.03)	0.15 (0.19)	0.04 (0.00)	0.04 (0.00)	0.05 (0.01)
TP (mg/L)	2.14 (2.37)	8.56 (1.44)	8.01 (1.77)	7.33 (1.85)	7.99 (1.69)	2.15 (2.36)
SO_4^{2-} (mg/L)	66.88 (9.79)	143.25 (13.30)	117.21 (12.70)	109.00 (9.05)	113.25 (10.19)	74.29 (12.18)
Cl^- (mg/L)	3.46 (1.26)	12.96 (3.35)	6.34 (1.49)	6.86 (0.52)	6.69 (0.88)	4.39 (0.78)
MBAS (mg/L)	0.64 (0.35)	790.0 (649.9)	1051.9 (1008.6)	825.2 (341.4)	651.8 (286.4)	664.1 (192.2)
E. coli (MPN/100mL)	-	70000 (50199)	4.80 (1.79)	3.17 (1.33)	19.83 (29.38)	-

Phase 3

Table B.III. Phase 3. Average and standard deviation (in parenthesis) over time of on-site and laboratory parameters of input GW and outflow from each level.

Parameters	Input GW	New panel			Old panel		
		Level 1	Level 2	Level 3	Level 1	Level 2	Level 3
T (°C)	9.03 (3.22)	7.86 (3.38)	7.02 (3.06)	7.34 (3.07)	8.39 (3.25)	7.31 (3.19)	6.96 (2.82)
DO (mg/L)	2.09 (0.73)	5.06 (1.29)	8.44 (2.06)	10.82 (0.91)	5.17 (0.83)	5.80 (1.68)	10.48 (1.30)
pH	7.34 (0.17)	7.31 (0.12)	7.39 (0.19)	7.73 (0.16)	7.48 (0.11)	7.46 (0.12)	7.76 (0.17)
EC (uS/cm)	696.60 (12.06)	693.40 (13.27)	696.80 (12.97)	699.00 (13.39)	696.73 (12.88)	701.30 (13.00)	705.10 (13.09)
TSS (mg/L)	41.06 (17.29)	19.77 (18.06)	2.67 (3.46)	1.12 (2.00)	43.28 (20.65)	16.68 (10.41)	3.79 (3.64)
COD (mg/L)	108.60 (21.83)	47.17 (19.76)	24.23 (5.39)	22.60 (4.51)	70.77 (19.34)	35.33 (12.07)	20.83 (1.43)
BOD (mg/L)	48.95 (15.50)	27.14 (14.25)	6.61 (6.24)	0.57 (0.98)	43.36 (6.17)	24.13 (12.99)	2.67 (3.90)
TN (mg/L)	1.57 (0.66)	1.48 (1.35)	0.79 (0.61)	0.73 (0.50)	1.60 (0.46)	1.31 (0.74)	0.74 (0.35)
NO_3^--N (mg/L)	0.31 (0.02)	0.31 (0.02)	0.30 (0.00)	0.30 (0.00)	0.30 (0.00)	0.30 (0.00)	0.30 (0.00)
NH_4^+-N (mg/L)	0.05 (0.01)	0.05 (0.01)	0.04 (0.01)	0.05 (0.02)	0.06 (0.01)	0.09 (0.12)	0.05 (0.01)
TP (mg/L)	8.70 (0.57)	8.40 (0.25)	8.18 (0.29)	8.18 (0.37)	8.51 (0.52)	8.63 (0.33)	8.52 (0.43)
Cl^- (mg/L)	43.34 (3.52)	39.23 (5.87)	35.56 (4.09)	34.84 (3.42)	42.67 (4.45)	39.38 (5.60)	35.61 (3.80)
MBAS (mg/L)	10.50 (6.27)	4.36 (2.64)	1.76 (2.35)	0.81 (0.74)	5.64 (3.35)	2.88 (1.53)	2.23 (1.18)

Phase 4

Table B.IV. Phase 4. Average and standard deviation (in parenthesis) over time of on-site and laboratory parameters of input GW and outflow from each level.

Parameter	Input GW	Variable load panel			Constant load panel		
		Level 1	Level 2	Level 3	Level 1	Level 2	Level 3
T (°C)	19.29 (5.94)	17.04 (5.70)	16.26 (5.72)	16.26 (5.64)	16.98 (5.58)	16.27 (5.58)	16.22 (5.57)
DO (mg/L)	2.29 (1.71)	7.95 (0.90)	9.22 (1.09)	9.51 (1.17)	7.59 (0.96)	9.25 (1.07)	9.53 (1.18)
pH	7.09 (0.14)	7.31 (0.07)	7.63 (0.02)	7.87 (0.04)	7.20 (0.03)	7.50 (0.03)	7.76 (0.12)
EC (uS/cm)	702.40 (20.72)	700.51 (1.68)	697.27 (1.57)	693.69 (1.73)	707.49 (12.41)	705.56 (2.32)	701.16 (2.24)
TSS (mg/L)	54.25 (54.12)	8.77 (1.91)	2.18 (1.86)	1.20 (1.99)	10.30 (4.92)	1.38 (0.80)	1.03 (0.96)
COD (mg/L)	120.07 (34.92)	41.69 (6.98)	23.82 (6.84)	20.82 (2.30)	40.00 (10.96)	20.31 (2.09)	20.11 (0.75)
BOD_5 (mg/L)	59.29 (17.15)	24.66 (5.51)	7.47 (3.06)	3.92 (1.57)	24.54 (5.38)	5.26 (1.57)	3.09 (2.16)
TN (mg/L)	1.75 (0.93)	0.84 (0.21)	0.53 (0.11)	0.59 (0.33)	0.87 (0.20)	0.63 (0.41)	0.54 (0.25)
NO_3^--N (mg/L)	0.30 (0.93)	0.30 (0.02)	0.30 (0.00)	0.30 (0.00)	0.30 (0.00)	0.30 (0.00)	0.30 (0.00)
NH_4^+-N (mg/L)	0.08 (0.08)	0.04 (0.00)	0.04 (0.00)	0.04 (0.00)	0.05 (0.03)	0.04 (0.02)	0.04 (0.00)
TP (mg/L)	8.82 (1.80)	7.79 (1.24)	7.77 (0.44)	7.69 (0.16)	8.22 (0.53)	8.18 (0.59)	8.10 (0.24)
Cl^- (mg/L)	51.31 (11.58)	40.43 (0.99)	38.20 (0.72)	37.93 (0.47)	40.49 (0.85)	37.96 (0.40)	37.98 (0.93)
MBAS (mg/L)	24.07 (8.46)	8.89 (2.30)	3.19 (1.06)	1.54 (0.30)	8.44 (2.73)	2.08 (1.62)	1.32 (1.49)